



THE UNIVERSITY OF
WAIKATO
Te Whare Wānanga o Waikato

Research Commons

<http://researchcommons.waikato.ac.nz/>

Research Commons at the University of Waikato

Copyright Statement:

The digital copy of this thesis is protected by the Copyright Act 1994 (New Zealand).

The thesis may be consulted by you, provided you comply with the provisions of the Act and the following conditions of use:

- Any use you make of these documents or images must be for research or private study purposes only, and you may not make them available to any other person.
- Authors control the copyright of their thesis. You will recognise the author's right to be identified as the author of the thesis, and due acknowledgement will be made to the author where appropriate.
- You will obtain the author's permission before publishing any material from the thesis.

**Spatial and Temporal Changes in Soil Climate and Active
Layer Depth in the Ross Sea Region, Antarctica**

1999-2018

A thesis

submitted in partial fulfilment

of the requirements for the degree

of

Master of Science in Earth Science

at

The University of Waikato

by

Annette G. Carshalton



THE UNIVERSITY OF
WAIKATO
Te Whare Wānanga o Waikato

2020

Abstract

The depth of seasonal thaw (the active layer depth) integrates a range of soil and atmospheric climate variables and has potential to provide a clear signal of a changing climate. Nine soil climate monitoring stations (SCS) were established between 1999 and 2012 and are currently operating in the Ross Sea Region of Antarctica. At each monitoring station soil temperature and moisture are measured at a range of depths down to 120 cm. Atmospheric variables measured include; air temperature, relative humidity, solar radiation, and windspeed and direction. Data validation has been carried out through the comparison of multiple sensors and has given confidence in the dataset. The objectives of this thesis were to; describe the active layer, assess the dataset for significant long-term trends, investigate the link between large scale climate systems and permafrost temperature, to test the model of Adlam et al. (2010), and develop a predictive model suitable for modelling all ice free areas in Antarctica.

Active layer depth (ALD) showed marked between-year variation, and between the SCS establishment and 2018. The mean ALD was 7.5 cm at Mt Fleming, 38 cm at the Wright Valley South Wall, 37 cm at the Wright Valley North Wall, 23 cm at Victoria Valley, 49 cm at the Wright Valley floor, 50 cm on the coast at Marble Point, 29 cm at Minna Bluff, 33 cm at Scott Base, and >90 cm at Granite Harbour. There were no significant trends of warming or cooling in either ALD or in temperature at top of the permafrost. Relationships between ALD and altitude ($R^2=0.71$), and with latitude ($R^2= 0.66$) were identified.

Wavelet analysis showed that both global and regional climate systems were significant drivers of de-seasonalised permafrost temperature ($p < 0.05$). The Southern Annular Mode showed relationships at both annual and biannual timescales; the Southern Oscillation Index had a relationship at a two to three year timescale; and the Amundsen Sea Low had an annual signal and some between season signals with de-seasonalised permafrost temperature, at the Wright Valley Floor, Victoria Valley, Marble Point and at Mt Fleming.

Nineteen potential models were developed using stepwise analysis and compared to the previous work of Adlam et al. (2010). Model 8 (Adj $R^2 = 0.75$) accounted for more variation in the data than the Adlam et al. (2010) model (Adj $R^2 = 0.69$)

and predicted the ALD within ± 10 cm at the five low altitude sites, using mean summer air temperature, mean winter air temperature, altitude and mean summer surface temperature. Model 14 ($\text{Adj } R^2 = 0.49$) was developed using data from all eight SCS sites, and was able to predict the ALD at high altitude sites within $< \pm 11$ cm, and the low altitude sites within $< \pm 20$ cm. Model 14 did not capture the between year variation with detail.

Future testing of model 8 and 14 is recommended using data from other parts of Antarctica, and both models could also be used to explore the use of satellite remote sensed surface temperature data in predicting ALD. The database comprises approximately 87,000,000 data points, collected from both soil and atmospheric sensors, and becomes more valuable with time as the record gets longer. This thesis did not use all the available data in the network, and further research is recommended. The SCS network provides a robust baseline to predict future change and understand how Antarctica is impacted by the changing global climate.

Acknowledgements

I would firstly like to thank my two primary supervisors, Megan Balks and Tanya O'Neill, for your considerable time and effort you have both invested in me and the completion of this thesis. The critical and steady eye in reading the drafts of figures, chapters, posters and papers, that have helped me develop my written communication skills and helped create a document that is able to pass these findings to the wider scientific community, is truly appreciated. Megan I would like to thank you for inviting me to work on the Soil Climate Monitoring project and allowing me to go to Antarctica and visit this spectacular environment. The added advantage of being able to add to the scientific understanding of such an important region and complete a project that most people would die for I am truly thankful.

To Karin Bryan, my third supervisor, your assistance with explaining time series analysis, wavelet analysis, and stepwise modelling has been invaluable along with your practical coding expertise, which has taught me some much-needed skills. Also, for the excitement and can-do attitude you held for every problem I came to you with, thank you- I always left feeling like the impossible was finally possible and that this thesis would be a success.

To Cheryl Ward, the most amazing librarian, you have taught me so much about how to find obscure references, along with how to manipulate end note and word. Without you, this thesis would be an unreadable mangled stack of papers- but your magical formatting skills and persistence has turned into some beautiful.

Thank you to Ray Littler for finding the original work he did with Leah Adlam, as well as explaining a range of statistical modelling skills and assisting me with the developing a site-specific model.

Funding assistance for this thesis by the Broad Memorial Fund was gratefully received.

Thank you to Chris Morcom for showing me how the soil climate stations worked in Antarctica, for developing and handing over the soil climate station data base and showing me the basics of coding in MatLab at the very start of my thesis.

Thank you to Aaron Wall, Joss Ratcliff for their extended guidance with fixing bugs and translating what I wanted to do into code.

To my wonderful office mates and fellow students Joss, Anne, Jamie, Matt, Cullum, Sarah, Amy, Jonno, while I may have dropped in and out, you have shared many cups of tea, positive encouragement, and friendship over the last two and a half years making this a doable and enjoyable process, so thank you.

To wonderful flat mates, David and Claire, who discussed (explained) math and proofread many drafts, along with my amazing friends Stew, Lucia, Andrew, Kerry, Henry and Paige, you have provided nights out, donuts, pizza, biltong as well as doing the dishes, and have helped me keep the end in sight, without your help this thesis would not have made it to completion.

And last but not least my family; Cecelia, David, Mom, Dad, Henry, Michelle and the nine niblings, you have believed in me through this journey, scraped me up and dusted me off whenever I have fallen, reminded me that you are behind me, sent me adorable photos while I've had to be locked away writing and proof read countless last minute drafts. The achievement of this thesis is as much yours as it is mine, I couldn't have done it without you. Thank you.

Mischief Managed. So long, and thanks for all the Fish.

Table of Contents

Abstract	i
Acknowledgements.....	iii
Table of Contents.....	v
List of Figures.....	viii
List of Tables.....	xi
1 Chapter One	1
Introduction	1
1.1 Introduction	1
1.2 Soil Climate monitoring network	1
1.3 Objectives.....	2
1.4 Thesis structure.....	3
2 Chapter 2.....	5
Literature Review	5
2.1 Introduction	5
2.2 Antarctic soils and their formation.....	6
2.2.1 Introduction	6
2.2.2 Antarctic soil formation	11
2.2.3 Soil formation processes	13
2.3 The Atmosphere.....	14
2.3.1 Introduction	14
2.3.2 Solar radiation	15
2.3.3 Large scale climate patterns	16
2.3.4 Regional climate patterns.....	17
2.3.5 Local meteorology.....	17
2.3.6 Precipitation	18
2.3.7 Microclimate	19
2.4 Soil thermal properties and processes	19
2.4.1 Introduction	19
2.4.2 Heat transfer	20
2.4.3 Soil thermal properties.....	21
2.4.4 Heat movement processes	22
2.4.5 Freezing, ice formation and water movement.....	25
2.5 Previous findings	25
2.5.1 Antarctic Peninsula.....	25

2.5.2	Ross Sea Region	27
2.6	Trend detection	30
2.7	Soil climate predictive models.....	32
2.7.1	Introduction	32
2.7.2	Empirical Modelling	33
2.7.3	Numerical modelling	36
2.8	Conclusion.....	37
3	Chapter Three.....	39
	Soil Climate Station Descriptions, Instrumentation and Data Assessment.....	39
3.1	Introduction	39
3.2	Climate station locations	39
3.3	Soil descriptions.....	42
3.4	Instrumentation	49
3.4.1	Temperature probes	50
3.4.2	Air Temperature	50
3.4.3	Relative above ground Humidity.....	51
3.4.4	Solar Radiation	51
3.4.5	Wind Speed and Direction	51
3.5	Data Validation.....	51
3.6	Summary	53
4	Chapter Four	55
	Climatic influences on Active Layer Depth between 2000 and 2018 in the McMurdo Dry Valleys, Ross Sea Region, Antarctica.....	55
4.1	Abstract	56
4.2	Introduction	56
4.3	Methods.....	59
4.3.1	Station locations	59
4.3.2	Monitoring equipment set up	61
4.3.3	Reliability of probes and data.....	61
4.4	Results	63
4.5	Discussion	69
4.6	Conclusion.....	71
4.7	Acknowledgements.....	72
4.8	References	72
5	Chapter Five.....	76
	Prediction of active layer depth from above ground variables, Ross Sea Region, Antarctica.....	76

5.1	Abstract	77
5.2	Introduction	78
5.3	Methods	80
5.4	Results	85
5.5	Discussion	94
5.5.1	Model options.....	94
5.5.2	High altitude modelling	95
5.5.3	Relative change model.....	95
5.5.4	Limitations	96
5.5.5	Future work	96
5.6	Conclusion.....	97
5.7	Acknowledgements.....	99
6	Chapter Six.....	100
	Discussion and Conclusion	100
6.1	Introduction	100
6.2	Summary	100
6.2.1	Thesis objectives	100
6.3	Discussion	104
6.3.1	Implications of research	104
6.3.2	Limitations of this research	105
6.3.3	Future research	106
6.4	Conclusion.....	107
	References	110
	Appendices	117
	Appendix I Soil Profile Descriptions	118
	Appendix II Soil Climate Station Instrumentation	128
	Appendix III Active Layer Depth Determination.....	133
	Appendix IV Cross wavelet Analysis Graphs	144
	Appendix V Predictive Model Options.....	151

List of Figures

Figure 2.1: Map of Antarctica, showing the basic Geomorphology of east and west Antarctica (Ward, n.d.).....	6
Figure 2.2: Schematic of the three-layer conceptual model of the cryosol soil profile, topped by the desert pavement found in Antarctic soils. The blue bodies depict some of the ice bodies found in the permafrost; A) ice lenses, B) segregated ice, which forms from the surface (top of the permafrost) down, and C) upward growth of secondary and tertiary ice wedges. Adapted from (Bockheim & Hinkel, 2005).....	8
Figure 2.3: Schematic of the Atmosphere closest to the land surface, adapted from descriptions by Kaimal & Finnigan (1994).	15
Figure 2.4: The net change in heat storage per flux type in wet and dry soils, with the arrows size denoting the relative amount of heat movement. Note the difference in sensible and latent heat flux between dry and wet soils. Adapted from (Shukla, 2014).....	21
Figure 2.5: Simplified diagram of variation in soil temperature through time with increasing depth. Illustrating the phase lag and attenuation (dampening) of the temperature signal as depth increases (Hillel, 2003)	24
Figure 2.6: Soil climate monitoring network based in the McMurdo Dry Valleys and the surrounding Ross Sea Region, Antarctica.	29
Figure 2.7: Schematic flow chart developed by the Ministry for the Environment and Statistics NZ (2017) for trend assessment decisions.....	31
Figure 2.8: Schematic of wavelet transform windows top, and the corresponding tie series represented in time and frequency space (Lau & Weng, 1995).....	32
Figure 3.1: Map of soil climate station locations, with labelled photos of each site. WV = Wright Valley. Photo Credit; a) Annette Carshalton (2017), b) Chris Morcom (2016 & 2017), c) 2015 team, d) 2014 team.	41
Figure 3.2: The Desert Pavement at Mt Fleming (photo by Annette Carshalton)	42
Figure 3.3: Restored desert Pavement at Granite Harbour, with head of MRC probe for scale (photo by Annette Carshalton).....	43
Figure 3.4: Soil Profile at the Wright Valley Floor (photo by Megan Balks)	44
Figure 3.5: Disturbed desert pavement (foot print) at the Wright Valley floor, 2017	44

Figure 3.6: Restored desert pavement at Victoria Valley SCS with MRC probe for scale (photo by Annette Carshalton).	45
Figure 3.7: Restored desert Pavement at Marble Point with head of MRC probe for scale (photo by Annette Carshalton).	45
Figure 3.8: Soil profile at Scott Base (Photo by Megan Balks)	46
Figure 3.9: Desert pavement at Scott Base, with head of the MRC probe for scale (photo by Annette Carshalton).....	46
Figure 3.10: Restored desert Pavement at Minna Bluff (photo by Annette Carshalton).	47
Figure 3.11: Desert pavement at the Wright Valley South Wall, with MRC probe head for scale.	48
Figure 3.12: Soil profile at the Wright Valley South Wall (Cathy Seybold).....	48
Figure 3.13: Desert pavement at the Wright Valley North Wall, with probe head for scale (photo by Annette Carshalton).....	48
Figure 3.14: Soil profile at the Wright Valley North Wall (Goddard, 2013).....	48
Figure 3.15: Atmospheric climate data monitoring site at Minna Bluff, with temperature probe housing and wind monitoring equipment visible (photo by Annette Carshalton).	49
Figure 3.16: Soil temperature and moisture probes before installation. a) Vitel probes, b) MRC probe with embedded sensors, and c) Campbell 107 and Vitel probe (photos by Megan Balks).....	50
Figure 3.17: Subset of the calibration between soil temperature MRC and Campbell 107 at approximately 45 cm in a) 2004 and b) 2018, at the Wright Valley Floor. The other SCS showed similar results.....	52
Figure 4.1: Soil climate monitoring sites location map, with the insert showing the McMurdo Dry Valley region (Red Square). WV = Wright Valley.	59
Figure 4.2: ALD at all sites from 1999/2000 summer to 2017/2018 summer. Note that the line connecting data points is smoothed.	64
Figure 4.3: Relationship between site mean ALD over 3-17 years with a: an altitudinal transect, from Marble Point on the coast, through to Mt Fleming at the head of the Wright Valley, ($R^2 = 0.7$); and b: a latitudinal transect from Granite Harbour ($77^{\circ}00'23.7''S$) to Minna Bluff ($78^{\circ}30'41.6''S$), ($R^2 = 0.6$).	64
Figure 4.4: Mean summer (Dec-Jan) temperature at the top of the permafrost at eight of the nine soil climate stations, years with incomplete data are shown as gaps.....	65

Figure 4.5: Mean annual temperature at the top of the permafrost; years with incomplete data are shown as gaps. Note the different y-axis when comparing to Figure 4.	65
Figure 4.6: Cross wavelet transform between de-seasonalised permafrost temperature data at the Wright Valley Floor (WVF) and climate drivers. a: Southern Annular Mode (SAM); b: Southern Oscillation Index (SOI); c: Amundsen Sea Low pressure (ASL). The amplitude is displayed by the colour bar. Yellow corresponds to strong signal (amplitude) and areas within the black contours are significant ($p < 0.05$). Data in the paler shaded areas are influenced by the ‘edge effect’ and so are less reliable. Arrows correspond to phase relationships, where pointing right is in phase, and pointing downward means the climate driver leads the soil temperature by a quarter cycle.	68
Figure 5.1: Soil climate monitoring sites location map, with the insert showing the location of the McMurdo Dry Valleys. WV = Wright Valley (Carshalton et al., 2019).....	82
Figure 5.2: Measured ALD plotted with ALD predicted using the equation of Adlam et al. (2010), the model was developed using data from 1999 to 2007, which is plotted on the left hand side of each graph (left of green line), and on the right hand side of the line is the results since the model was developed. Graphs f and g were not used to develop the model.	86
Figure 5.3: Measured ALD plotted with predicted ALD using the equation for model 8. The model was developed using data from 1999 to 2015, which is plotted on the left-hand side of each graph (left of vertical line), and on the right-hand side of the line is the results since the model was developed.	90
Figure 5.4: Measured ALD plotted with predicted ALD using the equation for model 12. The model was developed using data from 1999 to 2015, which is plotted on the left-hand side of each graph (left of vertical line), and on the right-hand side of the line is the results since the model was developed. Graphs f-h were not used to develop the model.....	91
Figure 5.5: Measured ALD plotted with predicted ALD using the equation for model 14 the model was developed using data from 1999 to 2015, which is plotted on the left hand side of each graph (left of vertical line), and on the right hand side of the line is the results since the model was developed.	92
Figure 5.6: Measured ALD plotted with predicted ALD using the equation for model 15. The model was developed using data from 1999 to 2015, which is plotted on the left-hand side of each graph (left of vertical line), and on the right-hand side of the line is the results since the model was developed.	93

List of Tables

Table 3.1: Description of each station in the Ross Sea Region monitoring network, including site location, site description and soil type. WV = Wright Valley. Adapted from Carshalton et al. (submitted).	40
Table 4.1: Soil climate stations site locations and descriptions. Notes: nd = not determined, summer = December and January	60
Table 4.2: Trend analysis results of ALD and mean annual top of the permafrost temperature for each climate station series. The null hypothesis that there is was a warming or cooling trend was rejected at all sites (WV = Wright Valley).	66
Table 4.3: Significant high amplitude periods identified with cross wavelet analysis between potential climate drivers and de-seasonalised permafrost temperature at listed soil climate stations.....	67
Table 4.4: Significant but low amplitude periods identified with cross wavelet analysis between potential climate drivers and de-seasonalised permafrost temperature at listed soil climate stations.	67
Table 5.1: Description for each site in the soil climate monitoring network, and including mean summer and winter atmospheric conditions, and mean active layer depth at each site across the stations record, from site establishment to 2018. WV = Wright Valley. Adapted from Carshalton et al. (submitted).....	83
Table 5.2: The four empirical model equations developed using stepwise analysis, to predict ALD* in the McMurdo Sound Region. Adlam et al. (2010) model also given.....	87
Table 5.3: Statistics of most viable stepwise multiple regression models. The number of years of data and number of sites used in development, along with the variation explained, the efficiency of the model (f-stat), where a larger number is preferred, and the residual mean standard error (RMSE). The same statistics for the model of Adlam et al. (2010) are also given from previously unpublished data (Personal communication, Littler 2019).	87

Chapter One

Introduction

1.1 Introduction

Climate change and global warming are currently at the forefront of scientific and general public thinking. The IPCC (International Panel for Climate Change) predicts that global mean surface air temperatures will be 1°C higher between 2016 and 2035 compared to the mean between 1850 and 1900 (IPCC, 2014). As well as the mean global long-term temperatures in 2100 being 1.5°C (high confidence) to 4°C (low confidence) greater than mean temperatures between 1850 and 1900 (IPCC, 2014). Most climate change models predict that warming will be amplified, and occur rapidly, in the polar regions (Budyko and Izrael, 1987; Maxwell and Barrie, 1989; Roots, 1989; MacCracken et al., 1990; Anisimov *et al.*, 1997). While changes in surface temperature have had a greater impact in the Arctic the Antarctic has been more affected by ozone depletion (Zawar-Reza & Katurji, 2014). Long-term monitoring of polar processes, including permafrost and air temperature has confirmed the predictions of climate models made in the 1990's (Zawar-Reza & Katurji, 2014).

Antarctica is considered a key region to study climate change, because of its theoretical sensitivity to small changes (Seybold *et al.*, 2009), and with only a small anthropological impact (Guglielmin, 2012) human-induced bias is reduced. The soil and permafrost climate in Antarctica is not fully understood, with research only having been undertaken in small areas for short periods of time. One of 80 key Horizon Scan questions to be answered in the next twenty years; “How will permafrost, the active layer, and water availability, in Antarctic soils and marine sediments change in a warming climate, and what are the effects on ecosystems and biogeochemical cycles?” (Kennicutt *et al.*, 2014, p. 9).

1.2 Soil Climate monitoring network

A soil climate monitoring network was set up in co-operation between Landcare Research NZ, the University of Waikato, and the USDA-NRCS (United States

Department of Agriculture – Natural Resources Conservation Service). The first four soil climate stations (here on as SCS) were set up in 1999 at: Scott Base, Marble Point, on the Wright Valley floor below Bull Pass and the fourth in the Victoria Valley with help from Ron Sletten from the University of Washington (Seybold *et al.*, 2009).

The network was extended in the 2002 and 2003 summers with a further two SCS installed along the Ross Sea coast at Minna Bluff and Granite Harbour, and a third site at 1700 m on Mt Flemming. In 2011 and 2012, a further two sites were installed on the walls of the Wright Valley, the first on the south wall above Don Juan Pond, and the following year one on the north wall east of Bull Pass bringing the total number of SCS to nine. At each SCS temperature sensors were placed into permafrost, as well as equipment to monitor atmospheric changes, with dataloggers recording hourly changes.

The purpose of the SCS network was to create a long-term record of temperatures and active layer thickness to act as a baseline, and potentially define “normal” conditions, which is vital for early detection of warming trends (Seybold *et al.*, 2009). The data from this network contributes to three international initiatives, CALM (Circumpolar Active Layer Monitoring network), the Scientific Committee for Antarctic Research expert group ANTPAS (Antarctic Permafrost, Soil and Periglacial Environments), and TSP-South (Thermal State of Permafrost).

1.3 Objectives

The overall objective of my thesis was to analyse the soil climate and permafrost temperature data to investigate the changes in active layer depth in the Ross Sea Region of Antarctica. My project builds on work by (Adlam, 2009) and (Goddard, 2013), with a further five years of data and two new SCS sites since the last effort to analyse and interpret the data from the soil climate monitoring network.

Specific objectives were to:

- Determine the spatial and temporal variability of the active layer;
- describe seasonal temperature cycles and any trends that occur across the dataset;

- assess the dataset for long-term trends in active layer depth and permafrost temperature, and determine if any trends are significant;
- investigate the link between large scale climate systems and permafrost temperature;
- test the model created by Adlam *et al.* (2010) to predict active layer depth from above-ground climate data; and
- trial the development of a more robust model that could potentially predict the ALD in all ice-free regions of Antarctica.

1.4 Thesis structure

This thesis comprises of two journal papers prepared for submission along with a range of supporting material.

- Chapter one offers an introduction to the thesis topic area, the SCS network and the objectives of the thesis.
- Chapter two reviews the literature on both previous study methods and previous findings of Antarctic soil climate.
- Chapter three provides a comprehensive overview of the SCS network, the location of each station, the soils found at each site, the instrumentation and the robustness of the data, along with the methods for how data validation was completed and how missing data was managed.
- Chapter four comprises of a submitted journal paper that reports the active layer depths, and mean permafrost temperatures at all sites, as well as reporting on the relationship between large scale atmospheric climate systems, namely the Southern Annular Mode, Southern Oscillation Index and Amundsen Sea Low, and mean annual de-seasonalised permafrost temperature. This paper has been submitted to the *Geoderma Regional* in June 2019 (Carshalton *et al.*, Submitted). Consequently, there is some repetition of material from the introductory, literature review and method chapters). The data analysis and first drafts were undertaken by myself, with input from my co-authors. The co-authors for this paper helped in the following ways: Megan Balks is my principle supervisor and aided with result interpretation, as well as input into the wording of each draft; Tanya

O'Neil assisted with proof reading of drafts and is the official University of Waikato supervisor for my thesis; Karin Bryan assisted with the methods and the interpretation of wavelet analysis between the climate systems and permafrost data, and Cathy Seybold is responsible for the maintenance and storage of the dataset.

- Chapter five is presented in journal paper format and will be submitted after this thesis is completed. The paper tests the model of Adlam *et al.* (2010) who developed a model from atmospheric variables from the same SCS network used here. Several further models were developed using both step wise analysis and restricted maximum likelihood analysis with the best options of each model presented. Assistance for this work came from my supervisors Megan Balks and Tanya O'Neil, in the form of reading drafts and interpreting each model, and from Ray Littler and Karin Bryan in practical assistance of carrying out the modelling work.
- Chapter six includes the summary and conclusions for this thesis, the limitations affecting this study and the soil climate network and concludes with recommendations for future research.
- Appendix 1 gives the detailed soil profile descriptions that were completed by the team initiating each SCS. Appendix 2 comprises of a summary of the instruments at each site and includes the effective range and tolerance of each instrument and when it was installed.
- Appendices 3 and 4 include the supplementary material for the first journal paper (Chapter 4), with appendix 3 consisting of the figures used to determine active layer, and appendix 4 including the detailed figures showing the significant ($p < 0.05$) relationship between the climate systems and de-seasonalised permafrost data.
- Appendix 5 is made up of tables detailing the statistics and equations of all the models developed using step wise analysis.

Chapter Two

Literature Review

2.1 Introduction

Antarctica is a place like no other on Earth; it is the coldest and one of the driest in the world. These two factors play a large role in Antarctic geomorphology and soil formation (Campbell & Claridge, 1987). It is the world's fifth-largest continent, with an approximate size of 14 million square kilometres. The majority of which is covered in ice. The profile of Antarctica is like an upturned bowl, with a steep increase in altitude from the coast. Antarctica can be broken into two main regions, east and west Antarctica (Figure 2.1), divided by the Transantarctic and Pensacola Mountains (not shown in Figure 2.1).

East Antarctica is the larger of the two regions and underlain with a continuous bedrock base (Campbell & Claridge, 1987). The bedrock is covered by an ice sheet, which, in places, is >4,000 m thick (Campbell & Claridge, 1987). West Antarctica is made up of a range of islands covered by an ice sheet that flows over the Transantarctic Mountains reaching a thickness of 1,500 m (Campbell & Claridge, 1987). The ice sheet stretches to the Antarctic Peninsula creating two large ice shelves and multiple small ones (Campbell & Claridge, 1987). Between 70 – 90% of Earth's fresh water is held in Antarctic ice (Denton et al., 1991; Ugolini & Bockheim, 2008). Due to the massive ice sheet, only 0.32% to 0.36% (Ugolini & Bockheim, 2008; Bockheim *et al.*, 2015) of the landmass in Antarctica is ice-free, comprising approximately 45,000 km². The largest areas of ice free land are within the Transantarctic Mountains, Pensacola Mountains, the McMurdo Dry Valleys, and the Antarctic Peninsula (Bockheim *et al.*, 2015).

The aims of this chapter are to give an overview of the information that needs to be understood to undertake Antarctic soil climate research. The chapter reviews the soil, atmospheric and general Antarctic environment, the physical processes driving the Antarctic climate, and the methods used to model and detect trends in soil climate. A description and critical evaluation of previous investigations into Antarctic soil climate and relationships with atmospheric variations and climate systems are also included.

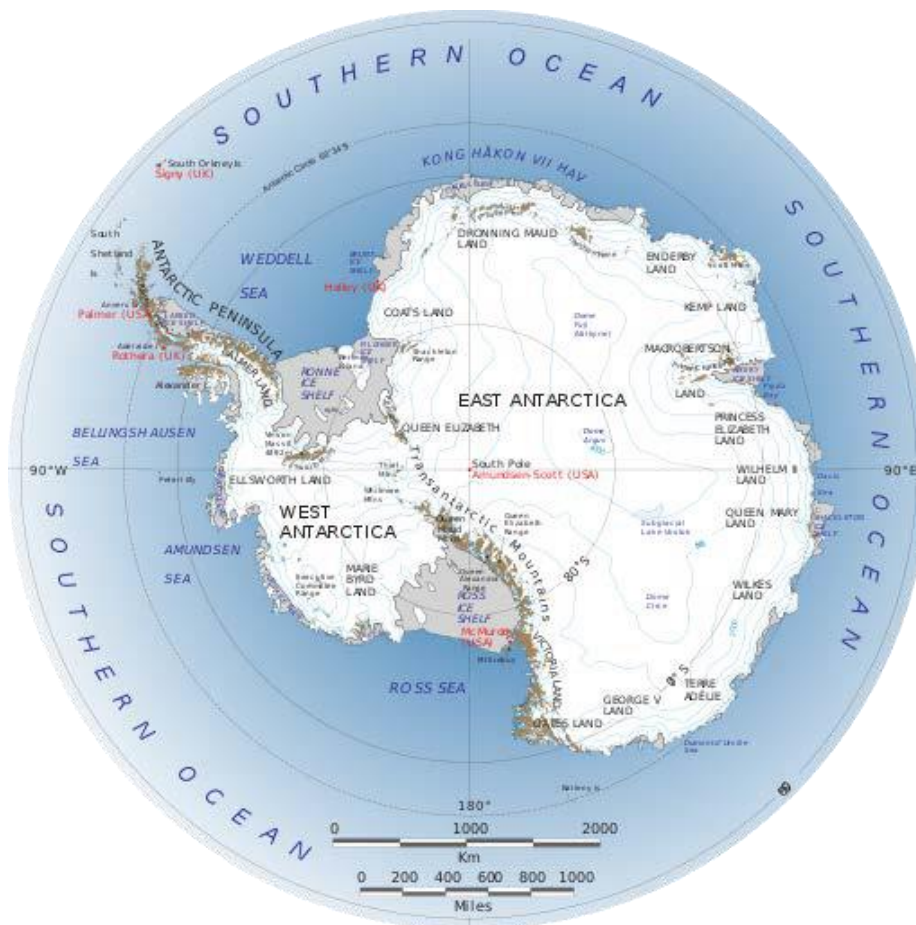


Figure 2.1: Map of Antarctica, showing the basic Geomorphology of east and west Antarctica (Ward, n.d.).

2.2 Antarctic soils and their formation

2.2.1 Introduction

When the soils of Antarctica were first explored, the scientific community did not have a term to define them, and many questioned if they could be considered soils due to being devoid of living matter, and unable to support plants, which we now know to be untrue (Bockheim *et al.*, 2015). Thus, at the time Antarctic soils did not classify as a soil. Soil Survey Staff (1999) updated the definition of a soil, to include Antarctic “soils” by defining it as:

“a natural body comprised of solids (minerals and organic matter), liquid and gasses that occurs on the land surface, occupies space, and is characterised by one or both of the following: horizons, or layers, that are distinguishable from the initial material as a result of additions,

losses, transfers and transformations of energy and matter *or* the ability to support rooted plants in a natural environment” (Soil Survey Staff, 1999, p. 1).

The World Reference Base for Soil Resources (2015), gives a more holistic and less technical definition under the belief that a simple definition is advantageous in discussing environmental problems in a systematic and timely manner. The WRB defines soil as:

“Any material within 2 m of the Earth’s surface that is in contact with the atmosphere, excluding living organisms, areas with continuous ice not covered by other material, and water bodies deeper than 2 m” (Food and Agriculture Organization of the United Nations, 2015. p. 4)

Frozen soils are defined in Soil Taxonomy, as Gelisols, and in the WRB (2015), as Cryosols. Gelisols and Cryosols are defined similarly as soils that have either permafrost (dry or ice-cemented) within 100 cm of the surface, or with material altered by cryoturbation and permafrost within 200 cm of the soil surface (Staff, 1999; Food and Agriculture Organization of the United Nations, 2015). From here on, frozen soils will be termed Cryosols.

Cryosols have three main layers: the active layer, a transition layer and permafrost (Figure 2.2). The three-layer system is defined by temperature fluctuations, in a way that is similar to thermoclines that occur in the atmosphere or lakes (Bockheim & Hinkel, 2005). The surface of the soil in Antarctica is unique in comparison to non-desert soils, due to sparse vegetation and organic matter. The lack of vegetation, a cold climate and high winds a desert pavement is formed.

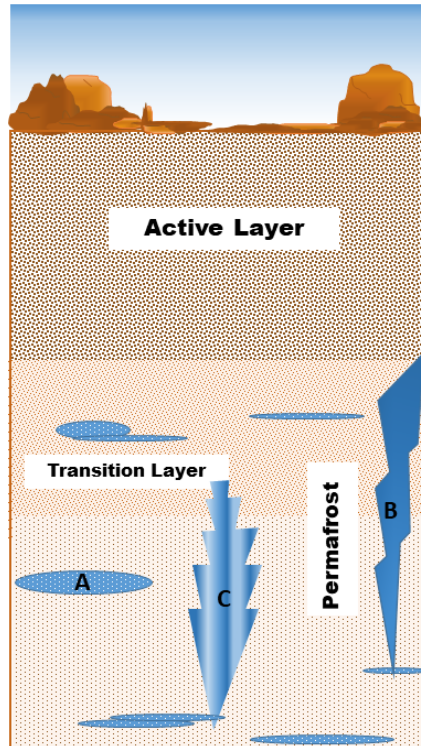


Figure 2.2: Schematic of the three-layer conceptual model of the cryosol soil profile, topped by the desert pavement found in Antarctic soils. The blue bodies depict some of the ice bodies found in the permafrost; A) ice lenses, B) segregated ice, which forms from the surface (top of the permafrost) down, and C) upward growth of secondary and tertiary ice wedges. Adapted from (Bockheim & Hinkel, 2005).

The desert pavements in Antarctica form on the soil surface and are made up of interlocking coarse sand, pebbles, and gravels through to boulders which, depending on age, may be coated with desert varnish, be pitted or ventifacted. The desert pavement is formed over time, as finer materials are eroded (Balks & O'Neill, 2016). Other methods of pavement formation include deflation, overland flow, upward migration of clasts, and weathering (Bockheim, 2010). Calcite deposits may occur on the desert pavement and within the soil, often underneath clasts (stones) (Claridge, 1965; McCraw, 1967; Balks & O'Neill, 2016).

The active layer is a layer of soil that freezes and thaws each year and is underlain by permafrost (Campbell & Claridge, 1987). To determine the depth of the active layer, it is necessary to undertake detailed temperature measurements to determine the maximum depth of summer thaw. In this thesis, the active layer depth was determined by calculating what depth of the soil profile the 0°C isotherm was crossed at maximum summer thaw. The soil material below the desert pavement, making up both the active layer and the permafrost, is generally unconsolidated and ranges in

texture from sands and sandy loams to boulders and gravels. In some areas fine sediments, dominated by silts and clays occur in areas such as former lake beds (Balks & O'Neill, 2016). Antarctic soils are like other desert soils, as precipitation exceeds evaporation in many areas, salts accumulate in the soil. Salts may be found dispersed through the soil, in discrete horizons or as incrustations in or on top of the soils (Balks & O'Neill, 2016). The mineralogy of the salts includes chlorides, nitrates, as well as sodium, potassium, calcium and magnesium sulphates (Campbell & Claridge, 1987). Soil moisture is generally low with moisture levels ranging from 1% ($0.013 - 0.015 \text{ m}^3 \text{ m}^{-3}$) in the McMurdo Dry Valleys to around 20-30% ($0.182 - 0.319 \text{ m}^3 \text{ m}^{-3}$) at the base of the active layer above the ice cement at some coastal sites (Seybold *et al.*, 2010).

The transition layer is increasingly becoming recognised as including the top of the permafrost (Bockheim & Hinkel, 2005). Continuous monitoring has allowed the detection of deep thaw events in the active layer during warm summers ((Bockheim & Hinkel, 2005; Bockheim, 2015; Bockheim *et al.*, 2015). Deep thaw events are those that thaw the transition layer in the permafrost with a temporal occurrence from sub-decadal to centennial (Bockheim & Hinkel, 2005).

Permafrost is defined as material that stays at or below 0°C for two or more consecutive years (Soil Survey Staff, 1999; Harris *et al.*, 1988). Depending on the moisture content for the soil, three types of permafrost may form; ice cemented; dry permafrost; and ice-cored moraine. Ice cemented permafrost is the most common (55%), followed by dry permafrost (43%) and ice-cored moraine (2%) (Bockheim *et al.*, 2007; Balks & O'Neill, 2016). Ice cemented permafrost has a moisture content of more than about 10%, and is difficult to dig through/ sample without a mechanical drill as the soil is cemented (Balks & O'Neill, 2016). Dry permafrost is found in some areas of Antarctica, particularly in old high-altitude areas, and on the dry valley floors. Dry permafrost forms when there is not enough water to form ice cement. The permafrost material remains loose and easy to excavate. To detect where the boundary between the active layer and the permafrost is careful temperature monitoring needs to be undertaken to detect the depth of maximum thaw each summer (Balks & O'Neill, 2016).

Ice-cored moraine forms where soil material accumulates over glacial ice. The overlying soil is formed from the “ablation till”, which is the rock material the

glacier has carried, and then left behind when the ice ablated. As the surface material thickens it eventually insulates the underlying ice from further ablation.

When stabilised from further melting soil can form in the ablation till and become strongly developed (Balks & O'Neill, 2016). Permafrost distribution can be broken into three types; continuous permafrost, which is found in Antarctica where permafrost underlies all terrestrial surfaces; discontinuous permafrost occurs in patches in the landscape, generally in heavily shaded areas, for example in the shadows of a mountain or under thick vegetation in the Arctic; and alpine permafrost, which occurs at high altitude in low latitude areas. The largest areas of alpine permafrost are in western China and the USA (Péwé, 1999).

Within ice cemented permafrost, ice bodies may form of which the shape and formation processes vary (Figure 2.2). There is often an ice-rich layer at the top of the permafrost in which condensed moisture has frozen at the permafrost interface (Balks & O'Neill, 2016); this layer, also called the primary ice vein, can be considered the maximum depth of thaw- with ice wedges extending from this into the transition layer (Lewkowicz, 1994; Bockheim & Hinkel, 2005). Ice formations in permafrost can be broken into five groups (Péwé, 1999):

- A. Pore ice; where pore water freezes in situ and no additional water enters the soil, creating ice cemented ground but no visible ice body;
- B. Segregated ice; which forms in layers or seams of ice up to 13 cm thick. Segregated ice forms from the soil surface down;
- C. Ice-wedges; where ice grows into the cracks of patterned ground, growing from the permafrost up into the transition zone
- D. Pingo ice; which forms in the horizontal lens developed from aquifers; and
- E. Buried ice, which can form from frozen seawater, river ice, or buried blocks from glaciers.

2.2.2 Antarctic soil formation

Five factors contribute, in varying degrees to soil formation in Antarctica. These are time; parent materials; climate; organisms; and relief (Jenny, 1941). In the central Trans-Antarctic Mountains soil formation started with rocks from the Precambrian with varying ages of material added through time (Cannone *et al.*, 2008; Seybold *et al.*, 2010). Local microclimate has been shown to be more influential in soil development than regional and environmental gradients, such as altitude (Cannone *et al.*, 2008; Seybold *et al.*, 2010).

Time

The dating of soil materials in Antarctica has included the characterisation of the weathering stage, with more weathered soils indicating longer time for soil development. Weathering stage is determined as a function of surface boulder frequency, relative abundance and the formation of soil salts and distinctiveness of soil horizons. The depths of each profile are also considered (Campbell & Claridge, 1987). The other main dating method utilises morphogenic salt assessment and electrical conductivity (Bockheim *et al.*, 2015).

Parent material

Some of Antarctica was formed in the Precambrian period; *i.e.* 4.5 billion years BP. Precambrian rocks underlie the majority of the Antarctic continent and are made up of gneisses and schists. The Trans-Antarctic Mountains have rock layers made up of the Beacon Group (Devonian – Jurassic), which characteristically are sandstone intruded with dolerites, beneath which lie Cambrian to Ordovician Granite Harbour intrusives (Bockheim *et al.*, 2015).

Transported soil parent materials are mainly of glacial origin, with some volcanic materials in the MDV and the South Shetland Islands, and debris flows in the east coast and the Antarctic Peninsula. Glacial products include tills, outwash, colluvium, and talus in varying amounts deposited over a long period. More recent volcanic activity in the Ross Sea region deposited scoria and a range of tephras in the immediate vicinity of Scott Base (Bockheim *et al.*, 2015).

Topography

The Antarctic continent can be divided into three climatic zones based on the climatological features. These are the Antarctic polar plateau, Antarctic slope, and Antarctic coast (Campbell & Claridge, 1987). Holdgate *et al.* (1977) recognised a fourth area as Maritime Antarctica, which encompasses the Antarctic Peninsula and its associated islands (Campbell & Claridge, 1987). The polar plateau is at high altitude, and is characterised by its high winds and low temperatures, while the coast has warmer and wetter conditions.

In Antarctica, the slope of a site plays the biggest topographic role in soil formation. An increasing slope accelerates the speed of weathering with the removal of weathered products, along with water and gravity (Campbell & Claridge, 1987). Changes in topography are the biggest driver in varying microclimates in the soil, such as large mountain chains acting as a barrier for incoming weather systems (Bertler *et al.*, 2004). Site aspect is also another important factor with north facing sites receiving more incoming solar radiation, allowing for warmer air and soil temperatures.

Organisms

Most soils in Antarctica do not support vascular plant life, due to them not being warm enough or having enough liquid water present. Soils with lichens and mosses are found in the Ross Sea Region, Antarctic Peninsula and the coastal areas in East Antarctica. In the Antarctic Peninsula areas exist where higher order plants have become established and have built higher carbon and nitrogen levels at the top of the soil profile. Organic nitrogen levels have been reported to reach up to 1.2% in the mineral surface below the humic layer (Campbell & Claridge, 1987). There is little detectable difference in physical and chemical weathering between soils with and without plant life. Most areas, particularly where soils with low soluble salt contents are found, while having no visible life, such as in the MDV, have an abundant microbiological community. The influence of microbial communities on the soil are virtually undetectable as these soils have extremely low organic carbon and nitrogen contents, and there are no detectable weathering differences between soils with, or without, abundant microbial communities (Campbell & Claridge, 1987).

Climate

Climate plays a major role in soil formation, and it has a greater influence on Antarctic soils than either time or parent material (Campbell & Claridge, 1987). Low amounts of solar radiation play a critical role in driving the atmospheric conditions, with the South Pole (90° latitude) experiencing only one true sunset and sunrise a year, and the whole Antarctic continent experiencing extended weeks or months of 24-hour darkness in winter. The lack of incoming solar radiation causes an extremely cold environment, as well as low humidity and precipitation amounts (Campbell & Claridge, 1987).

Due to the dark colour of the black scoriaeous ice-free land in some parts of Antarctica and extended periods of direct sunlight on the surface, it is not uncommon for soil surface temperatures of 14°C or higher to be seen with temperatures as great as 42°C being recorded in sheltered coastal areas (Campbell & Claridge, 1987). For soil formation, the length of time the ground is above freezing plays a key role, as most chemical weathering requires liquid water to occur. Soils in sheltered locations, with adequate soil moisture will develop faster than the surrounding area (Campbell & Claridge, 1987).

Long-lasting snow cover on the soil surface has a significant effect on soil temperature. In summer snow cover keeps the soil cool and reduces active layer depth by increasing the surface albedo which reduces the amount of incoming solar radiation. In winter snow cover will also insulate the soil, keeping it warm as heat exchange cannot occur between the soil and the air. These effects have been reported in the literature with a marked difference in temperature observed between snow covered soil, bare soil and air temperature (Guglielmin *et al.*, 2012; Hrbáček *et al.*, 2016).

2.2.3 Soil formation processes

There are several physical and chemical weathering processes which have helped to form the Antarctic soils present today processes include; salinization, rubification and cryoturbation. Physical processes which are more dominant include; abrasion, salt crystallisation and freeze-thaw action.

Salinization is the accumulation of soluble salt in the soil profile as soil moisture decreases. Rarely, the salt forms into a layer creating hard salt pans, which are not

easily broken with a spade (Bockheim & McLeod, 2006; Bockheim, 2015). In inland and high altitude areas, salt enriched layers usually occur a few centimetres below the surface, due to evaporation exceeding precipitation (Balks & O'Neill, 2016), whereas in coastal or sites with higher moisture salts are usually found as specks throughout the soil (Campbell & Claridge, 1987).

Rubification is a chemical process which changes the amount of redness in the soil (Oxford Dictionary, 2017). Otherwise known as staining, through the coating of rocks with weathered ferromagnesian minerals. The iron minerals come from within the rock and migrate to the rock surface before coating harder weathering resistant minerals, such as feldspar or quartz (Campbell & Claridge, 1987).

Cryoturbation is the movement of material due to frost action and is most identifiable from the observation of patterned ground in the environment. Cryoturbation occurs either through the contraction and expansion of rocks with changing temperature, causing cracking or through freeze-thaw action. Freeze-thaw weathering requires winter freezing of water in the active layer followed by thawing and subsidence allowing the material to move (Bockheim, 2015).

2.3 The Atmosphere

2.3.1 Introduction

The lowest layer of the atmosphere is the troposphere, which can be further broken into three layers (Figure 2.3), all driven by different atmospheric conditions. In the surface layer, airflow and structure are determined by surface topography and friction, solar radiation and air temperature (Kaimal & Finnigan, 1994). Kaimal and Finnigan (1994) defined the top boundary of the surface layer as 100 m theoretically, but this has some variance. Depending on the season, temperature, and if over land or sea. The outer layer can extend to a height between 500 m and 1200 m. The surface layer has a varying amount of shear stress caused by the landmass and is influenced more by regional conditions, such as synoptic circulation, and the Coriolis Effect (Kaimal & Finnigan, 1994).

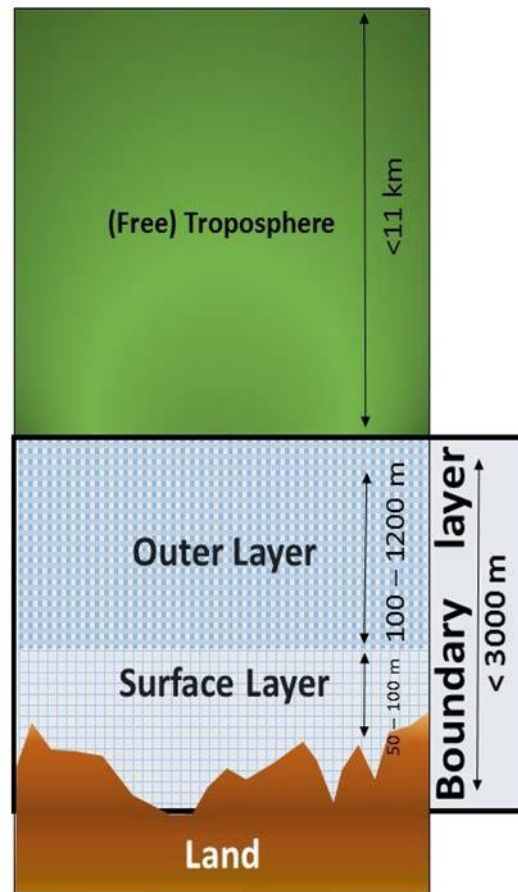


Figure 2.3: Schematic of the Atmosphere closest to the land surface, adapted from descriptions by Kaimal & Finnigan (1994).

The top of the boundary layer is usually well defined by a stable capped inversion layer. The turbulent surface (inner layer), and outer layer are not able to fully erode through the inversion layer (Garratt, 1994). Above the boundary layer is the Troposphere which is free from any effects from the surface.

2.3.2 Solar radiation

The Antarctic receives both short and long-term radiation, though the total amount received in Antarctica is less than in the tropics because of the low angle of the sun near the poles in summer and absence in winter. Radiation plays a key role in determining climatic conditions including; low-level temperature inversions, katabatic wind regimes; and the overall stabilisation of the atmosphere (King, 1997). Radiation on ice-free surfaces can lead to a strong temperature inversion within the first couple of micrometres above the surface; this is not possible to detect with an air temperature probe mounted at the standard height (King, 1997). Using a soil monitoring data set with a probe just below the surface could

be used as a proxy for this measurement. There is a large amount of variation in the amount of radiation that reaches the ground, six of the factors determining the amount are:

1. Aspect;
2. latitude and time of year;
3. elevation of the surface;
4. atmospheric water content;
5. amount of ozone;
6. amount of cloud; and
7. turbidity of the atmosphere, e.g. dust levels in the air (King, 1997).

The Albedo of the surface also plays a role in dictating the amount of radiation that will be absorbed by the surface, which leads on to heating of the surface. The albedo on bare ground measured at Bunger Oasis, East Antarctica, was 15% – 20% (Solopov, 1969; King, 1997) meaning that 15% – 20% of solar radiation will be reflected off the ground and 80% - 85% is absorbed.

2.3.3 Large scale climate patterns

Synoptic weather processes are large processes and have a far-reaching effect. In Antarctica, they are important for influencing the amount and distribution of precipitation (Noone et al. 1999; Noone & Simmonds 2002; Cohen *et al.*, 2013). Synoptic weather processes link closely to large-scale atmospheric circulation patterns such as the Southern Annular Mode (SAM) and the Southern Ocean Oscillation Index (SOI). The link between regional conditions and the SOI and SAM circulation indices is not fully clear, but they are known to have strong influences on the Antarctic atmosphere. The SAM plays the greatest role in dictating the regional circulation patterns in Antarctica from short to inter-annual or longer time scales (Cohen *et al.*, 2013).

The Southern Annular Mode (SAM) and its associated index (SAMI) is based on the zonal pressure difference between the 65° S latitude and the 45° S latitude (Marshall, 2003) and is controlled by the expansion and contraction of the polar vortex (Thompson and Wallace, 2000; Cohen *et al.*, 2013). The SAM can describe 30% of the Southern Hemisphere's weather patterns. The positive phase of the SAMI relates to when there are high-pressure systems over Antarctica and low-

pressure systems over the high latitude areas (65° S), and the negative phase has the opposite orientation (Marshall, 2003).

The Southern Ocean Oscillation and its index (SOI) are a measure of the pressure difference between the east and west sides of the Pacific Ocean. Observational measurements are taken in Darwin, Australia and Tahiti. A positive difference in the values is defined when there are high-pressure systems in the west (Tahiti) and is known as “La Nina”. A negative difference occurs when there are high-pressure systems over the east Pacific (Australia) known as “El Nino” (Ropelewski & Jones, 1987).

2.3.4 Regional climate patterns

The Ross Sea region is dominated by a permanent, seemingly stationary region of low pressure, known as the Amundsen Sea Low (ASL). The ASL stretches across the South Pacific Ocean between the Ross Sea and the Antarctic Peninsula (Hosking *et al.*, 2013), approximately between 60°S and 75°S (Cohen *et al.*, 2013). Variations in the ASL strongly influences the West Antarctic atmospheric circulation and climate including the wind velocity, precipitation, sea ice concentration, and near-surface (2 m) air temperature (Turner *et al.* 2009; Küttel *et al.* 2012; Hosking *et al.*, 2013). The ASL shows seasonal movements shifting generally towards the Antarctic Peninsula in summer and autumn (December to May) and centring over the Ross Sea in winter and spring (June to November). The ASL is influenced by larger climate systems and shows a strong correlation with the SAM and SOI in spring (Cohen *et al.*, 2013).

2.3.5 Local meteorology

Antarctica, and in particular the MDVs, are impacted by a range of wind types, which greatly influence temperature, moisture levels, and air movement (or lack thereof). Topography plays a major role in the speed, direction and frequency of wind at each site. Thus there are large differences in wind regimes between sites that are close to each other. Regional circulation patterns, particularly cyclonic activity (Campbell & Claridge, 1987) also play a role, as do other atmospheric processes, such as solar radiation and temperature.

Katabatic winds are defined as gravitational forced cold winds flowing from the high polar plateau down into the coastal environment. In general, the steeper the

slope, the greater amount of cold air will flow, until stabilisation through friction retardation is reached (Schwerdtfeger, 1984). Katabatic winds flow off the polar plateau and mix up the cold air cells in the valleys (Doran *et al.*, 2002a). Anabatic winds are warm gentle winds that flow up slopes or up a valley. In the MDVs, anabatic winds dominate in summer, as coastal winds (McKendry & Lewthwaite, 1992).

Foehn winds are the result of alteration in the wind flow on the lee side of a mountain barrier. For a foehn event to occur, airflow needs to be within 30° perpendicular to the ridgeline and have a steep pressure gradient between each side of the mountain range (Speirs *et al.*, 2013). In Antarctica, foehn winds have been attributed to rapid temperature changes of greater than 40°C particularly in winter and like katabatic winds, foehn winds will break up the cold inversion layers. Strong outer layer flow deflected into the valley system causes foehn winds in the MDVs, which then flow into the adjacent coast. The outer layer winds are by caused by deepening low surface pressure in the Ross Sea (Speirs *et al.*, 2013).

2.3.6 Precipitation

The amount of precipitation varies across Antarctica, with the interior (namely MDVs) receiving much lower amounts of precipitation compared to the coast. Wall (2004) identified around five summer wetting events a year at coastal sites compared to one event in the Wright Valley over a three-year period. Variation in precipitation in the Ross Sea Region has been attributed to variation in the Amundsen Sea Low (Turner *et al.*, 2009; Küttel *et al.*, 2012; Hosking *et al.*, 2013). In the MDV's and other interior sites evaporation exceeds precipitation, which is similar to other desert soils (Balks & O'Neill, 2016). In the MDV's snowfall amounts are increased at higher altitudes and at the eastern and western ends of the valleys, compared to the centre of the valleys. The lowest recorded mean annual precipitation was 45 mm at Lake Vanda in the Wright Valley (Campbell & Claridge, 1987; Balks & O'Neill, 2016). Snowfall generally sublimates within two hours in the MDV's (Balks & O'Neill, 2016).

At the coast precipitation events occur all year round, with snow accumulating in the winter, where later snowmelt is identifiable in soil moisture monitoring (Balks & O'Neill, 2016).

2.3.7 Microclimate

The microclimate responses to local and regional weather changes are amplified due to the lack of relative humidity, soil moisture and surface vegetation. The microclimate can quickly adjust to changing atmospheric conditions, with air temperature showing a close to instant response to changes winds or incoming radiation, compared to the lagged effect in soil (Katurji *et al.*, 2013). The soil takes longer to adjust to atmospheric changes due to its physical properties and the soils ability to absorb and hold heat (Katurji *et al.*, 2013).

Shading occurs where the Antarctic topography blocks the sun; this effect can mimic early evening transition period conditions through the loss of direct light. The Early Evening Transition Period (EEP), is defined as occurring when one of the following occurs: wind surface speed and variance decrease, sensible heat flux changes from ground heating to ground cooling; near-surface water vapour increases; or the surface layer is no longer linked to the outer layer caused by a decrease in downward transfer of horizontal motion (Katurji *et al.*, 2013). Studies in the Miers Valley found that the following a change in incoming solar radiation, a small change in air temperature (2°C) was detectable within a few minutes. In comparison, soil surface temperature dropped by between 8°C and 10°C over two-to-three hours, in response to shading. This is because the surface temperature is affected by the absorption of solar radiation, so it takes time once shading starts to release the balance of the heat flux. While air temperature is more greatly affected by wind speed, which reduces to close to 0 ms⁻¹ on shading (Katurji *et al.*, 2013).

2.4 Soil thermal properties and processes

2.4.1 Introduction

While atmospheric conditions are the drivers of changes in active layer temperature, they are not the only factors controlling the dynamics of soil temperature. The mineral properties and soil structure along with water content are key factors that alter how heat moves through the soil profile (Wilhelm & Bockheim, 2016). It is important to understand how heat travels and behaves in the soil, to accurately study, assess for trends, and model potential changes in soil climate. The changes in the

soil climate impacts both life within the soil as well as abiotic processes such as soil weathering (Hartge, 2016).

2.4.2 Heat transfer

Soil temperature is controlled by two properties, how much heat energy is needed to increase the soil temperature by a specific amount, and the soil materials ability to conduct heat downwards (Hartge, 2016). The main source of incoming heat to the soil is net solar radiation (Figure 4); net solar radiation being the long-wave radiation not reflected by the earth back into the atmosphere (Shukla, 2014). The ability of the soil to reflect short-wave radiation is known as albedo, with lighter coloured surfaces (higher albedo) reflecting more energy. Fresh snow has the highest albedo with 80 – 90% of incoming radiation being reflected back to the atmosphere, while sand can reflect between 20-45% depending on moisture content and parent material (Gates & Hanks, 1980; Shukla, 2014).

The heat energy absorbed by soil from the net solar radiation can be partitioned into three (Figure 2.4); sensible heat flux, latent heat flux, and soil heat flux. A diurnal pattern generally occurs with sensible and latent heat flux higher at night, and soil heat flux higher during the day (Shukla, 2014).

Sensible heat flux is the removal of heat through the movement of warm air from the shallow soil and soil surface to the cooler atmosphere. Latent heat flux is the energy associated with a change in state of soil water, either through evaporation (liquid water to gas state), condensation (gas to liquid water), freezing (liquid water to ice) or through sublimation (ice to gas state) to the atmosphere (Shukla, 2014). In Antarctica, and other areas of soil that are influenced by freezing and thawing, the latent heat flux dominates the heat flow, though sensible and soil heat fluxes play a role, thus in modelling it is important to account for the movement of water out of the soil (Riseborough *et al.*, 2008).

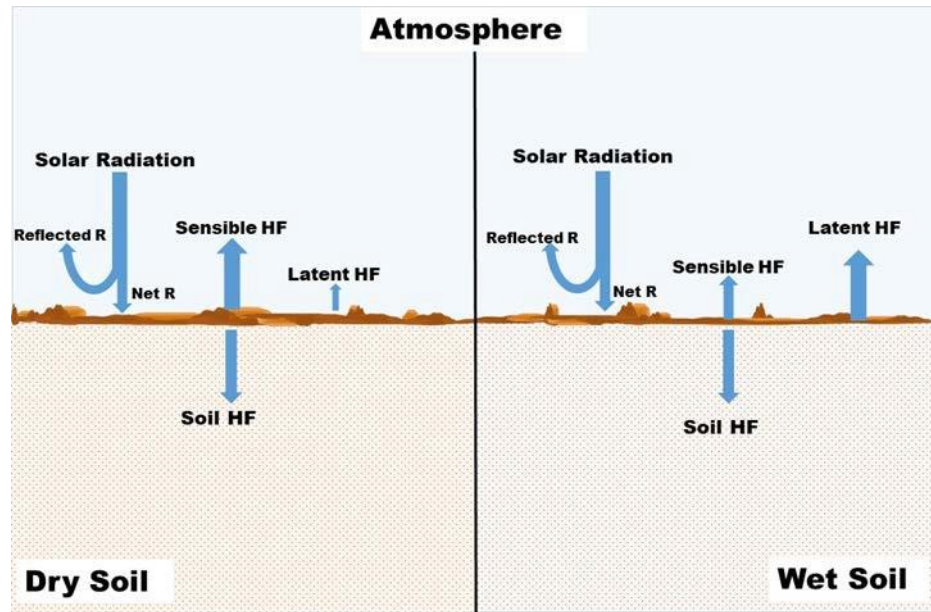


Figure 2.4: The net change in heat storage per flux type in wet and dry soils, with the arrows size denoting the relative amount of heat movement. Note the difference in sensible and latent heat flux between dry and wet soils. Adapted from (Shukla, 2014)

Soil heat flux is the movement of heat into the soil profile from the surface (Sauer & Horton, 2005). The ability of a soil to move heat down the profile determines how variable the change of temperature in the soil is during the day and between seasons (Sauer & Horton, 2005). The soil heat flux is controlled by three key parameters, which are all interconnected, these are thermal conductivity, thermal diffusivity, and volumetric heat capacity (Hartge, 2016). The methods of heat movement in the soil are also needed to understand the propagation of the soil heat flux.

2.4.3 Soil thermal properties

Heat capacity, thermal conductivity and diffusivity are well linked, and knowing two of these parameters can allow for the calculation of the third, using the equation:

$$\lambda = \alpha * C_v \quad (2-1)$$

where λ represents thermal conductivity, α represents thermal diffusivity and C_v represents the volumetric heat capacity (Hartge, 2016). The heat capacity of a soil is found through the calculation of the volumetric heat capacities of the fractions that make up a soil profile; air, water, and mineral substrate. With the definition of volumetric heat capacity being:

“The amount of heat that will lead to a temperature increase of 1°C of a unit volume (m³) of soil.” (Hartge, 2016, p. 202)

The heat capacity of a soil will vary considerably with changing water content, because of the high specific heat of water 4.19 MJ/(m³ °C) compared to the low specific heat of air 0.00126 MJ/(m³ °C) (De Vries, 1963; Hartge, 2016).

Heat capacity changes when soil freezes for two reasons: a volume increase of about 9 % occurs; and the volumetric heat capacity of ice [1.88 MJ/(m³°C)] is lower than that of water (De Vries, 1963; Hartge, 2016). The transition from water to ice does not occur directly at 0°C, rather somewhere between the freezing point and -20°C, with the level of supercooling increasing with increasing clay or salt content ((Hoekstra, 1965; Hartge, 2016).

The conduction of heat is defined as the amount of heat energy (J s⁻¹), which in a steady state, travels across 1 m² and a distance of 1 m at a temperature gradient of 1°C/m (Hartge, 2016). The thermal conductivity of a soil depends on the makeup of the solid fraction, and the interfacial contact between solids and between solids and water or air. As porosity increases thermal conductivity decreases (Shukla, 2014).

Thermal diffusivity is the measure of the rate at which heat dissipates through a profile and through time (Correia *et al.*, 2012). The thermal diffusivity is defined as the ratio between thermal conductivity and heat capacity. The greater the thermal diffusivity the faster heat travels through a material (Hartge, 2016).

2.4.4 Heat movement processes

The movement of heat through the soil usually involves transfer through conduction from warmer layers to cooler layers. Heat movement is consequently usually downward in summer due to solar radiation warming the surface, and upwards in winter when the air temperature cools below the mean annual temperature maintained at depth.

Heat transfer direction can, and often does, change direction diurnally as well. Heat flow in the soil is directly related to the heat capacity and thermal conductivity of a soil, which are influenced by the bulk density and water content (Shukla, 2014). Other influences include; soil compaction, snow cover,

vegetation, and topography (Shukla, 2014). The three principles of heat flow are radiation, conduction and convection.

Thermal radiation can come from all material that is warmer than zero Kelvin, through electromagnetic waves (Shukla, 2014). The transfer of energy through radiation plays a significant role at the surface, but within the soil profile, heat flow by thermal radiation is insignificant (Hartge, 2016).

Heat transfer by conduction is the flow of heat through direct contact, either between molecules of the same substance or between different substances within direct contact of each other. Thus, in the soil, heat is conducted through the direct contact of solid soil particles with each other (Shukla, 2014). Increasing soil compaction or bulk density will result in improved, and faster, conductive heat flow. While increasing porosity will give a decrease in the thermal contact between solids and a decrease in the ability for heat to be transferred through conduction (Shukla, 2014).

Convection is the transfer of heat through the movement of fluids, either air or water, within the pore space of the soil, and is the dominant process globally (Shukla, 2014). The movement of heat by convection is slower than the conduction of heat (Blanco et al., 2007; Gruber and Haeberli, 2007; Wilhelm & Bockheim, 2016), except where movement is through very coarse material, where meltwater can travel quickly through a profile (Humlum, 1997; Wilhelm & Bockheim, 2016). It is thought that conduction is the main heat flow process at low temperatures, e.g. below freezing (Hartge, 2016), and in cold environments. In polar environments non-conductive heat transfer methods, via water and water vapour are significant and at times the dominant method of heat transfer in the soil (Kane *et al.*, 2001), such as in spring and summer within the active layer where there is little snow cover, and soil water is in a liquid state (Ling and Zhang, 2003; Wilhelm & Bockheim, 2016).

In practice, heat transfer is often a combination of conduction (between molecules) and convection (fluid movement), with heat transferring from fluids to solid particles as it moves down the profile. Heat transfer via pure convection is more important in understanding atmospheric heat movement than soil heat movement (Shukla, 2014).

Along with heat transfer theory, other physical processes also influence the near soil surface temperature in frozen soils. These include pore water pressure, solute concentration gravity and other similar gradients (Kane *et al.*, 2001)

Two phenomena that are the result of heat transfer in the soil are the damping effect and the phase lag effect. The damping effect is seen with the amplitude of the temperature propagation wave decreasing with depth (Figure 2.5), this is caused by the absorption and release of heat by the soil material as temperature progresses downwards (Hillel, 2003). The amplitude of the wave at any depth can be calculated by finding the difference between the maximum (or minimum) temperature and the mean temperature; with the difference between the maximum and mean decreasing with depth.

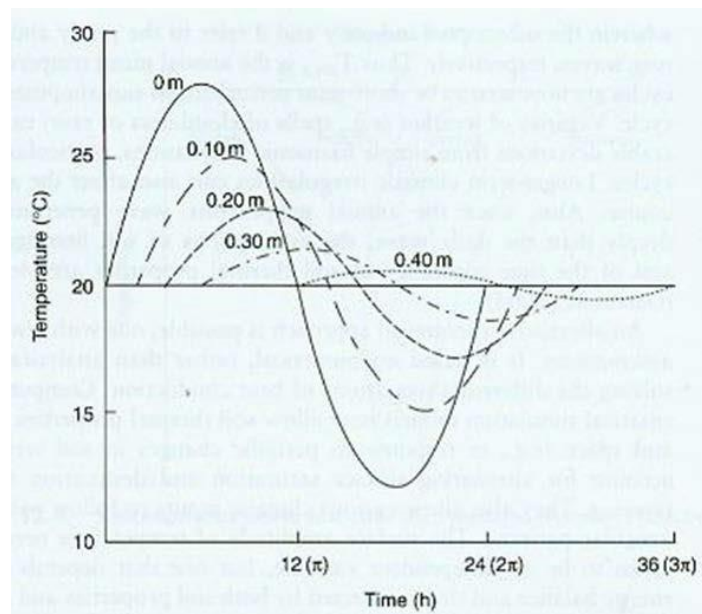


Figure 2.5: Simplified diagram of variation in soil temperature through time with increasing depth. Illustrating the phase lag and attenuation (dampening) of the temperature signal as depth increases (Hillel, 2003)

The rate of decreasing temperature amplitude and the speed that the signal travels depends on the thermal properties of the soil and on the frequency and pattern of incoming solar radiation (Smerdon *et al.*, 2006). The diurnal wave reaches depth of zero amplitude, the point where there is a negligible difference between the mean and maximum temperature, approximately 50 cm, depending on the site conditions (e.g. Balks *et al.*, 1995; Thompson *et al.*, 1971, as cited in Adlam 2009; Shukla, 2014; Florides & Kalogirou, 2019). The annual depth of zero amplitude,

where a seasonal cycle can no longer be detected varies widely, from between 15 to 20 m in the Arctic (Linell & Tedrow, 1981), to 10 and 11 m in Northern Victoria Land, Antarctica (Guglielmin, 2006) and greater than 25 meters in the McMurdo Dry Valleys, Antarctica (Guglielmin *et al.*, 2011). The depth of annual zero amplitude can be estimated, assuming thermal diffusivity does not change with depth using the equation proposed by Carslaw and Jaeger (1959, as cited in Guglielmin, 2006):

$$ZAA(m) = (\pi k P)^{1/2} \quad (2-2)$$

Where ZAA is the depth of zero amplitude (m), k is the thermal diffusivity (m^2s^{-1}) and P is 1 year/s (Guglielmin, 2006). The term depth to zero amplitude in practices is reliant on the accuracy and preciseness of data collected. For this reason (Adlam, 2009) proposed that instead of referencing the depth of zero amplitude, the depths where the temperature amplitude was $< 1^\circ C$, $< 0.5^\circ C$ and $< 0.1^\circ C$ are reported instead. Using this new scale Adlam (2009) found an amplitude of $< 1^\circ C$ around 15 m, at $< 0.5^\circ C$ around 17.5 m and at $< 0.1^\circ C$ around 26 m (Guglielmin *et al.*, 2011).

2.4.5 Freezing, ice formation and water movement

The formation of ice in soil is a complex process, and depends on water availability, pore size, and both matrix and external pressure. When ice forms, under standard conditions, the water expands, and takes up approximately 9% more volume (Shukla, 2014).

2.5 Previous findings

2.5.1 Antarctic Peninsula

Monitoring of soil climate and permafrost on the Antarctic Peninsula started to in the late 1950's. Oliva *et al.* (2017b) undertook a project reassessing previously published trends across ten sites situated along the Peninsula and in the surrounding islands, with the additions of more recent data. The warming trends between 1960 and the early 1990's was correlated with warming temperature trends and deepening of active layers. Further data analysis of newer data showed that

between the 1990s and early 2000's any deepening of the active layer was reversed by a cooling trend, with cooling ongoing until 2015 (Oliva *et al.*, 2017b). The thinning of the active layer was thought to result from cooler conditions and increased snow cover keeping soil temperatures low (Oliva *et al.*, 2017b). The short stretch of time that Oliva *et al.* (2017b) covered (20 years) likely shows a short-term cycle rather than trends in warming or cooling. Oliva *et al.* (2017b) noted that the average trend did not occur at all sites, with sites in the N- NE of the Antarctic Peninsula having a greatly pronounced cooling effect while at sites in the SW of the Antarctica Peninsula showed only inter-season variation in permafrost temperature. There has been no cooling trend in other fields of measurement, for example, sea ice or atmospheric temperatures (Oliva *et al.*, 2017b).

Atmospheric warming trends were identified in the 20th century, across the continent (Vaughan *et al.*, 2001; Steig *et al.*, 2009; Schneider *et al.*, 2012; Bromwich *et al.*, 2013; Oliva *et al.*, 2017b). However, a cooling between 1999 and 2014 was also documented (Turner *et al.*, 2016) and a decrease in ALD in the Antarctic Peninsula has been reported between 2006 and 2014 (Goyanes *et al.*, 2014; Hrbacek *et al.*, 2016 Ramos *et al.*, 2017; Oliva *et al.*, 2017b). Evidence has suggested that one driver of short term cooling in Antarctica is in the Southern Oscillation when in an El Niño phase (Bertler *et al.*, 2004).

In the western coastal Antarctic Peninsula, a decrease in ALD was reported between 2006 and 2014. It was suggested that the trend was due to increased snow cover, since no trend in mean annual air temperature was noted (Ramos *et al.*, 2017). Other Antarctic Peninsula sites showed high inter-year variation and it was suggested that further monitoring would be needed to assess if long term change to ALD was occurring (Almeida *et al.*, 2017; Hrbáček *et al.*, 2017; de Pablo *et al.*, 2018).

Historic warming has been detected across Antarctica from ice-cores and other paleotemperature proxy records. The Medieval Climate Anomaly (MCA), the period between 1000 – 1200 CE, had distinct climate fluctuations which were documented around the world, as a phase of pronounced warming (Lüning *et al.*, 2019). Antarctica was generally warmer in the MCA when compared to the Little Ice Age, with warming trends identified in the Sub Antarctic Islands, the Antarctic

Peninsula, Victoria Land and central West Antarctica Lüning *et al.*, 2019). The MCS and other multi-centennial scale variability in climate seems to be driven by the Southern Annular Mode and the Southern Oscillation Index (Lüning *et al.*, 2019).

2.5.2 Ross Sea Region

Investigations into soil temperature, and permafrost and soil moisture content were undertaken at three sites in the summers of 1992/1993 and 1993/1994 by (Balks *et al.*, 1995). At Scott Base, mean January soil temperatures across a ten-day period ranged between 1°C & 6°C at the soil surface, 3°C & -1°C at 15 cm and -2°C & -1°C at 60 cm. Marble Point soil temperatures ranged between +15°C and -34°C between January 1993 and January 1994. Variation in summer solar radiation saw steep fluctuation of soil near-surface temperature at Marble Point and Scott Base. In winter periods of warming of up to 15°C was likely due to winter storms mixing the inversion layer. At the Beacon Heights site, which is about 600 m above the Taylor Glacier, temperatures ranged between 3.5°C and 1°C at the surface, to between -9.5°C and -10°C at a depth (Balks *et al.*, 1995).

In the Ross Sea region, both warming and cooling soil temperature trends have been reported. A cooling trend in the MDV was reported between 1986 and 2000 (Doran *et al.*, 2002b). While warming with thickening ALD was reported in northern Victoria Land after 2000 and was attributed to increased incoming solar radiation (Guglielmin & Cannone, 2012).

Current day Ross Sea region soil climate monitoring network

The ice-free area of interest for this project is situated in central Victoria Land, where nine soil climate-monitoring stations have been set up (Figure 2.6). The four most far-reaching points are; Granite Harbour in the north, Minna Bluff in the south, Mt Fleming in the east, and Scott Base in the west. The SCS stations form two transects. An altitudinal transect starting at Mt Fleming (1700 m), through the North and South Wright Valley Walls, Victoria Valley, and Wright Valley Floor, cumulating at Marble Point. The second, a latitudinal transect, extended from Minna Bluff in the south through Scott Base, Marble Point, to Granite Harbour in the north.

Adlam (2009) and Goddard (2013) previously studied the soil climate data of the Ross Sea region network. The results from these two efforts were MSc theses, as well as one published paper and several conference publications. Both Adlam (2009) and Goddard (2013) used seven of the current stations, with Goddard (2013) also including data from Cape Hallett and Darwin Glacier (Not pictured). Since Adlam (2009) and Goddard (2013), two new soil climate stations have been established on the Wall of the Wright Valley in the summers of 2011 and 2012 (Figure 2.6). Adlam (2009) reported that ALD calculated using the SCS network decreased with increasing altitude ($R^2=0.95$) and increased with decreasing latitude ($R^2=0.94$).

Goddard (2013) and Adlam (2009) had slightly different focuses in their research. Adlam (2009) worked to find trends in soil climate and potential correlations of these to atmospheric climate data. While Goddard (2013) characterised wind speed and air and soil temperatures, followed by an investigation into any trends. Key findings of similarity between Goddard (2013) and Adlam (2009) included the lowest winter temperatures recorded at Victoria Valley, while not stated by Goddard (2013), Adlam (2009) put this down to being due to strong inversion layers at Victoria Valley and fewer winter storms.

Adlam (2009) did not find any long-term trends of warming or cooling at any of the sites with R^2 of 0.20 for air temperature and an R^2 of 0.27 for soil temperatures. Goddard (2013) found significant trends ($p < 0.05$) in air ($R^2 = 0.59$) and shallow soil ($R^2 = 0.61$) temperatures at Marble Point and in shallow soil (5.5 cm) temperature at Granite Harbour ($R^2 = 0.72$). Though caution was advised when interpreting significance at Granite Harbour due to the potential impacts meltwater at the site had on shallow soil temperatures. No other trends were found at the other seven sites studied (Goddard, 2013).

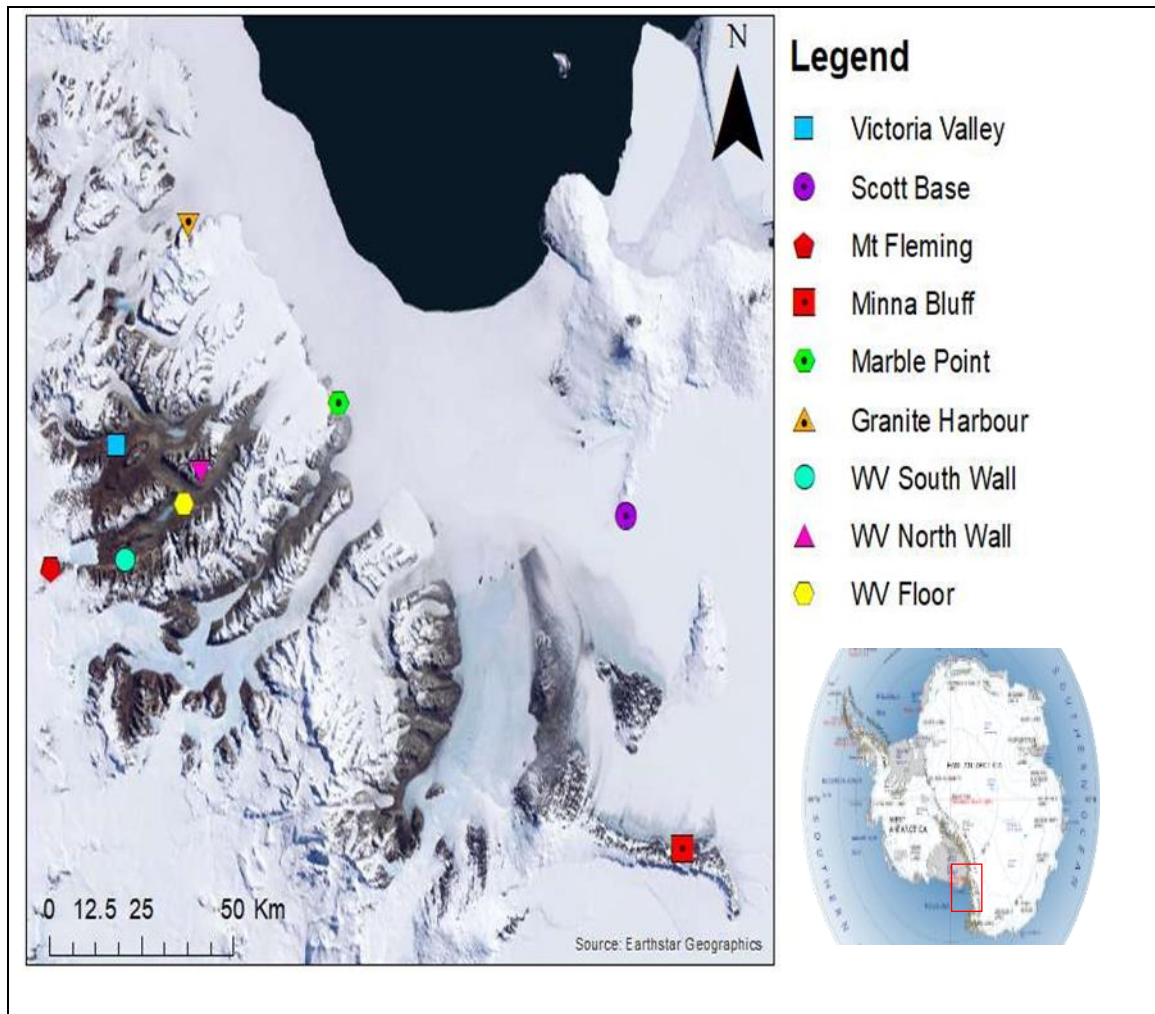


Figure 2.6: Soil climate monitoring network based in the McMurdo Dry Valleys and the surrounding Ross Sea Region, Antarctica.

Soil moisture contents were studied by Seybold *et al.* (2010) using ten years of data from the soil climate monitoring network. Mean volumetric soil moisture contents were lowest in the surface soils of the MDV with a mean range of 0.013 – 0.015 $\text{m}^3.\text{m}^{-3}$, and highest at Scott Base and Granite Harbour, near these soils ice-cemented layers, with a mean range of 0.182 – 0.319 $\text{m}^3.\text{m}^{-3}$. Balks *et al.* (1995) reported very low (1.1 % by weight) moisture contents near Lake Vanda. At Beacon Heights, the moisture content above the ice-cemented layers averaged 1.5%. At Scott Base moisture content approached 100% when approaching the permafrost boundary.

Moisture contents correlated to the mean air temperature (R^2 0.76) and relative air humidity (R^2 0.68). There was a weak relationship between soil moisture content and latitude with local microclimate and topography having a greater influence.

When all the sites are compared decreasing moisture content correlated with increasing elevation, and with increasing distance from the coast (Ugolini & Bockheim, 2008; Seybold *et al.*, 2010). Moisture content increased with depth at Lake Vanda, Beacon Heights, and Scott Base (Balks *et al.*, 1995).

Up to five soil moistening events (Rainfall, snow melt) were identified at Scott Base and Marble Point each summer between 1999 and 2002. While one soil moistening event was identified over the same period on the Wright Valley Floor (WVF) (Wall, 2004). During these events, volumetric liquid moisture contents increased by between 6% at the WVF, 23% at Scott Base, and 32% at Marble Point. The drying period on average was six days for surface soils, which extended to twelve days when freeze-thaw cycles were occurring (Wall, 2004).

2.6 Trend detection

The accepted best practice in assessing climate data for trends was to assess a minimum of 30 years of data. The 30 year period to allows for normalisation and the ability for findings to be easily compared throughout the world (WMO-No.100, 2018). However, a 30-year period is not generally the most optimal to study many variables, with temperature trends detectable in shorter time frames, while precipitation trends needing longer time frames. A 5 – 10 year period of temperature data was found to have a similar predictive ability as a 30 year period (WMO-No.100, 2018).

There are many methods to look for trends and patterns in the time series, depending on the number of data points and the type of data present. In this thesis Non-Parametric (Mann Kendal) trend testing was undertaken, as linear regression assumptions did not hold (Figure 2.7) Cross-correlation using wavelets was also used which allows for the comparison between site-specific data and both continental and regional synoptic weather patterns.

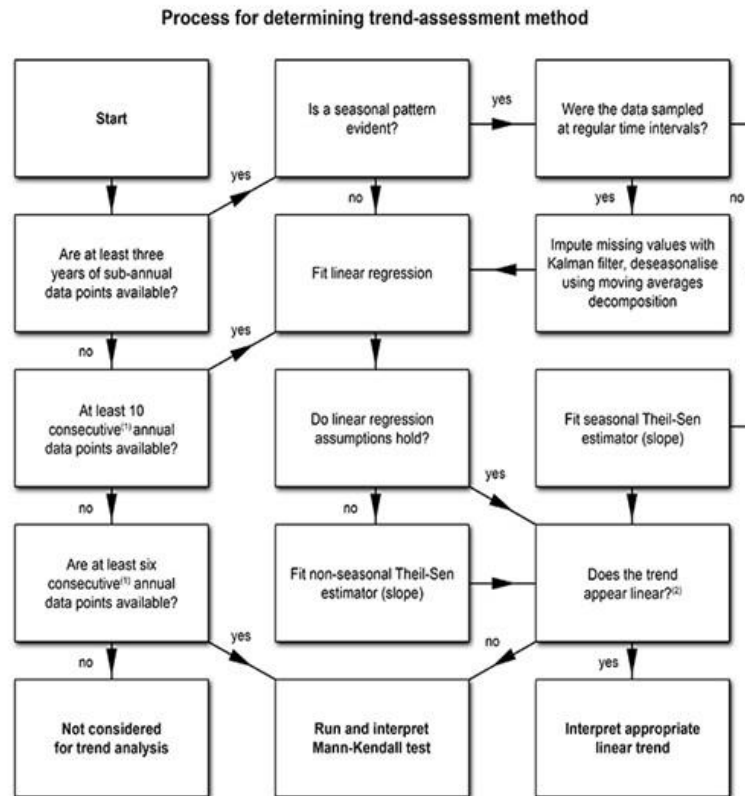


Figure 2.7: Schematic flow chart developed by the Ministry for the Environment and Statistics NZ (2017) for trend assessment decisions.

The Mann-Kendal test is a non-parametric (distribution-free) test, that looks for both upward and downward monotonic trends through time, resulting in a null hypothesis being accepted or rejected for a set significance threshold. The Tau-b test measures the strength and direction of the relationship between pairs of variables, such as time and ALD, with results ranging between 1 (perfect association) and -1 (perfect reversed association), with 0 indicating no relationship (Agresti, 2010).

Wavelet and cross wavelet analysis allows for the comparison between site-specific data and both continental and regional synoptic weather patterns

Wavelet

Wavelet and cross wavelet analysis allow for the study of time dominated data sets to be studied at multiple time and frequency scales simultaneously. The wavelet analysis transform allows the signal to be manipulated in frequency (occurrence rate) and can identify the occurrence of both high and low-frequency signals through the use of flexible windows (Figure 2.8), to create narrow windows appropriate for

high-frequency signals and wide windows for low-frequency signals or background noise. To compare the cross wavelets of different time series, the wavelet function is normalised to have a “unit energy”. The more active a signal at a particular period/frequency, the higher the unit energy. A unit energy greater than a value of one is deemed to be more significant than white noise (Lau & Weng, 1995).

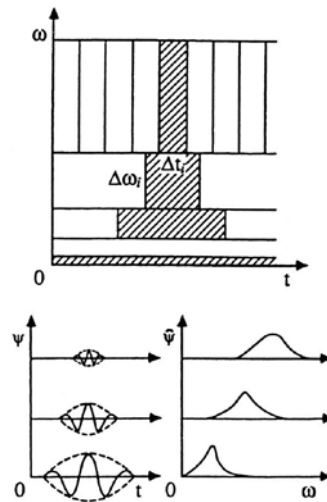


Figure 2.8: Schematic of wavelet transform windows top, and the corresponding time series represented in time and frequency space (Lau & Weng, 1995).

Wavelet analysis has been used successfully to study climate drivers and their relationship to Antarctica (Torrence & Compo, 1998; Grinsted *et al.*, 2004; Hosking *et al.*, 2016).

2.7 Soil climate predictive models

2.7.1 Introduction

A model uses various input variables to create a mathematical representation of an observed phenomenon. Models are particularly useful to test a range of hypotheses and scenarios (Riseborough *et al.*, 2008), or by allowing for the interpolation of data where real-life observations are not possible. Both uses are valuable in Antarctica due to the expensive nature of Antarctic science, along with the limitations the extreme climate poses. Scientists understand the value that

studying the Antarctic soil climate, and its implications in the current global climate extremes. The ability to model the potential changes to the permafrost can allow for better management and monitoring of climate change at a large scale.

The atmospheric climate has been monitored since the beginning of Antarctic exploration; research and continuous long term records are available from the 1950's (Martin, 2016). Atmospheric monitoring is spread across the continent with many more sites are in action compared to the number of soil-climate monitoring sites.

Remote sensing and the increasing data volumes, together with high resolutions, allow for modelling the permafrost depth and changing soil climate at a regional and continental scale. Furthermore, these data allow more accessible continuous monitoring, though without easy access to comprehensively ground-truth the findings the results must be questioned. Satellite-derived surface temperature data was assessed for accuracy across the Miers Valley, Antarctica in 2009. A reliable relationship was found for all four Landsat 7 data sets studied (January, February, March, and November), compared to 45 in-ground sensors with an $R^2 = 0.9$ and $p < 0.001$ (Brabyn *et al.*, 2014). The relationship found in the Miers valley is consistent with Suga *et al.* (2003), giving support to satellite data as a reliable method of determining surface temperature, where vegetation is limited (Brabyn *et al.*, 2014).

Models can be divided into several categories, each with their distinct uses, advantages and limitations: these include: numerical, empirical, and spatial modelling. As with all modelling, it is important to remember the adage that “all models are wrong, some are useful” when interpreting the findings. The usefulness of a model should be assessed on how well it fits its purpose and how user-friendly it is. A simple model can be more useful as it requires less data, while a sophisticated model requires more data to produce credible results (Riseborough *et al.*, 2008).

2.7.2 Empirical Modelling

Empirical models use one or more known variables to predict what an unknown variable will be. There is a range of statistical methods to assess the relationship between the known and unknown variables and to produce an equation from a

model. Easily measured topographic and climatic variables are used in permafrost analysis, though some models will also use soil climate variables. Empirical models normally assume that the variables are in equilibrium (Riseborough *et al.*, 2008). There are three well-known models, used to predict the depth and distribution of permafrost, which vary in complexity, these are the Stefan Model, Kudryavtsev Model, and the Top of the Permafrost Model (TTOP) (Riseborough *et al.*, 2008).

Stefan model

The Stefan equation (Lunardini, 1981) is the most widely used in permafrost modelling, where the solution predicts the boundary between the permafrost and active layer (Equ 2-3). The idea behind the equation is that when the thermal diffusivity changes are small compared to the rate of the front movement and the initial temperature of the ground is around 0°C. The equation can be simplified to:

$$X = \sqrt{\frac{2 \lambda I}{L}} \quad (2-3)$$

Where X is the thaw depth (m), λ is the thermal conductivity ($\text{W}\cdot\text{m}^{-1}\cdot\text{K}^{-1}$), I is the accumulated ground surface degree-day total (either the freeze or thaw index) ($^{\circ}\text{C}$) and L is the volumetric latent heat of fusion ($\text{J}\cdot\text{m}^{-3}$) (Lunardini, 1981; Riseborough *et al.*, 2008). The simplified Stefan equation above (Equ 2-3) has been used widely to characterise the active layer spatially by estimating the soil properties, and empirically using summer temperature (e.g. Nelson *et al.*, 1997; Shiklomanov and Nelson, 2003; Zhang T. *et al.*, 2005; reported in Riseborough *et al.*, 2008).

Kudryavtsev Model

The Kudryavtsev Model (Kudryavtsev *et al.*, 1977) is a more complex model that has become commonly used through time, which predicts active layer depth (ALD) and the mean annual permafrost temperature. The Kudryavtsev model utilises surface temperature, soil properties, and air temperature variables and studies have indicated that it provides a more accurate estimate of the maximum ALD (Romanovsky and Osterkamp, 1997; Shiklomanov and Nelson, 1999; Riseborough *et al.*, 2008). The Kudryavtsev Model has been successful at creating spatial models of active layer depth (e.g. Romanovsky and Osterkamp, 1997; Anisimov *et al.*, 1997; Shiklomanov and Nelson, 1999; Sazonova and Romanovsky,

2003; Stendel *et al.*, 2007; reported in Riseborough *et al.*, 2008). The Kudryavtsev Model relies on the assumption that the periodic steady-state will remain with phase change (Kudryavtsev *et al.*, 1977; Riseborough *et al.*, 2008).

TTOP Model

The top of the permafrost (TTOP) model, developed by Smith *et al.* (1996) measures the mean annual temperature at the boundary of the permafrost and the active layer. The top model utilises the understanding of the modelled thermal offset effect, where the mean annual temperature is affected by the differences between frozen and thawed soil thermal conductivity (Romanovsky and Osterkamp, 1995; Riseborough *et al.*, 2008). The TTOP model also uses freezing and thawing indices of the lower atmosphere and ground surface through the utilisation of n factors, which are related to degree-day totals for freezing or thawing (Lunardini, 1978; Riseborough *et al.*, 2008). The TTOP model has been shown to be reasonably accurate, at a resolution of 1 km² with work in the arctic, with the boreholes to ground truth model results (eg Wright *et al.* (2003); Riseborough *et al.*, 2008).

Previous modelling work in Antarctica applied the Stephan Model and Kudryavtsev Model to three sites between 2011 and 2014 across the Western Antarctic Peninsula, with reasonable success (Wilhelm *et al.*, 2015). In bedrock material the Stephan Model was a reasonable fit, predicting a shallower ALD (11.9 m ± 1.4), while the Kudryavtsev Model predicted a deeper ALD (18.6 m ± 4.9) than measured in bedrock material (12.5 – 14.5 m) (Wilhelm *et al.*, 2015). It was suggested by Uxa (2017) that the ALD's modelled using Stephan and Kudryavtsev Models by (Wilhelm *et al.*, 2015) were overestimated, due to the models assuming that little latent heat was absorbed.

Work utilising the TTOP model, and MODIS land surface temperature satellite data was carried out at a 1 km² scale for eight ice free regions in Antarctica (Obu *et al.*, 2019). Ground truthing results were positive, with the difference between measured and predicted mean annual ground temperature at the top of the permafrost ranged across Antarctica between +0.8 °C to -4.2 °C (Obu *et al.*, 2019). Corrections were made for snow cover, though the biggest variations between predicted and measure permafrost temperatures were in areas subjected to wind-driven snow distribution (Obu *et al.*, 2019).

Above ground variables are more widely monitored in Antarctica, with continuous monitoring since the 1950's (Martin, 2016). The relationship between above ground variables and soil temperature has been well established, in Antarctica (Waelbroeck, 1993; Adlam *et al.*, 2010; Lacelle *et al.*, 2016) and offer a useful tool for modelling ALD in areas where soil climate monitoring is not viable.

Adlam (2009) found a positive correlation between air temperature and near-surface soil temperature ($R^2 > 0.79$). The soil temperature also correlated with incoming solar radiation ($R^2 \approx 0.8$) in some areas of the Ross Sea Region, Adlam (2009) did not find a relationship between wind speed and soil temperature at a seasonal scale.

Adlam *et al.* (2010) developed a model to predict ALD, using data from five low altitude sites between 1999 and 2007 was completed using stepwise analysis and gave the following equation:

$$ALD = 222 + 5.69(MSAT) + 3.63(MWAT) - 10.6(TSSR) - 2.84(MSWS) \quad (2-4)$$

Where ALD (cm) is active layer depth, MSAT ($^{\circ}C$) is mean summer (December – January (DJ)) air temperature, MWAT ($^{\circ}C$) is mean winter (June – August) air temperature, TSSR is total summer (DJ) solar radiation (100 kW/m^2) and MSWS (ms^{-1}) is mean summer (DJ) wind speed. The overall model had an $R^2 = 0.7$ (Adlam *et al.*, 2010).

Research in the Quartermain Mountains, in the McMurdo Dry valleys, found a strong relationship between mean air and surface temperatures ($R^2 = 0.92$, $p < 0.01$), as well as a strong relationship with mean incoming solar radiation ($R^2 = 0.72$, $p < 0.01$) (Lacelle *et al.*, 2016). Both incoming solar radiation and measured surface temperature were used to model at a whole valley scale, where the surface temperature remains perennially frozen, and where an active layer is present (Lacelle *et al.*, 2016).

2.7.3 Numerical modelling

Numerical models allow for the study of potential environments, and unlike empirical models, they are flexible enough to work with limited data and highly

varied materials, boundaries and geometry (Riseborough *et al.*, 2008). By using finite equations, a simulated environment can be solved for in either one, two or three dimensions with the input needed being set outside boundaries, the continuous space thermal and other properties of the soil, a specified starting temperature, and the use of theories to specify how energy (heat?) will flow through the material. Many of the specific properties needed to fill the model can be collected from ground surface temperature data or derived from atmospheric data either collected on-site (e.g. Outcalt *et al.*, 1975; Ng and Miller, 1977; Mittaz *et al.*, 2000; Riseborough *et al.*, 2008) or derived from remote sensing (e.g. Hinzman *et al.*, 1998; Chen *et al.*, 2003; Anisimov, 1989; Zhang *et al.*, 2007; Riseborough *et al.*, 2008). There are many limitations with numerical models due to the number of assumptions they make, so care needs to be taken in their interpretation.

2.8 Conclusion

Antarctica's cold, dry, climate has created a distinct environment not found anywhere else on earth. Most of the 14 million km² continent is covered with ice, with an estimated 0.32 -0.36% of Antarctica being ice free. Most of the ice-free land is situated in the Transantarctic Mountains and on the Antarctic Peninsula.

Antarctic soils are classified as Cryosol's (Food and Agriculture Organization of the United Nations, 2015) or Gelisol's (Soil Survey Staff, 1999). The Cryosol soil profile can be broken into four main layers;

- a desert pavement,
- an active layer which freezes and thaws annually, and is moderately weathered,
- a transition layer which thaws episodically, though meets all the requirements of the permafrost,
- and finally the fourth layer is the permafrost, which is material that stays below 0°C, and has a varied moisture content.

The dominant soil-forming factors in Antarctica are climate and temperature, which are mainly controlled by incoming solar radiation. In the Ross Sea region, there have been both warming and cooling trends reported, but none currently remain over a long period of time. Climate drivers such as the SAM and SOI have been identified as drivers the Antarctic climate at decadal to multi-centennial scales (Lüning *et al.*, 2019).

Caution should be used in interpreting the significance of trends in Antarctica, particularly in soil climate, as most data sets are shorter than the recommended 30-year period (WMO-No.100, 2018).

Chapter Three

Soil Climate Station Descriptions, Instrumentation and Data Assessment

3.1 Introduction

The objectives of this chapter are to describe the:

- soil climate station network;
- soils at each site;
- instrumentation at each site; and
- how the data is collected and processed before interpretation.

3.2 Climate station locations

Nine automated soil climate stations (SCS) were installed in the McMurdo Dry Valleys and the adjacent coastal area in the Ross Sea Region, Antarctica, between 1999 and 2012 (Figure 1, Table 1). As stated above, along the coast is a latitudinal transect with Granite Harbour in the north ($77^{\circ}00'23.7''$ S), through Scott Base and Marble Point, to Minna Bluff in the south ($78^{\circ}30'41.6''$ S). An altitudinal transect runs from a coastal margin station at Marble Point (60 m) through two stations on the McMurdo Dry Valley floors, in the Wright Valley (160 m) and the Victoria Valley (410 m) and through mid-altitude stations on the walls of the Wright Valley (South Wall 728 m; North Wall, 832), to Mt Fleming at the head of the Wright Valley (1700 m). Seven of the soil climate stations (SCS) were set up between 1999 and 2003 and have been running continuously since then. Two further SCS were installed on the Wright Valley walls in 2011 and 2012. Along with the SCS two bedrock borehole sites in 2005, continuously measuring soil temperature to a depth of 30 m (Adlam *et al.*, 2009). One borehole is situated approximately 150 m west of the Wright Valley Floor SCS and the second 2 km north of the Marble Point SCS.

Table 3.1: Description of each station in the Ross Sea Region monitoring network, including site location, site description and soil type. WV = Wright Valley. Adapted from Carshalton et al. (submitted).

	GPS coordinates	Site location	Site description (elevation, aspect, slope)	Soil classification, permafrost type
Granite Harbour (2003)	77°00'23.7"S 162°31'32.4"E	On 10 m wide boulder lateral moraine ledge between coast and base of cliff.	4.5 masl, NW facing (300°), 10°,	Typic Haplorthel, Ice cemented
Marble Point (1999)	77°25'10.6"S 163°40'55"E	400 m E of the Wilson-Piedmont Glacier, 620 m S of USA helicopter refuelling station.	60 masl S facing (180°), 3%,	Calcic Anhyorthel, Ice cemented
Minna Bluff (2003)	78°30'41.6"S 166°45'58"E	75 km S of Scott Base, on N side of Minna Bluff Peninsula.	37 masl, N facing (360°), < 5°	Typic Haploturbel, Ice cemented
Mt Fleming (2002)	77°32'42.7"S 166°17'24.6"E	Flat rocky platform on N side of Mount Fleming, near edge of Polar Plateau.	1700 masl, S facing (180°), <5°	Typic Haploturbel, Ice cemented
North Wall Wright Valley (2012)	77° 30' 07.9" S 162° 03' 53.1" E	On a flat gravely plain, overlooking the Wright Valley, E of Bull Pass.	832 masl, S facing (180°), 5%	Typic Anhyorthels, Dry permafrost
Scott Base (1999)	77°50'53.6"S 166°45'44"E	Approximately 100 m N, behind Scott Base on a rocky gentle slope.	38 masl, SE facing (135°), 6%	Typic Haplorthel, Ice cemented
South Wall Wright Valley (2011)	77° 34' 26.0" S 161° 14' 19.6" E	On a sandy ridge 700 m above Don Juan Pond.	728 masl, E facing (90°), 5%	Typic Haplorthel, Ice cemented
Victoria Valley Floor (1999)	77° 19'51.3"S 161°36'02.2"E	On the Victoria Valley floor in the centre of an old lake pedon. 300 m NW from the bottom of Lake Victoria.	410 masl, flat	Typic Haplorthel, Ice cemented
Wright Valley Floor (1999)	77°31'06.1"S 161°51'57"E	On the floor of the Wright Valley, below Bull Pass.	160 masl, S facing (180°), 3%	Salic Anyorthel, Dry permafrost

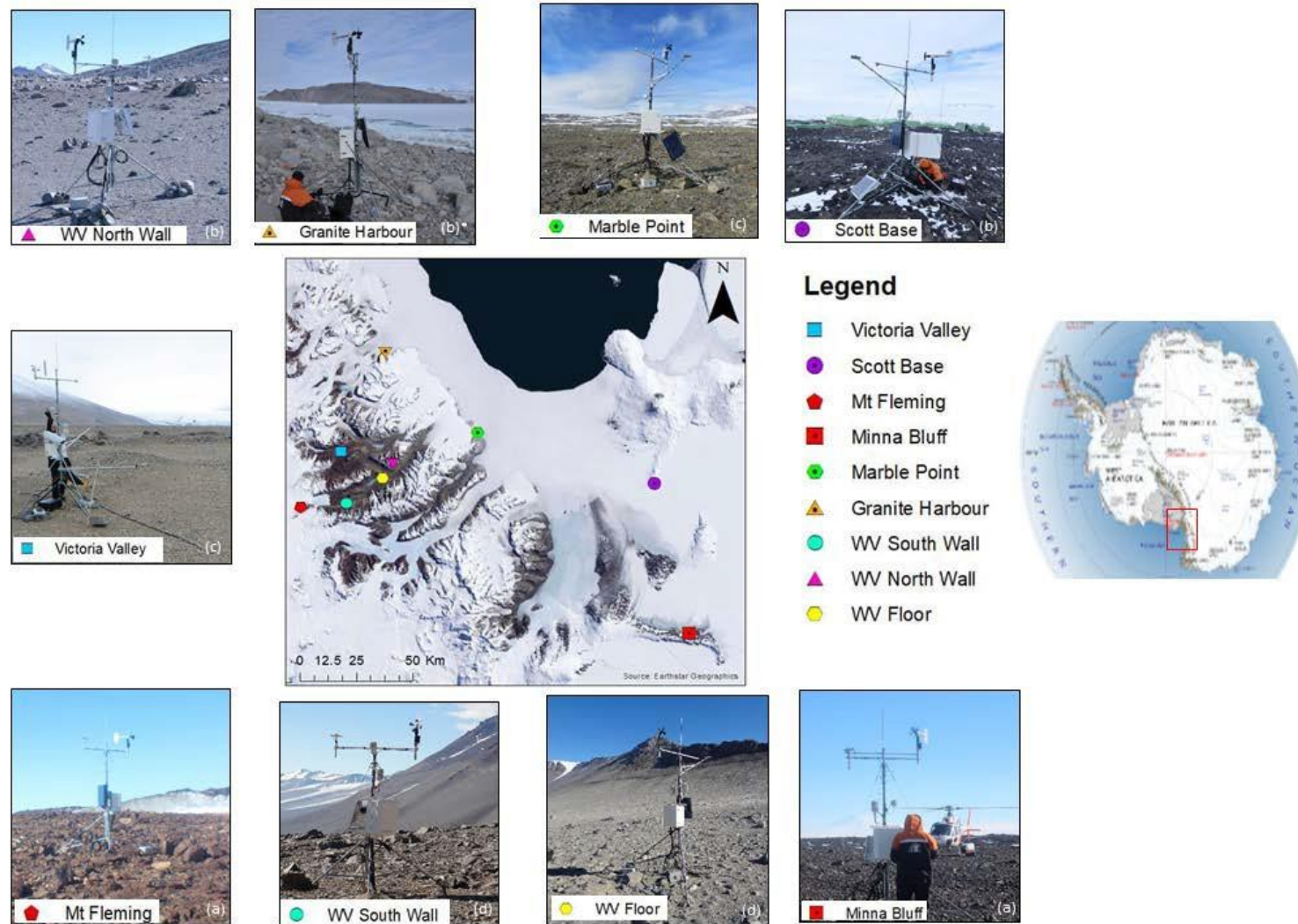


Figure 3.1: Map of soil climate station locations, with labelled photos of each site. WV = Wright Valley. Photo Credit; a) Annette Carshalton (2017), b) Chris Morcom (2016 & 2017), c) 2015 team, d) 2014 team.

3.3 Soil descriptions

The soil at each site was described, classified and samples collected for analysis by the United States Department of Agriculture National Soil Survey Centre at the same time as the SCS was installed (Seybold *et al.*, 2009). The soils in the SCS network are classified as Gelisols which are soils with permafrost or features associated with freeze-thaw action. The detailed soil profile descriptions (Appendix 1) were completed following USDA methods and are summarised below.

Mt Fleming

The SCS at Mt Fleming, is the highest altitude site in the soil climate monitoring network (1700 m) and was installed in January 2002, on a cirque on the north side of Mt Fleming at the head of the upper Wright Valley (Table 3.1). The desert pavement comprises coarse patterned ground, dominated by dolerite boulders, with sandy material built up in patterned ground cracks (Figure 3.2). The desert pavement is strongly weathered. The parent material is a mixed glacial till dominated by dolerite, with subsidiary granite and sandstone. Massive ground ice (ice-cored moraine) is probably present beneath (Balks, 2002, pers. Comm).

The soil profile at Mt Fleming was described to 70 cm by Balks (2002, pers. comm.; Appendix I) and classified as a Typic Haploturbel. Ice-cemented permafrost was present from 45 cm downwards. Soil moisture ranged between 2 and 7% above 45 cm, and was 16% between 45 and 70 cm, causing the sample to appear saturated when thawed.



Figure 3.2: The Desert Pavement at Mt Fleming (photo by Annette Carshalton)

Granite Harbour

The SCS at Granite Harbour is in a sheltered site situated at the foot of a north-facing slope, on a bouldery lateral moraine between the sea edge and a cliff (Table 3.1) and is subject to subsurface meltwater flowing through the site from the adjacent cliff. The site was chosen due to its proximity to Botany Bay which is a “site of special scientific interest” due to extensive moss growth, and thus the Granite Harbour SCS captures data of an exceptional microclimate not typical of the wider area.

The desert pavement is made up of predominately of angular granite blocks and boulders, with finer material below showing signs of weathering. At the base of the slope close to the sea edge the surface is made up of rounded granite boulders and unweathered sands similar to beach sand (Figure 3.3). Moss and lichen are growing in moist sheltered areas among the rock’s upslope of the SCS.

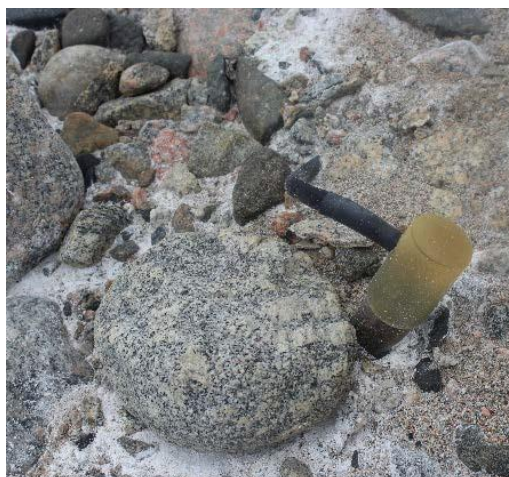


Figure 3.3: Restored desert Pavement at Granite Harbour, with head of MRC probe for scale (photo by Annette Carshalton)

The soil was classified by Balks (2003, pers. comm.; Appendix I) as a Typic Haplorthel (Appendix I). Ice- cement was at 80 cm at the time of sampling in 2003. The gravimetric moisture content was approximately 1%.

Wright Valley Floor

The SCS on the Wright Valley Floor (WVF) was established on the foot slope on the side of an out-wash terrace on the floor of the Wright Valley below Bull Pass in December 1999 (Table 3.1). The soil was described to 130 cm by Kimble (1999;

Appendix I) and classified as a Subactive Hygergillic Typic Anhyorthel (Figure 3.4), with a granite dominated parent material. The desert pavement consists of loose gravely sand (Figure 3.5). Ice-cemented permafrost was not reached, therefore the WVF has dry permafrost to > 1.8 m.

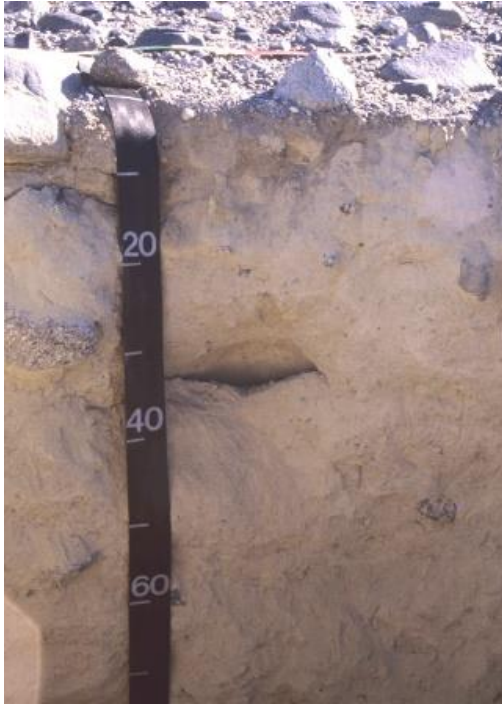


Figure 3.4: Soil Profile at the Wright Valley Floor (photo by Megan Balks)



Figure 3.5: Disturbed desert pavement (foot print) at the Wright Valley floor, 2017

Victoria Valley

A SCS was set up in the Victoria Valley in January 2002, on the true right bank of Lake Victoria, about 20 m down valley of a dolerite dominated recessional moraine (Table 3.1). The soils and landscape were described by Balks and Sletten (2002; Appendix I). The local landscape is dominated by large (15 -30 m diameter), low centred and fairly flat (< 1 m vertical relief), polygonal patterns. The desert pavement is made up of gravels and sands with few rocks evident, and dominated by granite and dolerite, with some marble and sandstone (Figure 3.6). The surface is about 10 000 years old and is a former lakebed. The soil was described to 120 cm, with ice cement present at 40 cm. The soil was classified using USDA taxonomy as a Typic Haplorthel.



Figure 3.6: Restored desert pavement at Victoria Valley SCS with MRC probe for scale (photo by Annette Carshalton).

Marble Point

The Marble Point SCS station was established in January 1999, 620 m south of the USA helicopter refuelling station, on a backslope of a fluvial terrace (Table 3.1). The soil profile was described to 100 cm, by Kimble, Campbell, Balks and Paetzold. (1999; Appendix I) All horizon samples had effervescence with HCl, thus the soil was classified as a Sandy-Skeletal, Mixed, Superactive Calcic Haplorthel, under USDA taxonomy. The desert pavement consisted of gravelly sand with small stones, comprising marble, gneiss and granite fragments (Figure 3.7).



Figure 3.7: Restored desert Pavement at Marble Point with head of MRC probe for scale (photo by Annette Carshalton).

Scott Base

The SCS station at Scott Base was set up in January 1999, on a back slope on the side of a mountain behind the buildings of Scott Base (Table 3.1). The soils were described to 75 cm by Kimble, Campbell, Balks and Paetzold (1999, Appendix I) and classified using the USDA taxonomy as a Typic Haplorthel (Figure 3.8). The parent material comprised of scoreacious basalt. The desert pavement is made up of gravelly sand, along with common small rocks and pebbles (Figure 3.9). Ice-cement is present but was not measured at the time of sampling. There are a few small areas with moss growing in the wider vicinity.



Figure 3.8: Soil profile at Scott Base (Photo by Megan Balks)



Figure 3.9: Desert pavement at Scott Base, with head of the MRC probe for scale (photo by Annette Carshalton).

Minna Bluff

The SCS at Minna Bluff was installed in January 2003 and is located on the north side of Minna Bluff directly south of Scott Base (Table 3.1). The station is situated two thirds of the way between the Ross Ice Shelf and the steep side of the bluff, on rectangular patterned ground. The site and soils were described to 80 cm Balks (2003; Appendix I) and classified as Typic Haploturbel. The parent material was ablation till and dominated by basalt and granite rock material. The desert pavement consists of coarse sands and common rocks, the material was moderately rounded, with some desert varnishing (Figure 3.10). Ice-cement

occurred at 34 cm, and no vegetation was present. The dry bulk density between 4-10 cm depth was 2.5 g.cm^{-3} and between 10 – 30 cm it was 1.9 g.cm^{-3} .



Figure 3.10: Restored desert Pavement at Minna Bluff (photo by Annette Carshalton).

Wright Valley Walls

Two further sites were set up in the Wright Valley eight years after the original seven sites were established. The first WV wall station was developed in 2011, on the WV South Wall, on a narrow terrace above Don Juan Pond (Table 3.1). The parent material was from a colluvial fan, over glacial till and was dominated by granite, with some dolerite. The desert pavement is made up of pitted boulders and weathered gravels and a part of moderately developed polygons that are about 10 m square, along 30 cm wide pattern ground cracks dominated by stony material (Figure 3.11).

The soil profile at the WV South Wall was described by McLeod Seybold (2011; Appendix I), to a depth of 120 cm (Figure 3.12). The soil was classified as a hypergellic Typic Haplorthel. Ice-cemented ground was detected at 24 cm at the time of sampling.



Figure 3.11: Desert pavement at the Wright Valley South Wall, with MRC probe head for scale.



Figure 3.12: Soil profile at the Wright Valley South Wall (Cathy Seybold)

The final SCS was installed on the Wright Valley North Wall, situated on a terrace east of Bull Pass (832 m) in 2012 (Table 3.1). The parent material was predominantly colluvium dominated by granite with some dolerites. The desert pavement made up of weathered stones and gravels (Figure 3.13). The soil profile was described to 120 cm, by Seybold and Goddard (2011; Appendix I). The soil was classified as a hypergellic Typic Haplorthel (Figure 3.14). Ice-cement was not encountered.



Figure 3.13: Desert pavement at the Wright Valley North Wall, with probe head for scale (photo by Annette Carshalton).



Figure 3.14: Soil profile at the Wright Valley North Wall (Goddard, 2013)

3.4 Instrumentation

Across the nine SCS the soil variables monitored are temperature and moisture levels. Atmospheric variables measured include: air temperature, relative humidity, solar radiation and wind speed & direction (Figure 3.15). At the SCS sites, instruments used to measure each variable were similar. At least two instruments were used at each site to measure soil temperature and moisture because the regular calibration of the in-ground sensors is not possible. Having at least two different instruments making duplicate measurements provides a means to check for instrument changes over time. There is also a backup if one of the sensors malfunctions. Above ground supporting equipment, includes the data logger hardware, solar panels, batteries and the tower structure. Atmospheric data were measured every 10 seconds, and soil data every 20 minutes, with hourly means recorded. Manual data download and station maintenance is undertaken annually.



Figure 3.15: Atmospheric climate data monitoring site at Minna Bluff, with temperature probe housing and wind monitoring equipment visible (photo by Annette Carshalton).

3.4.1 Temperature probes

To measure soil and permafrost temperature three probes are utilised across the nine SCS sites (Appendix 2). The Campbell 107 (Figure 3.16c) probes are present at all sites. Vitel Soil Moisture and Temperature probes are deployed in the seven SCS sites installed between 1999 and 2003 (Figure 3.16a). The Vitel probe has more recently been manufactured under the name Hydra probe and were installed at the two Wright Valley wall sites in 2011 and 2012. MRC probes were installed at all sites except Mt Fleming (Figure 3.16b). The MRC probe is a 1.2 m long plastic rod which has 11 sensors imbedded along its length. The MRC probe was generally installed to 1.2 m depth, but due to difficult rocky conditions at Granite Harbour it was installed on an angle with the base at 90 cm, and at Minna Bluff it was installed with the probe 10 cm above the ground surface. All measurements were recorded in degrees Celsius.



Figure 3.16: Soil temperature and moisture probes before installation. a) Vitel probes, b) MRC probe with embedded sensors, and c) Campbell 107 and Vitel probe (photos by Megan Balks).

3.4.2 Air Temperature

Most of the stations have two probes measuring air temperature at a single height between 1.6 m and 3.0 m (Appendix 2). The probe types currently used are the Campbell 107, Campbell 109, HMP35C and HMP45C. The later model probes (45C and 109) have a wider measuring range (between -50°C and $+70^{\circ}\text{C}$), and are

an improvement in cold conditions by up to 15°C. Thus, the later models have been installed when replacements were needed and at the newer sites on the walls of the Wright Valley.

3.4.3 Relative above ground Humidity

Relative Humidity (RH) of the air is measured with a Vaisala HMP35C probe at Minna Bluff and with a Vaisala HMP45C probe all other sites (Appendix 2). The 45C is an improved model compared to the 35C model, but the key specifications are the same and have the same tolerance levels of $\pm 2\%$.

3.4.4 Solar Radiation

A LiCor LI2000X is installed at each site to measure incoming solar radiation (W m^{-2}). The mounting height of each probe is between 2.2 m and 3.0 m. The waveband stretches from 400nm to 1,100nm with a tolerance of $\pm 3\%$ (Appendix 2). Net radiation was also measured at Scott Base, and using a Q-7.1 Net Radiometer sensor, which was installed at the end of 2000.

3.4.5 Wind Speed and Direction

One of two probes were used to measure wind speed and direction (Appendix 2) at each SCS site. The original probe installed was the Met One; which is capable of recording wind speed up to 45 m s^{-1} with an accuracy of $\pm 0.11 \text{ m s}^{-1}$. The newer probe is the RM Young; it was installed at sites on the Wright Valley walls and replaced the Met One probe at Marble Point in 2008 and on the Wright Valley floor in 2006. The RM Young can measure wind speeds of up to 100 m s^{-1} with a tolerance of $\pm 0.3 \text{ m s}^{-1}$.

3.5 Data Validation

Before starting analysis of the data at each SCS, the data was checked to ensure it was continuous and reliable, and what years were suitable to use. As the desert pavement at each site changes in height with time, the height of the MRC protruding from the ground is measured every year. The sensor depth of the MRC was adjusted before comparing to other soil probes, and before the calculation of ALD.

Data quality

Data gaps were assessed manually to check for gaps and illogical data (instrument errors). To check for measurement drift and other inconsistencies in the soil probes, the soil temperature at approximately 45 cm deep was compared between the MRC probe data and either the C107, C109 or Vitel probes at the same depth, for 2004 (Figure 3.17a) and 2018 (Figure 3.17b). The MRC and Campbell probes where compared were highly correlated ($R^2 > 0.9$). When the MRC probe was compared to the Vitel probes the correlation was lower ($R^2 \approx 0.7$) due to the Vitel probe “flatlining” at approximately -14°C . When only summer month values were compared the Vitel and MRC probes were highly correlated ($R^2 > 0.9$). Full calibration of the individual soil probes is not possible without disturbing the soil profile and stopping continuous measurement.

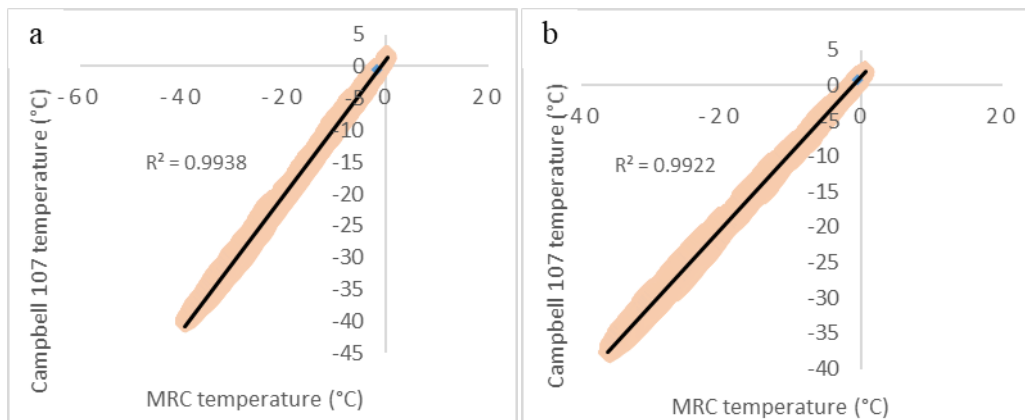


Figure 3.17: Subset of the calibration between soil temperature MRC and Campbell 107 at approximately 45 cm in a) 2004 and b) 2018, at the Wright Valley Floor. The other SCS showed similar results.

The data was filtered manually to avoid accidentally removing winter storm data. The dataloggers are programmed to record faulty recordings as “-6999”, all of these values were removed, and these spaces were filled with “not a number” values (NaN). For the temperature data, all spike values under -100°C were removed, as this is way below the measurement range for the data. “Once-off” spikes of $> +20^\circ\text{C}$ within the permafrost data were also removed. Hourly plots of the data were also assessed to check that the data remained in the logical range for the whole data set and was complete for each site. Several sections of erroneous temperature

data were recorded at Minna Bluff and at Scott Base, causing a few years of data to not be used.

Missing data

Most of the research done in this thesis used seasonal and annual means. The SCS at the WVF and at Marble Point did not have any gaps in their soil data. At the other sites most sites have multiple gaps in July, August and September, due to batteries running out during late winter and before they were recharged via solar panels. Minna Bluff, Scott Base and the newest station on the North Wall of the Wright Valley, had some larger gaps where instruments or datalogger malfunction occurred.

Where the gaps were large, e.g. greater than a week, or repetitively occurring through winter or spring, the data was removed from analysis; most sites have at least one year with a period of missing data. For smaller gaps, interpolation by taking the mean of the measurement an hour before and after and taken as that measurement, for bigger gaps the data from the previous day was used to infill the gap. The means and calculated ALDs taken from years with interpolated data were compared to years at the same site where the data were complete for the specific year and if they had a large difference that was not explainable, the interpolated data year was removed.

Where constant issues were found with an instrument, or with the whole station running out of power, these details have been passed onto the technical team to allow for maintenance planning.

3.6 Summary

The Ross Sea Region SCS network is made up of nine stations set up between 1999 and 2012 within the McMurdo Dry Valleys and along the adjacent coast (Table 3.1). The soils at each site are affected by freeze-thaw and action and classified in the Gelisol order. All stations have a well-developed desert pavement, and all but the sites on the WVF and on the WV North Wall have ice-cemented permafrost (Appendix 1).

At each SCS soil temperature and moisture is monitored down to 1.2 m. The atmospheric climate is measured between 1.6 – 3.0 m from the ground surface and variables measured include air temperature, wind speed and direction, relative humidity, incoming solar radiation and net solar radiation (Appendix 2).

An assessment of the data quality was undertaken, with erroneous data replaced with null values, measurement drift and instrument error in the soil probes was completed by comparing the ALD between the MRC and Campbell probes at each site, with $R^2 > 0.9$ found at all sites.

Most sites had small gaps of missing data, particularly in early spring. Where there were large gaps, analyses were not undertaken for that season or year for that SCS. Smaller gaps were interpolated from the hours before and after or using infilling from the previous day. Sections of interpolated data were assessed against other years at the same site to check for reliability. Repeated breakdowns at any SCS have been reported to the technical team. Detailed station maintenance records are kept and can be found at:

https://www.nrcs.usda.gov/wps/portal/nrcs/detail/soils/survey/climate/?cid=nrcs142p2_053772

Chapter Four

Climatic influences on Active Layer Depth between 2000 and 2018 in the McMurdo Dry Valleys, Ross Sea Region, Antarctica

(Paper submitted to Geoderma Regional, as part of special issue on extreme soils)

Authors: A. G. Carshalton¹, M. R. Balks¹, T. A. O'Neill¹, K. R. Bryan¹, C. Seybold²

¹University of Waikato, Waikato, New Zealand

²NRCS, USDA, Nebraska, USA

4.1 Abstract

The maximum seasonal depth of thaw (the active layer depth) in permafrost soils is influenced by a range of soil and atmospheric variables. The depth of the active layer, along with the temperature at the top of the permafrost, have potential to provide a clear signal of a changing climate, with less “noise” than atmospheric variables. A monitoring network of nine soil climate stations was established in the McMurdo Dry Valleys between 1999 and 2012. Each station monitors soil temperature to a depth of up to 1.2 m, along with a range of atmospheric variables including air temperature, solar radiation, and wind speed.

There was marked between-year variation but no trends of warming or cooling over time, in either active layer depth or temperature at the top of the permafrost. Wavelet analysis showed that both global and regional climate systems were a significant driver of permafrost temperature. The Southern Annular Mode showed relationships at both annual and biannual timescales ($p < 0.05$); the Southern Oscillation Index had a relationship at a two to three year timescale ($p < 0.05$); and the Amundsen Sea Low had an annual signal and some between season signals ($p < 0.05$).

The data set is too short to draw conclusions on potential longer-term changes in the soil climate. Nevertheless, the database provides a baseline against which future change can be assessed and will increase in value the longer it is maintained.

4.2 Introduction

The International Panel for Climate Change (IPCC) predicts that global mean surface air temperatures will be 1°C higher between 2016 and 2035 compared to the mean between 1850 and 1900; and that the mean global long term temperatures in 2100 will be 1.5°C to 4°C greater than mean temperatures between 1850 and 1900 (IPCC, 2014). One of the key questions identified in an Antarctic Horizon Scan was “How will permafrost, the active layer, and water availability, in Antarctic soils and marine sediments change in a warming climate, and what are the effects on ecosystems and biogeochemical cycles?” (Kennicutt et al., 2014).

The active layer is the layer of soil that freezes and thaws annually and is underlain by permafrost (Campbell and Claridge, 1987). Active layer depth (ALD) provides an indicator of climate that is less “noisy” than atmospheric data as the ALD integrates variations that occur in air temperature, solar radiation and wind conditions over short (hourly) time scales. Therefore, changes in ALD have potential to provide an indicator of climate change. An understanding of the relationship between climate, ALD, and other soil and ecological properties can provide a basis for predicting effects of potential future changes in climate.

Atmospheric trends in temperature across Antarctica have been well documented, with warming trends identified in the 20th century (Vaughan et al., 2001; Steig et al., 2009; Schneider et al., 2012; Bromwich et al., 2013; Oliva et al., 2017). However a cooling trend between 1999 and 2014 has also been reported (Turner et al., 2016) and a decrease in ALD in the Antarctic Peninsula has been reported between 2006 and 2014 (Goyanes et al., 2014; Hrbacek et al., 2016 Ramos et al., 2017; Oliva et al., 2017). Evidence has suggested that one driver of short term cooling in Antarctica is in the Southern Oscillation when in an El Niño phase (Bertler et al., 2004).

Previous climate monitoring in the Ross Sea Region of Antarctica has provided a range of outcomes. A cooling trend was reported in the McMurdo Dry Valleys between 1986 and 2000 (Doran et al., 2002b), however no trends of overall increase or decrease in ALD were observed in the Ross Sea Region between 1999 and 2007 (Adlam et al., 2009). A weak warming trend in mean air and mean soil temperatures was reported at one site (Marble Point) between 2000 and 2011 (Goddard, 2013). A warming trend with thickening ALD was reported in northern Victoria Land since 2000 and was attributed to increased incoming solar radiation (Guglielmin and Cannone, 2012). In the western coastal Antarctic Peninsula a decreasing trend in ALD was reported between 2006 and 2014, it was suggested that the trend was due to increased snow cover, since no trend in mean annual air temperature was noted (Ramos et al., 2017). Other Antarctic Peninsula sites showed high between-year variation and it was suggested that further monitoring would be needed to assess if long term change to ALD was occurring (Almeida et al., 2017; de Pablo et al., 2018; Hrbáček et al., 2017).

Changes in soil temperature, and thus the ALD, may be influenced by larger climate systems that affect all Antarctic weather. These are the Southern Annular Mode (SAM), the Southern Oscillation Index (SOI), and the Amundsen Sea Low (ASL). The SAM, also known as the Antarctic Oscillation, is a pressure system situated between the latitudes of 40° and 65° South, and is defined as being in a positive phase, when the higher pressure zone is situated about 40° S and in a negative phase when the higher pressure zone is closer to 65° S. The SAM is the main mode of atmospheric variability in the high latitudes of the southern hemisphere (Marshall, 2003). The SAM has been shown to contribute significantly to climate variability both at high and low frequency time scales (Kidson, 1999; Baldwin, 2001; Marshall, 2003).

The SOI is an index of the change in surface pressure across the South Pacific based on the difference in pressure between Tahiti and Darwin (Australia), and stretches over a 100 year period (Ropelewski and Jones, 1987). The ASL is a seemingly stationary area of low atmospheric pressure that stretches across the South Pacific ocean between the Ross Sea and the Antarctic Peninsula (Hosking et al., 2013). Variation in the ASL has been shown to influence southerly wind velocity, near surface air temperature, and precipitation (Turner et al., 2009; Küttel et al., 2012; Hosking et al., 2013). The ASL is influenced by larger scale climate circulation systems, such as the SAM and the SOI (Kwok and Comiso 2002; Turner 2004; Hosking et al., 2013), with the SAM having a significant relationship with the central pressure of the ASL for all seasons, and the SOI (Niño3.4 index), having a significant relationship in summer (December to February) (Hosking et al., 2013).

The objectives of this paper are to: 1) report on the variation in ALD and temperature at the top of the permafrost both spatially and temporally in the Ross Sea Region of Antarctica; 2) to assess if any warming or cooling trends are evident in the dataset; and 3) assess the potential driving relationship between the SOI, SAM, ASL and the temperature at the top of the permafrost.

4.3 Methods

4.3.1 Station locations

Nine automated soil climate stations were installed in the McMurdo Dry Valleys and the surrounding area (Figure 4.1, Table 4.1). Along the coast is a latitudinal transect with Granite Harbour in the north ($77^{\circ}00'23.7''$ S), through Scott Base and Marble Point, to Minna Bluff in the south ($78^{\circ}30'41.6''$ S). An altitudinal transect runs from a coastal margin station at Marble Point (60 m) through two stations on the McMurdo Dry Valley floors, one in the Wright Valley and the other in the Victoria Valley and through mid-altitude stations on the walls of the Wright Valley, to Mt Fleming at the head of the Wright Valley (1700 m). Seven of the stations were set up between 1999 and 2003 and have been running continuously since then. Two further stations were established on the Wright Valley walls in 2011 and 2012.

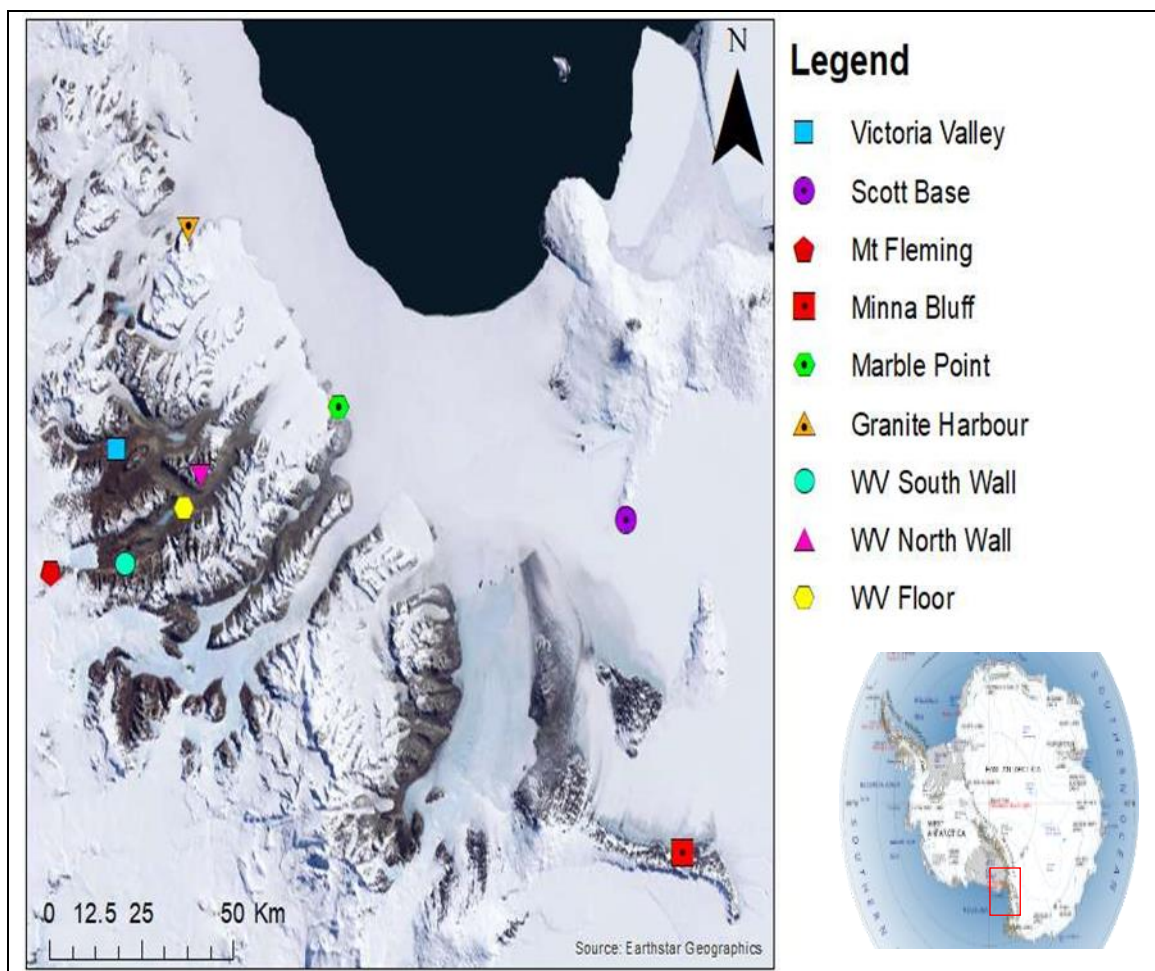


Figure 4.1: Soil climate monitoring sites location map, with the insert showing the McMurdo Dry Valley region (Red Square). WV = Wright Valley.

Table 4.1: Soil climate stations site locations and descriptions. Notes: nd = not determined, summer = December and January

	GPS coordinates	Site location	Site description (elevation, aspect, slope, vegetation cover)	Mean soil (15 cm) temp		Mean air temp		Soil classification, permafrost type
				Annual °C	Summer °C	Annual °C	Summer °C	
Granite Harbour (2003)	77°00'23.7"S 162°31'32.4"E	On 5 m wide bouldery beach between coast and base of cliff.	4.5 masl, NW facing (300°), 10°, moss patches present	-14.5	4.5	-16	-1	Typic Haplorthel, Ice cemented
Marble Point (1999)	77°25'10.6"S 163°40'55"E	400 m E of the Wilson-Piedmont Glacier, 620 m S of USA helicopter refuelling station.	60 masl S facing (180°), 3%, no vegetation	-18	1	-17.5	-3.5	Calcic Anhyorthel, Ice cemented
Minna Bluff (2003)	78°30'41.6"S 166°45'58"E	75 km S of Scott Base, on N side of Minna Bluff Peninsula.	37 masl, N facing (360°), < 5°, no vegetation	-16.5	-1.5	-17	-3	Typic Haploturbel, Ice cemented
Mt Fleming (2002)	77°32'42.7"S 166°17'24.6"E	Flat rocky platform on N side of Mount Fleming, near edge of polar plateau.	1700 masl, S facing (180°), <5°, no vegetation	-23.3	-9	-24	-11.5	Typic Haploturbel, Ice cemented
North Wall Wright Valley (2012)	77° 30' 07.9" S 162° 03' 53.1" E	On a flat gravelly plain, over looking the Wright Valley, E of Bull Pass.	832 masl, S facing (180°), 5%, no vegetation	nd	1	nd	-3	Typic Anhyorthels, Dry permafrost
Scott Base (1999)	77°50'53.6"S 166°45'44"E	Approximately 100 m N, behind Scott Base on a rocky gentle slope.	38 masl, SE facing (135°), 6%, no vegetation	-17.5	-0	-16.5	-5.5	Typic Haplorthel, Ice cemented
South Wall Wright Valley (2011)	77° 34' 26.0" S 161° 14' 19.6" E	On a sandy ridge 700 m above Don Juan Pond.	728 masl, E facing (XXX), 5%, no vegetation	-17	1	-17	-3	Typic Haplorthel, Dry permafrost
Victoria Valley Floor (1999)	77° 19'51.3"S 161°36'02.2"E	On the Victoria Valley floor in the centre of an old lake pedon. 300 m NW from the bottom of Lake Victoria.	410 masl, flat, no vegetation	-23	-0	-23	-3	Typic Haplorthel, Ice cemented
Wright Valley Floor (1999)	77°31'06.1"S 161°51'57"E	On the floor of the Wright Valley, below Bull Pass.	160 masl, S facing (180°), 3%, no vegetation	-19.5	3	-19.5	-3.5	Salic Anyorthel, Dry permafrost

4.3.2 Monitoring equipment set up

Each soil climate monitoring station records both soil and atmospheric climate variables. Soil temperature and soil moisture are measured at a range of depths up to between 90 – 120 cm using three types of sensors; Vitel soil temperature and moisture probes (installed at a range of depths at all stations), MRC (Measurement Research Corporation, Gig Harbour, WA) temperature probes installed at all stations except Mt Fleming (which measure the soil temperature at 11 depths along the 1.2 m probe), and Campbell Scientific 107 probes (installed at Mt Fleming to a depth of 75 cm, and at all other sites from depths near the surface to between 75 – 90 cm). Atmospheric variables measured at all stations include: solar radiation (measured at 3 m using a LiCor LI200x); air temperature, (measured between 1.6 and 2 m above ground using either a Vaisala HMP45C, a Vaisala HMP53C, a Campbell Scientific 107 or a Campbell Scientific 109 probe); and wind speed and wind direction (at 3 m using a RM Young sensor), (Appendix 2)

Data from all stations are downloaded manually every January, data are stored in a database and are available to the public along with station soil descriptions, and soil characterizations at:

https://www.nrcs.usda.gov/wps/portal/nrcs/detail/soils/survey/climate/?cid=nrcs142p2_053772

4.3.3 Reliability of probes and data

The stations on the Wright Valley Floor and at Marble Point, do not have any gaps in the data set, all other stations have at least one, sometimes more, multiple day gaps in data in August and September, caused by the batteries at the station running out before the sun has begun to charge them. Thus annual means cannot be calculated for years where there were large data gaps, however summer data collection was generally reliable. Minna Bluff, Scott Base and the newest station on the North Wall of the Wright Valley, have larger gaps where instruments or datalogger malfunction has occurred. The number of days missing in any period/section of data was assessed against the total number of years of data being analysed to determine whether there was a large or significant potential effect on the calculated results.

ALDs for each year were determined as the maximum depth of the zero isotherm between the summer months of December and January. To calculate the ALD, the maximum temperature for each sensor in the MRC probe was plotted against the corresponding depths (Appendix 3). The depth where the line crossed the zero isotherm was manually extracted using the 'ginput' function in MatLab and recorded in Microsoft Excel as the ALD for the corresponding summer. The temperature at the top of the permafrost, at each site, was recorded as the temperature of the sensor below the deepest ALD across the record at that site.

To assess trends through time, the Mann-Kendal method was utilised, along with Kendal's Tau-b test. The Mann-Kendal test is a non-parametric (distribution free) test, that looks for both upward and downward monotonic trends through time, resulting in a null hypothesis being accepted or rejected for a set significance threshold, and a p-value was also calculated. The Tau-b test measures the strength and direction of the relationship between pairs of variables, such as time and ALD, with results ranging between 1 (perfect association) and -1 (perfect reversed association), with 0 indicating no relationship (Agresti, 2010). The computation of the Tau-b, significance test, and testing of the null hypothesis was undertaken following the work of Burkey (2006), with alpha set as standard at 0.05, for the ALD at each station in the soil climate monitoring network.

The time series of soil temperature both at the surface and at the top of the permafrost were inspected for long term trends. Cross wavelet analyses, between de-seasonalised soil temperature from the top of the permafrost at four soil climate stations (Mt Fleming, Wright Valley Floor, Marble Point, and Victoria Valley) and the larger climate systems potentially driving the temperature (SOI, SAM, ASL), were undertaken (Appendix 4).

Wavelet analysis allows for the study of a time series over multiple scales, through utilising a scaled generalised local function that can be stretched and manipulated in both frequency and time, to create narrow windows appropriate for high frequency signals and wide windows for low frequency signals or background noise (Lau and Weng, 1995). Results were plotted with time as the abscissa, wavelet frequency/fourier period as the ordinate, and signal strength/amplitude distribution displayed using contour plotting. To calculate the wavelet, tool boxes from Torrence and Compo (1998) and Grinsted et al. (2004)

were used, with the wavelet shape chosen being the complex Morlet wavelet, which is the most commonly used in analysis of climate oscillations (Torrence and Compo, 1998). Significance levels were set at 95%, or 0.05. Daily Southern Annular Mode data were retrieved from:

https://www.cpc.ncep.noaa.gov/products/precip/CWlink/daily_ao_index/aao/aao.Shtml

with monthly means calculated from the daily values. Monthly data for the Southern Oscillation Index was sourced from:

https://www.esrl.noaa.gov/psd/gcos_wgsp/Timeseries/SOI/.

Data for the Amundsen Sea Low were retrieved from:

https://legacy.bas.ac.uk/data/abs/ASL-index-Version2-Monthly-ERA-Interim_Hosking2016.txt

and the relative central pressure calculated following the methods given in Hosking et al. (2016) with the equation:

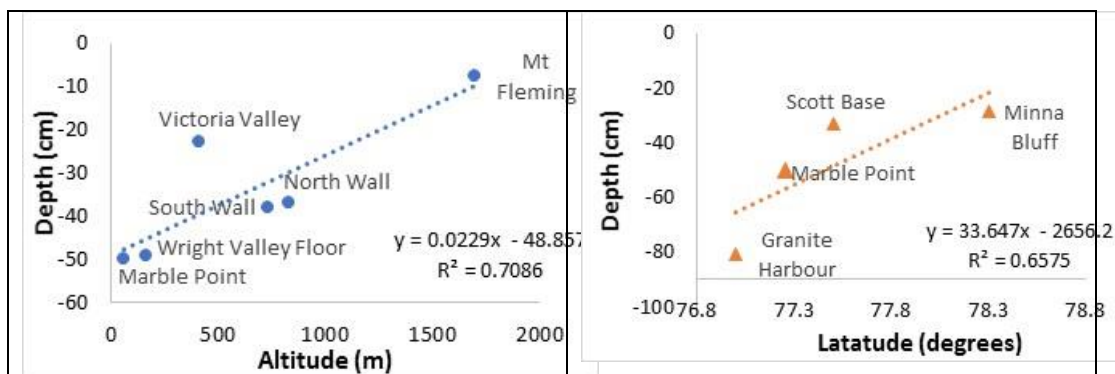
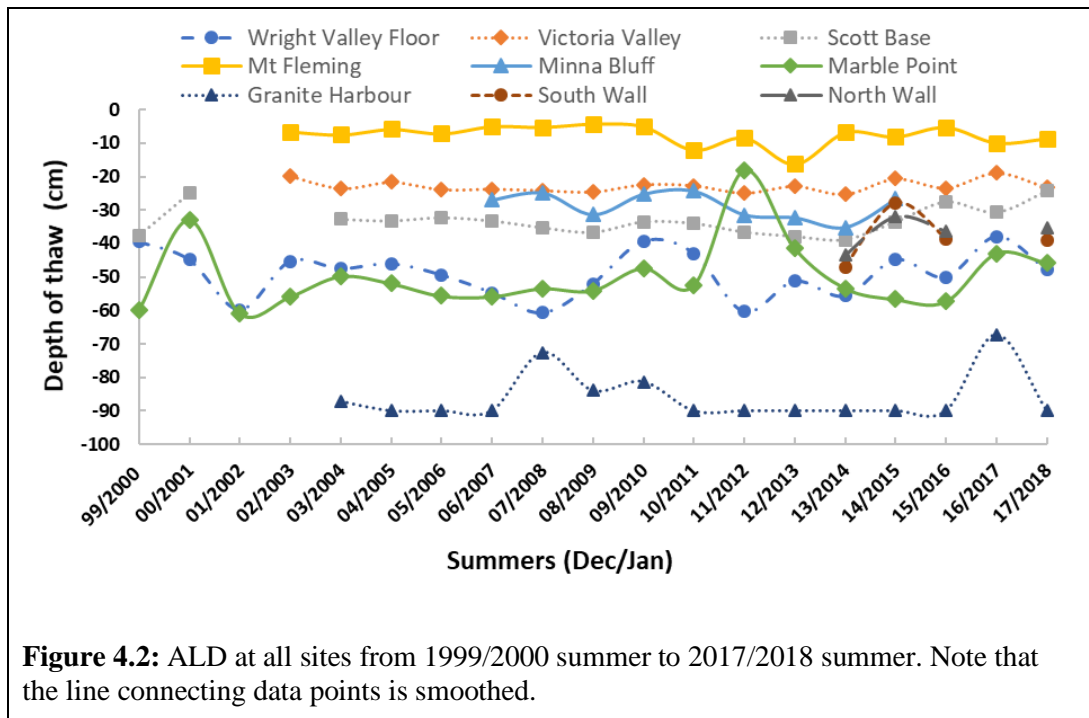
$$RelCenPres = ActCenPres - SectorPres$$

Where the ActCenPres is the pressure at the actual location of the ASL, and the SectorPres is the area-averaged pressure over the whole ASL region. The RelCenPres is a preferred measure as the actual pressure is strongly modulated by the SAM (Hosking et al., 2016).

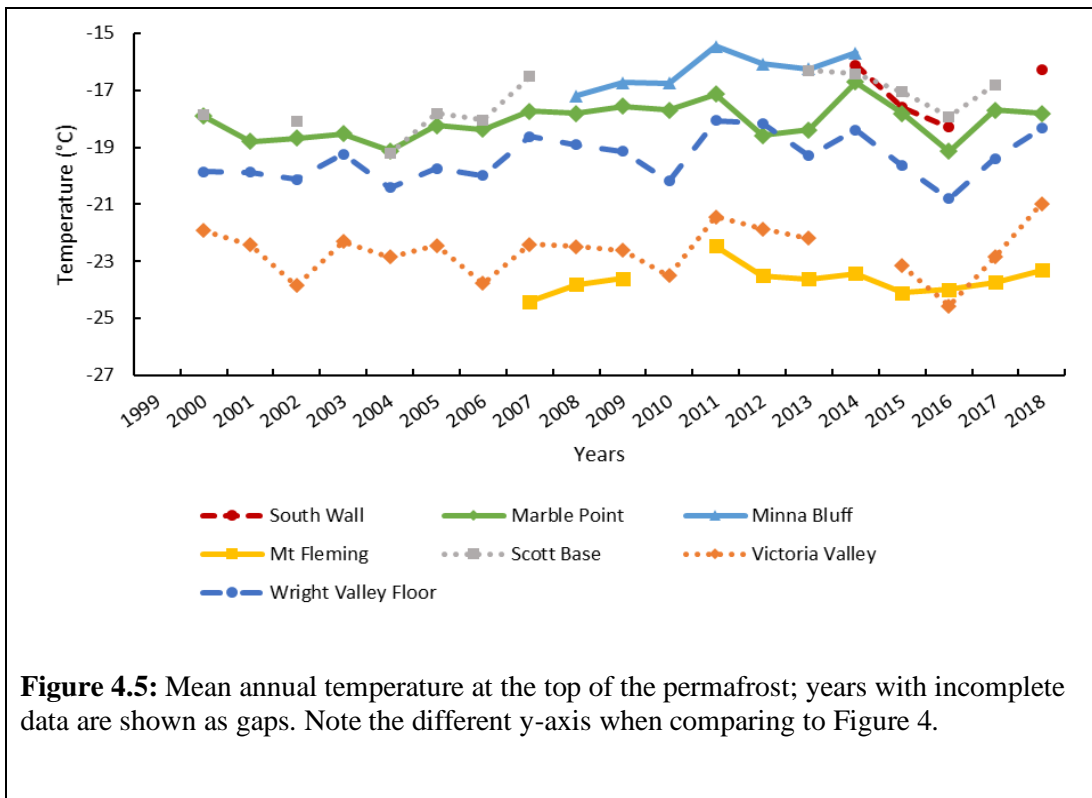
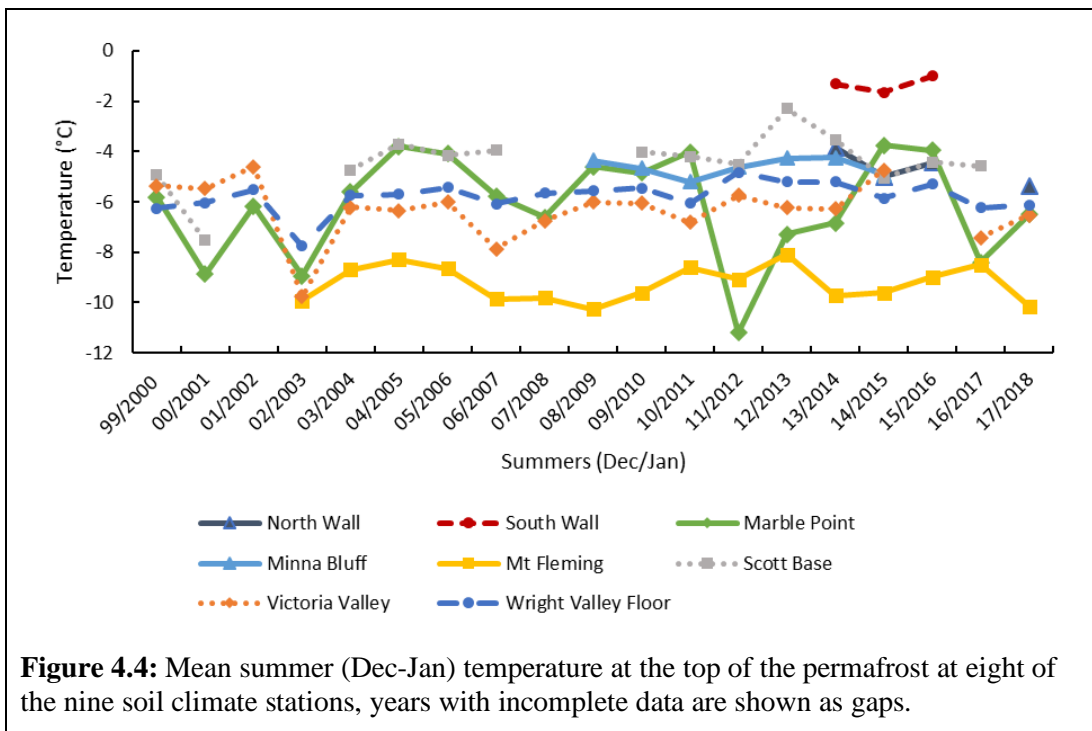
4.4 Results

The ALD showed some between-year variation (Figure 4.2). The high altitude Mt Fleming site had the shallowest active layer depth, and the deepest active layer was at Granite Harbour. At the Granite Harbour site the soil is subjected to melt water warming and the ALD, were shown as 90 cm but should be interpreted as >90 cm (the depth of the deepest sensor). The coastal station at Marble Point in both the 2000/2001 summer and the 2011/2012 summer had a particularly shallow ALD, which differed from the general pattern at other stations. The mean ALD for each site was recorded using all available years, and plotted in two transects: an altitudinal transect including Mt Fleming, the North and South

Wright Valley Walls, Victoria Valley, Wright Valley Floor, and Marble Point; and a latitudinal transect; from Minna Bluff in the south through Scott Base, Marble Point, to Granite Harbour in the north. ALD decreased with increasing altitude ($R^2 = 0.71$) and increased with increasing latitude ($R^2 = 0.66$) (Figure 4.3).



Assessing the mean summer (December/January) temperature at the top of the permafrost showed between year variation (Figure 4.4). The mean annual temperature at the top of the permafrost (Figure 4.5) also showed between year variation.



The Mann-Kendall test was used to test the null hypothesis that there was significant warming or cooling trends in ALD and mean annual temperature at the top of the permafrost and the null hypothesis was rejected at all sites across the

time series for both tests. P-values were all greater than 0.05 (Table 4.2). This was followed by Kendall's Tau-b test showing no association between time and ALD, as no values were close to 1 or -1. In the mean permafrost temperature trend at, Marble Point had a p-value of 0.08 and so was the closest to showing a trend. Kendall's Tau-b test showed a weak positive association between time and mean annual permafrost temperature at Minna Bluff but no association at other sites (Table 4.2). Likewise, there were no significant trends in mean summer permafrost temperature (Carshalton, 2019).

Table 4.2: Trend analysis results of ALD and mean annual top of the permafrost temperature for each climate station series. The null hypothesis that there is was a warming or cooling trend was rejected at all sites (WV = Wright Valley).

ALD	Mean Annual Permafrost temp			
	p-value	Tau-b	p-value	Tau-b
Granite Harbour	0.6775	-0.1008	ND	ND
Marble Point	0.2342	0.2047	0.0802	0.2982
Minna Bluff	0.2515	-0.3333	0.1331	0.5238
Mt Fleming	0.1917	-0.25	0.5334	0.1636
North Wall WV	0.7341	0.3333	ND	ND
Scott Base	0.9671	-0.0147	0.1611	0.3455
South Wall WV	0.7341	0	0.7341	-0.3333
Victoria Valley	0.8926	-0.0333	0.9698	-0.0065
WV Floor	0.8337	-0.0409	0.2079	0.2164

For wavelet analysis, temperature at the top of the permafrost was used as these data are naturally smoothed with less hourly variability relative to air temperature, and they are also influenced by other atmospheric variables, such as incoming radiation. Cross wavelet analysis between three climate drivers (SOI, SAM, and ASL) and four sites showed significant high power events between 1999 and 2018. In the Wright Valley significant ($p < 0.05$) periods with high power were identified between: the SAM (\approx 1-2 year cycle); the SOI (\approx 3 year cycle); and the ASL (\approx 1 year cycle) (Figure 4.6 a, b, c). Similar results were recorded at Marble Point, Victoria Valley and Mt Fleming (Table 4.3). Significant ($p < 0.05$) low energy relationships occurred between the climate drivers and the four soil climate stations at similar periods and dates (Table 4.4).

Table 4.3: Significant high amplitude periods identified with cross wavelet analysis between potential climate drivers and de-seasonalised permafrost temperature at listed soil climate stations.

Cross wavelet	SAM (years)	SOI (years)	ASL (years)
Marble Point	1 - 2	1 & 3	0.75 - 1
Mt Fleming	1	6 - 1 & 3	0.75 - 1
Victoria Valley	1 - 2	2 - 3	0.75 - 1
Wright Valley Floor	1 - 2	1 & 2- 3	0.75 - 1

Table 4.4: Significant but low amplitude periods identified with cross wavelet analysis between potential climate drivers and de-seasonalised permafrost temperature at listed soil climate stations.

Coherence	SAM (years)	SOI (years)	ASL (years)
Marble Point	< 1 & 2	0.5 - 1	0.5 - 1 year
Mt Fleming	< 1	< 1 and 2	< 1 year
Victoria Valley	< 1 & 1-2	3 - 4 years	4, 2 & <1
Wright Valley Floor	0.5 - 2	0.5 - 1 & 2 -4	< 1

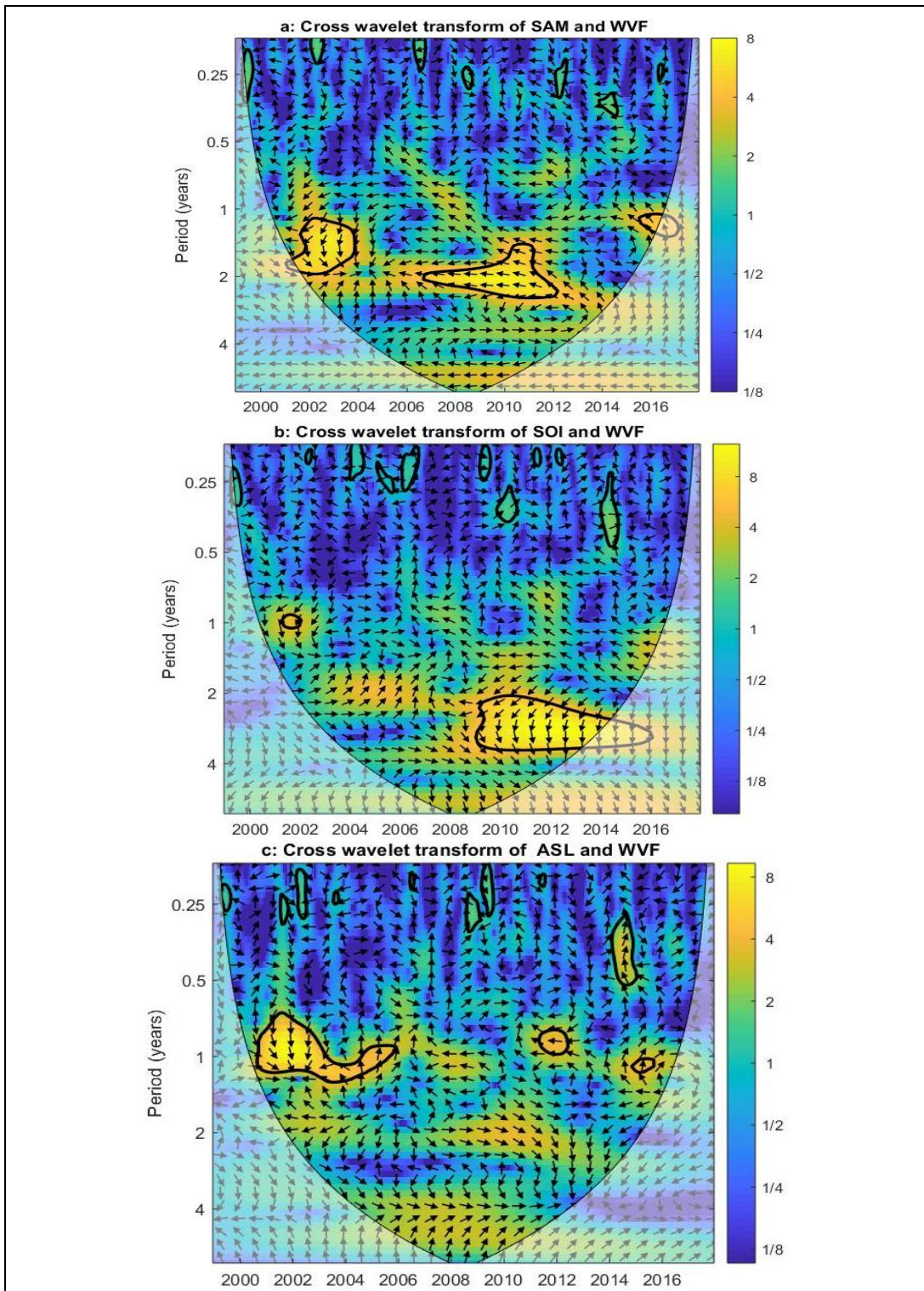


Figure 4.6: Cross wavelet transform between de-seasonalised permafrost temperature data at the Wright Valley Floor (WVF) and climate drivers. a: Southern Annular Mode (SAM); b: Southern Oscillation Index (SOI); c: Amundsen Sea Low pressure (ASL). The amplitude is displayed by the colour bar. Yellow corresponds to strong signal (amplitude) and areas within the black contours are significant ($p < 0.05$). Data in the paler shaded areas are influenced by the ‘edge effect’ and so are less reliable. Arrows correspond to phase relationships, where pointing right is in phase, and pointing downward means the climate driver leads the soil temperature by a quarter cycle.

4.5 Discussion

The ALD across all sites followed a similar pattern of variation between 1999 and 2018. Mt Fleming, on the edge of the Polar Plateau, had the shallowest ALD and coldest temperatures (Table 4.1, figures 4.2 and 4.3). While the deepest ALDs were at Granite Harbour, with the depth of thaw exceeding 90 cm in some years. The soil climate station at Granite Harbour is on a north facing slope that has subsurface water flow, which transfers heat to depth, so the site has a deeper ALD than typical of the wider area. New sites, not previously reported, on the walls of the Wright Valley had ALD values between those of Mt Fleming and the Wright Valley Floor but were deeper than at Victoria Valley, which is at a lower altitude. The Wright Valley Floor and Marble Point on the coast had similar ALDs (Figure 4.2) — although Marble Point had a particularly shallow ALD in 2011/2012 summer. There was more snow than usual recorded on the ground at Marble Point during the 2011/12 summer, which would have had an insulating effect on the soil reducing the overall thaw depth. Both the altitudinal transect from Mt Fleming to Marble Point (Figure 4.3a) and the latitudinal transect from Minna Bluff to Granite Harbour (Figure 4.3b), showed a linear relationship to ALD similar to previous findings in the Ross Sea Region (Adlam et al., 2009).

The ALD at Victoria Valley was shallower than all three sites in the Wright Valley, even though it is at a lower elevation than the sites on the Wright Valley walls (Figure 4.2). Victoria Valley also has colder mean annual permafrost and air temperatures than all three Wright Valley sites, though the mean summer temperatures on the Wright Valley floor and at Victoria Valley were similar (Figure 5). The likely reason for the shallower ALD and colder mean annual temperatures at Victoria Valley is topographic, with the Victoria Valley experiencing long periods of stable calm weather in winter, allowing a cold air cell (inversion layer) to settle over the valley bottom and drive winter temperatures down (Doran et al., 2002a). Weaker winter storms tend to flow over the cold cell and into downhill valleys through mountain passes (such as Bull Pass into the Wright Valley), rather than breakup the inversion layer. In summer the Victoria Valley receives coastal winds and, like the Wright Valley, the wide flat bottom allows for easy solar heating (Doran et al., 2002a), which is observable when comparing the mean summer temperatures (Figure 4.4).

Both warming (Goddard, 2013; Guglielmin and Cannone, 2012; Guglielmin et al., 2014; Guglielmin et al., 2012; Oliva et al., 2017) and cooling trends (Doran et al., 2002b; Oliva et al., 2017; Ramos et al., 2017) in Antarctica and the McMurdo Dry Valley area have been previously reported. Non-parametric trend testing was used in this study as the data set was reasonably short (maximum of 18 points), and no linear trends were observed. Goddard (2013) The weak warming trend in permafrost temperature reported by (Goddard, 2013) between 2000 and 2011 at Marble Point did not continue.

Figure 6-a shows a significant ($p < 0.05$) high energy event between the SAM and the Wright Valley Floor cross wavelet in 2002, with downward arrows showing that the SAM was leading (driving) the Wright Valley Floor temperature; the same event was also observed at Victoria Valley and Marble Point (Carshalton, 2019). The cross wavelet signal is observable in the ALD, with a deeper ALD recorded in the 2001/2002 summer (Figure 4.2) at the Wright Valley Floor and Marble Point. The warmer 2001/2002 summer was previously studied (Foreman et al. 2004; Barrett et al. 2008; Adlam et al., 2009) and a blocking high was identified in the South Atlantic in September 2001 which dominated the meteorology of the Southern Ocean, influencing the atmospheric wave patterns and air pressure, in both the Amundsen and Weddell seas (Turner et al., 2002; Massom et al., 2006). The pattern was shown to resemble the SAM, with the index having positive values for the 2001/2002 summer- linked to strong westerly winds (Simmonds and Keay 2000; Thompson et al. 2000; Massom et al., 2006). A small low pressure system was also present over the Ross Sea during this time, which may be associated with the ASL, which may have contributed to the warmer temperatures (Adlam et al., 2009; Turner et al., 2002).

Since the 2001/2002 event further significant warming events have occurred between the local climate and the SAM and SOI, firstly on the west of the Antarctic Peninsula in 2008 and 2010, and the north-east of the Antarctic Peninsula in 2001, 2008, 2005 and 2010 (Clem and Fogt, 2013). These events were evident in wavelet energy spectra between 2008 and 2010 between the SAM and the Wright Valley Floor data (Figure 4.6a) and from 2009 onwards between the SOI and the Wright Valley Floor data (Figure 4.6b). The ASL had a clear seasonal pattern that generally correlated with both the SAM and the SOI, with the strongest relationship occurring in spring (Cohen et al., 2013).

Due to the length of the data set and the ‘edge effect’, the significant relationship between the Wright Valley Floor data and the SOI in 2015 and 2016 (Figure 4.6b) should be interpreted with caution, but this period of time corresponds with a strong El Niño event in the SOI, as well as the SAM in a strong negative stage, the second lowest since satellite recording began (Schlosser et al., 2018). Cooling and growing sea ice occurred throughout 2015 and the start of 2016 and then there was a sudden warming and reduction of sea ice in spring the of 2016 (Stuecker et al., 2017). The change in sea ice extent, and the cross wavelet correlations between the climate systems and the Wright Valley Floor data, may also correspond to the cooling (2014 – 2016) then warming (2016 - 2018) pattern in the mean annual permafrost temperature in the majority of the soil climate stations (Figure 4.5).

4.6 Conclusion

The soil climate and ALD have been monitored continuously across nine sites in the McMurdo Sound Region, Antarctica between 1999 and 2018. Between the 1999/2000 and 2017/2018 summers the ALD varied between summers and ranged from a mean of -7.6 cm at Mt Fleming to > 90 cm at Granite Harbour. There was an expected relationship in between mean ALD and both altitude ($R^2= 0.71$) and latitude ($R^2= 0.66$). The mean annual temperature at the top of the permafrost ranged between -15°C and -24.5°C, and the mean summer temperature (December and January) was between -3°C and -11°C across the soil climate stations. The local environment plays a strong role in controlling the soil climate at some sites. The ALD at Granite Harbour is deeper than the surrounding area due to the effect of melt water transferring heat. At Victoria Valley mean annual temperatures are cooler other sites due to long lasting winter inversion layers and less storms.

While past research has reported both warming and cooling trends in soil temperature and ALD around Antarctica, no trends in warming or cooling were evident in ALD or mean annual and mean summer temperatures at the top of the permafrost at any sites. Cross wavelet analysis between de-seasonalised permafrost temperature and the SAM, SOI and ASL, showed significant ($p<0.05$) periods reoccurred through the data sets. With corresponding events in ALD in the 2001/2002 summer, and in mean annual permafrost temperature between 2014

and 2018. Conclusions on long-term trends or predictions cannot be drawn as the data set is too short. Continued monitoring is highly recommended.

4.7 Acknowledgements

This research was partly funded by Landcare Research - Ross Sea Region Terrestrial Data Analysis research programme, MBI contract no. C09X1413 and logistic support from Antarctica New Zealand. Thanks to John Kimble, Ron Paetzold, Don Huffman, Iain Campbell, Jackie Aislabie and Deb Harms for assisting in the initial climate station establishment. Thanks to Chris Morcom, Dean Sandwell, Fraser Morgan and Aaron Wall for ongoing technical support. Funding assistance for Annette Carshalton was provided by the Broad Memorial Fund.

4.8 References

- Adlam, L.S., Balks, M.R., Seybold, C.A., Campbell, D.I., 2009. Temporal and spatial variation in active layer depth in the McMurdo Sound Region, Antarctica. *Antarctic Science* 22(1), 45-52. <https://doi.org/10.1017/S0954102009990460>.
- Agresti, A., 2010. *Analysis of Ordinal Categorical Data*. John Wiley & Sons, New York. <https://doi.org/10.1002/9780470594001.ch1>.
- Almeida, I.C.C., Schaefer, C.E.G.R., Michel, R.F.M., Fernandes, R.B.A., Pereira, T.T.C., de Andrade, A.M., Francelino, M.R., Fernandes Filho, E.I., Bockheim, J.G., 2017. Long term active layer monitoring at a warm-based glacier front from maritime Antarctica. *CATENA* 149, 572-581. <https://doi.org/10.1016/j.catena.2016.07.031>.
- Bertler, N.A.N., Barrett, P.J., Mayewski, P.A., Fogt, R.L., Kreutz, K.J., Shulmeister, J., 2004. El Niño suppresses Antarctic warming. *31(15)*. <https://doi.org/10.1029/2004gl020749>.
- Burkey, J., 2006. A non-parametric monotonic trend test computing Mann-Kendall Tau, Tau-b, and Sen's Slope written in Mathworks-MATLAB implemented using matrix rotations. In: ktaub.m (Ed.), *Mathworks-MATLAB*. King County, Department of Natural Resources and Parks, Science and Technical Services section, Seattle, Washington. USA, <http://www.mathworks.com/matlabcentral/fileexchange/authors/23983>
- Campbell, I.B., Claridge, G.G.C., 1987. *Antarctica: Soils, weathering processes and environment*. Elsevier Science Pub. Co. Inc., New York, NY; None,

- Carshalton, A.G., 2019. 18 years of Active layer and soil climate monitoring, Ross Sea Region, Antarctica. Universtiy of Waikato Hamilton, New Zealand,
- Clem, K.R., Fogt, R.L., 2013. Varying roles of ENSO and SAM on the Antarctic Peninsula climate in austral spring. 118(20), 11,481-411,492.<https://doi.org/10.1002/jgrd.50860>.
- Cohen, L., Dean, S., Renwick, J., 2013. Synoptic Weather Types for the Ross Sea Region, Antarctica. *Journal of Climate* 26(2), 636-649.<https://doi.org/10.1175/jcli-d-11-00690.1>.
- de Pablo, M.A., Ramos, M., Molina, A., Prieto, M., 2018. Thaw depth spatial and temporal variability at the Limnopolar Lake CALM-S site, Byers Peninsula, Livingston Island, Antarctica. *Science of The Total Environment* 615, 814-827.<https://doi.org/10.1016/j.scitotenv.2017.09.284>.
- Doran, P.T., McKay, C.P., Clow, G.D., Dana, G.L., Fountain, A.G., Nylen, T., Lyons, W.B., 2002a. Valley floor climate observations from the McMurdo dry valleys, Antarctica, 1986–2000. 107(D24), ACL 13-11-ACL 13-12.<https://doi.org/10.1029/2001jd002045>.
- Doran, P.T., Priscu, J.C., Lyons, W.B., Walsh, J.E., Fountain, A.G., McKnight, D.M., Moorhead, D.L., Virginia, R.A., Wall, D.H., Clow, G.D., Fritsen, C.H., McKay, C.P., Parsons, A.N., 2002b. Antarctic climate cooling and terrestrial ecosystem response. *Nature* 415(6871), 517-520.<https://doi.org/10.1038/nature710>.
- Goddard, H.E., 2013. Investigation of air and soil climate across the latitudinal and altitudinal gradient of the Ross Sea region of Antarctica. Masters Thesis, University of Waikato, Hamilton, New Zealand, <http://hdl.handle.net/10289/7908>.
- Grinsted, A., Moore, J.C., Jevrejeva, S., 2004. Application of the cross wavelet transform and wavelet coherence to geophysical time series. *Nonlin. Processes Geophys.* 11(5/6), 561-566.<https://doi.org/10.5194/npg-11-561-2004>.
- Guglielmin, M., Cannone, N.J.C.C., 2012. A permafrost warming in a cooling Antarctica? 111(2), 177-195.<https://doi.org/10.1007/s10584-011-0137-2>.
- Guglielmin, M., Dalle Fratte, M., Cannone, N., 2014. Permafrost warming and vegetation changes in continental Antarctica. *Environmental Research Letters* 9(4), 045001.[10.1088/1748-9326/9/4/045001](https://doi.org/10.1088/1748-9326/9/4/045001).
- Guglielmin, M., Worland, M.R., Cannone, N., 2012. Spatial and temporal variability of ground surface temperature and active layer thickness at the margin of maritime Antarctica, Signy Island. *Geomorphology* 155, 20-33.<http://dx.doi.org/10.1016/j.geomorph.2011.12.016>.
- Hosking, J.S., Orr, A., Bracegirdle, T.J., Turner, J., 2016. Future circulation changes off West Antarctica: Sensitivity of the Amundsen Sea Low to

projected anthropogenic forcing. 43(1), 367-376.<https://doi.org/10.1002/2015gl067143>.

Hosking, J.S., Orr, A., Marshall, G.J., Turner, J., Phillips, T., 2013. The Influence of the Amundsen–Bellingshausen Seas Low on the Climate of West Antarctica and Its Representation in Coupled Climate Model Simulations. 26(17), 6633-6648.<https://doi.org/10.1175/jcli-d-12-00813.1>.

Hrbáček, F., Kňázková, M., Nývlt, D., Láska, K., Mueller, C.W., Ondruch, J., 2017. Active layer monitoring at CALM-S site near J.G.Mendel Station, James Ross Island, eastern Antarctic Peninsula. *Science of The Total Environment* 601-602, 987-997.<https://doi.org/10.1016/j.scitotenv.2017.05.266>.

IPCC, 2014. How will permafrost, the active layer and water availability in Antarctic soils and marine sediments change in a warming climate, and what are the effects on ecosystems and biogeochemical cycles? ,

Kennicutt, M.C., Chown, S.L., Cassano, J.J., Liggett, D., Peck, L.S., Massom, R., Rintoul, S.R., Storey, J., Vaughan, D.G., Wilson, T.J., Allison, I., Ayton, J., Badhe, R., Baeseman, J., Barrett, P.J., Bell, R.E., Bertler, N., Bo, S., Brandt, A., Bromwich, D., Cary, S.C., Clark, M.S., Convey, P., Costa, E.S., Cowan, D., Deconto, R., Dunbar, R., Elfring, C., Escutia, C., Francis, J., Fricker, H.A., Fukuchi, M., Gilbert, N., Gutt, J., Havermans, C., Hik, D., Hosie, G., Jones, C., Kim, Y.D., Le Maho, Y., Lee, S.H., Leppe, M., Leitchenkov, G., Li, X., Lipenkov, V., Lochte, K., López-Martínez, J., Lüdecke, C., Lyons, W., Marensi, S., Miller, H., Morozova, P., Naish, T., Nayak, S., Ravindra, R., Retamales, J., Ricci, C.A., Rogan-Finnemore, M., Ropert-Coudert, Y., Samah, A.A., Sanson, L., Scambos, T., Schloss, I.R., Shiraishi, K., Siegert, M.J., Simões, J.C., Storey, B., Sparrow, M.D., Wall, D.H., Walsh, J.C., Wilson, G., Winther, J.G., Xavier, J.C., Yang, H., Sutherland, W.J., 2014. A roadmap for Antarctic and Southern Ocean science for the next two decades and beyond. *Antarctic Science* 27(1), 3-18.<https://doi.org/10.1017/S0954102014000674>.

Lau, K.-M., Weng, H., 1995. Climate Signal Detection Using Wavelet Transform: How to Make a Time Series Sing. 76(12), 2391-2402.[10.1175/1520-0477\(1995\)076<2391:Csdwt>2.0.Co;2](https://doi.org/10.1175/1520-0477(1995)076<2391:Csdwt>2.0.Co;2).

Marshall, G.J., 2003. Trends in the Southern Annular Mode from Observations and Reanalyses. 16(24), 4134-4143.[https://doi.org/10.1175/1520-0442\(2003\)016<4134:Titsam>2.0.Co;2](https://doi.org/10.1175/1520-0442(2003)016<4134:Titsam>2.0.Co;2).

Massom, R.A., Stammerjohn, S.E., Smith, R.C., Pook, M.J., Iannuzzi, R.A., Adams, N., Martinson, D.G., Vernet, M., Fraser, W.R., Quetin, L.B., Ross, R.M., Massom, Y., Krouse, H.R., 2006. Extreme Anomalous Atmospheric Circulation in the West Antarctic Peninsula Region in Austral Spring and Summer 2001/02, and Its Profound Impact on Sea Ice and Biota. 19(15), 3544-3571.<https://doi.org/10.1175/jcli3805.1>.

Oliva, M., Navarro, F., Hrbáček, F., Hernandez, A., Nývlt, D., Pereira, P., Ruiz-Fernandez, J., Trigo, R., 2017. Recent regional climate cooling on the Antarctic Peninsula and associated impacts on the cryosphere. *The Science*

of the total environment 580, 210-223.<https://doi.org/10.1016/j.scitotenv.2016.12.030>.

Ramos, M., Vieira, G., de Pablo, M.A., Molina, A., Abramov, A., Goyanes, G., 2017. Recent shallowing of the thaw depth at Crater Lake, Deception Island, Antarctica (2006–2014). *CATENA* 149, 519-528.<https://doi.org/10.1016/j.catena.2016.07.019>.

Ropelewski, C.F., Jones, P.D., 1987. An extension of the Tahiti-Darwin Southern Oscillation Index. *Monthly Weather Review*, 115,, 2161-2165,

Schlosser, E., Haumann, F.A., Raphael, M.N., 2018. Atmospheric influences on the anomalous 2016 Antarctic sea ice decay. *The Cryosphere* 12(3), 1103-1119.<https://doi.org/10.5194/tc-12-1103-2018>.

Stuecker, M.F., Bitz, C.M., Armour, K.C., 2017. Conditions leading to the unprecedented low Antarctic sea ice extent during the 2016 austral spring season. 44(17), 9008-9019.<https://doi.org/10.1002/2017gl074691>.

Torrence, C., Compo, G.P., 1998. A Practical Guide to Wavelet Analysis. 79(1), 61-78.[https://doi.org/10.1175/1520-0477\(1998\)079<0061:Apgtwa>2.0.Co;2](https://doi.org/10.1175/1520-0477(1998)079<0061:Apgtwa>2.0.Co;2).

Turner, J., Harangozo, S.A., Marshall, G.J., King, J.C., Colwell, S.R., 2002. Anomalous atmospheric circulation over the Weddell Sea, Antarctica during the Austral summer of 2001/02 resulting in extreme sea ice conditions. 29(24), 13-11-13-14.<https://doi.org/10.1029/2002gl015565>.

Turner, J., Lu, H., White, I., King, J.C., Phillips, T., Hosking, J.S., Bracegirdle, T.J., Marshall, G.J., Mulvaney, R., Deb, P., 2016. Absence of 21st century warming on Antarctic Peninsula consistent with natural variability. *Nature* 535, 411.<https://doi.org/10.1038/nature18645>.

Chapter Five

Prediction of active layer depth from above ground variables, Ross Sea Region, Antarctica

(Submission in preparation)

5.1 Abstract

Soil temperature and active layer depth (ALD) are strongly influenced by atmospheric variables, as well as soil properties. Nineteen potential models were developed using stepwise analysis and compared to the previous work of Adlam et al. (2010), using data from a soil climate monitoring network made up of nine soil climate stations (SCS) within the McMurdo Dry Valleys and along the adjacent coast.

The Adlam et al. (2010) model, used mean summer air temperature (MSAT), mean winter air temperature (MWAT), total summer solar radiation (TSSR), and mean summer wind speed (MSWS), and had an adjusted $R^2 = 0.69$. The Adlam et al. (2010) model was tested using a further ten years of data from the same five low altitude sites the model was developed on and produced reasonable results (average ± 20 cm). At a further two mid-altitude sites (700 – 800 m) on the walls of the Wright Valley, the ALDs were also predicted with reasonable accuracy (± 15 cm North Wall, $> \pm 20$ cm South Wall).

A statistically improved model, Model 8, was developed using 16 years of data from the five low-altitude SCS, using altitude, air temperature and surface temperature (Adjusted $R^2 = 0.75$; $p < 0.001$). Model 8 predicted the ALD within ± 10 cm at all five low altitude sites, but when applied to the three higher altitude sites Model 8 was unable to accurately predict ALD ($> + 32$ cm).

Model 14 (Adjusted $R^2 = 0.49$; $p < 0.001$) was the best option of the models explored to produce a large scale, low-resolution model of the ALD across Antarctica. Model 14 was developed using data from eight SCS (low, mid, and high altitude sites), using MSAT and mean surface temperature provided an improved fit between measured and predicted ALD at the mid and high altitude sites (average $< \pm 11$ cm). At the lower altitude sites, Model 14 failed to show the detailed between year variation accurately but provided a reasonable fit (average $< \pm 20$ cm).

To determine the robustness of the models it would be advantageous to test them on data from other Antarctic sites. As ground-surface temperature has been shown to be a strong predictive factor for ALD, future investigation into the use of satellite data in predicting ALD at a regional scale should be considered.

5.2 Introduction

As the global climate changes monitoring is needed to better understand the effect of climate perturbations and predict future change. Approximately 0.36% of Antarctica is ice-free (Bockheim et al., 2015). This area growing with time as glaciers retreat and coastal ice-free areas expand, though currently such changes have only been observed on to the Antarctic Peninsula (Lee et al., 2017). With the continued could see the ice free land to expand by up to 25% by the end of the 21st century (Lee et al., 2017). Thus, the need to understand and quantify the changes in soil climate is important.

The active layer is the top layer in the cryosol soil profile which freezes and thaws each year, while permafrost underlies the active layer and remains frozen for two or more years (Campbell and Claridge, 1987). It is important to understand changes occurring in active layer depth (ALD) as the ALD is able to integrate the variation of multiple atmospheric climate variables that change on short (minute to hourly) time scales, thus ALD is potentially a reliable indicator of climate change. Active layer and permafrost monitoring in Antarctica is limited to isolated areas, including the Antarctic Peninsula and maritime islands (Almeida et al., 2017; de Pablo et al., 2018; Guglielmin et al., 2012; Hrbáček et al., 2017; Michel et al., 2012; Oliva et al., 2017; Ramos et al., 2017), Continental West Antarctica (Mauro et al., 2014; Schaefer et al., 2016), the McMurdo Dry Valleys and Victoria Land (Adlam et al., 2010; Balks et al., 1995; Conovitz et al., 2006; Guglielmin, 2006; Ikard, 2009) and generally, continuous monitoring has only occurred since about 2000. The monitoring of atmospheric variables has been more widespread with short and long-term projects, with varying parameters measured starting in 1909 by Ernest Shackleton, with the longest continuous running weather monitoring programme in Antarctica was initiated by the British Antarctic Survey in the 1950's (Martin, 2016).

Due to logistical constraints monitoring the soil climate more widely in Antarctica is not generally viable and thus modelling needs to be considered. With a range of atmospheric climate data available, along with satellite remote sensing data, attempting to model the soil climate by utilising atmospheric variables, allows for a greater understanding of the current Antarctic soil climate and the ability to study how the soil environment might change with a changing global climate.

Previous attempts to model the soil ALD (or depth to permafrost), using both empirical and numerical methods, have been made in the Arctic and Antarctic (Riseborough et al., 2008). Most models focused on using soil characteristics such as bulk density, thermal conductivity and thermal diffusivity, with the two most well-known models being the Stephan Model and the Kudryavtsev Model (Riseborough et al., 2008). The Stephan Model (Lunardini, 1981; Riseborough et al., 2008) relies on knowing the soil properties, as well as the location's summer air temperature, and representative ALD data (Nelson et al., 1997; Shiklomanov and Nelson, 2003; Zhang T. et al., 2005; Riseborough et al., 2008). The Kudryavtsev Model (1974) is a more complex model than the Stefan Model, and is used to predict ALD and the mean annual permafrost temperature, and utilises surface temperature, soil properties, and air temperature variables. The Kudryavtsev Model has successfully predicted ALD at a regional and continental scale in the Arctic (Anisimov et al., 1997; Shiklomanov and Nelson, 1999; Sazonova and Romanovsky, 2003; Stendel et al., 2007; Riseborough et al., 2008).

In Antarctica, both the Stephan and the Kudryavtsev models were applied at three sites between 2011 and 2014 across the Western Antarctic Peninsula, with reasonable success (Wilhelm et al., 2015). In bedrock material the Stephan Model was a reasonable fit, predicting a shallower ALD ($11.9 \text{ m} \pm 1.4$), while the Kudryavtsev Model predicted a deeper ALD ($18.6 \text{ m} \pm 4.9$) than measured in bedrock material ($12.5 - 14.5 \text{ m}$) (Wilhelm et al., 2015). In unconsolidated material, the predicted ALD's were unable to be verified as the measurement boreholes were not deep enough (Wilhelm et al., 2015). Though it was suggested by Uxa (2017) that the ALD's modelled by both the Stephan and Kudryavtsev models by Wilhelm et al. (2015) were overestimated, due to the models assuming that little latent heat was absorbed during thawing.

The relationship between atmospheric variables and ALD is well established, and in the Ross Sea Region (RSR) of Antarctica (Adlam et al., 2010; Lacelle et al., 2016; Waelbroeck, 1993). In the Quartermain Mountains, above the Taylor Glacier, a strong relationship was found between mean air and surface temperatures ($R^2 = 0.92$, $p < 0.01$), as well as a strong relationship with mean incoming solar radiation ($R^2 = 0.72$, $p < 0.01$) (Lacelle et al., 2016). Both incoming solar radiation and measured surface temperature were used to model at a whole valley scale, where the surface temperature remains perennially frozen, and

areas where an active layer forms, though the ALD was not modelled, in the Beacon and University valleys of the Quartermain Mountains (Lacelle et al., 2016). Guglielmin et al. (2012) reported that air temperature explained between 50 % and 80 % of the seasonal variation in ground surface temperature across four years of data at study sites in the South Orkney Islands. Wind speed and incoming solar radiation had a minor role in driving surface temperature, with air temperature as the main driver (Adlam et al., 2010; Guglielmin et al., 2012). However, the relationship between surface temperature and ALD was not reported as significant (Guglielmin et al., 2012).

Adlam et al. (2010) developed a model to predict ALD utilising atmospheric data collected between 1999 and 2007 from the RSR soil climate monitoring network (Figure 5.1). The model developed by Adlam et al. (2010) was completed using stepwise multiple regression, and gave the following equation:

$$\text{ALD} = 222 + 5.69(\text{MSAT}) + 3.63(\text{MWAT}) - 10.6(\text{TSSR}) - 2.84(\text{MSWS})$$

Where ALD (cm) is active layer depth, MSAT (°C) is mean summer (December – January (DJ)) air temperature, MWAT (°C) is mean winter (June – August) air temperature, TSSR is total summer (DJ) solar radiation (100 kW/m²) and MSWS (ms⁻¹) is mean summer (DJ) wind speed. The overall model had an adjusted R² = 0.69 (Adlam et al., 2010). The soil climate monitoring network has been recording continuously since 1999 and the data from the network, up to the end of 2018, was used for the work in this paper.

The objectives of this paper were to (1) test the model developed by Adlam et al. (2010) with an additional decade of data and (2) develop improved models to predict ALD using both stepwise regression and restricted maximum likelihood methods.

5.3 Methods

A soil and atmospheric climate network made up of nine soil climate stations was installed in the McMurdo Dry Valleys (MDVs) and along the Southern Ross Sea coast (Figure 5.1, Table 5.1). An altitudinal transect runs through the MDVs from Mt Fleming at the head of the Wright Valley (1700 m), through two stations located on the walls of the Wright Valley (832 m and 728 m), and two valley floor sites, one in the Wright Valley below Bull Pass (160 m) and the other in the

Victoria Valley (410 m) next to Lake Victoria, culminating on the coast at Marble Point (60 m). A latitudinal transect is present along the coast with Minna Bluff (78°30'41.6" S) in the south, through Scott Base and Marble Point to Granite Harbour in the north (77°00'23.7" S). The atmospheric conditions vary across the nine sites as expected with higher windspeeds and cooler temperatures at higher altitudes (Mt Fleming) and southern latitudes (Minna Bluff), while warmer conditions are experienced in more northern and sheltered locations. The ALDs follow a pattern similar to the atmospheric conditions at each site, except at Granite Harbour where the ALD is deeper (>90 cm) compared to the rest of the network (Table 5.1). The deeper ALD depth at the Granite Harbour soil climate station is likely to be due to the sites' micro-climate, that has subsurface water flow transferring heat to depth, causing a deeper ALD than the wider area (Carshalton et al., submitted). Thus, the Granite Harbour soil climate data was excluded from modelling efforts. The hourly atmospheric and soil climate data used in this paper is available at:

https://www.nrcs.usda.gov/wps/portal/nrcs/detail/soils/survey/climate/?cid=nrcs142p2_053772

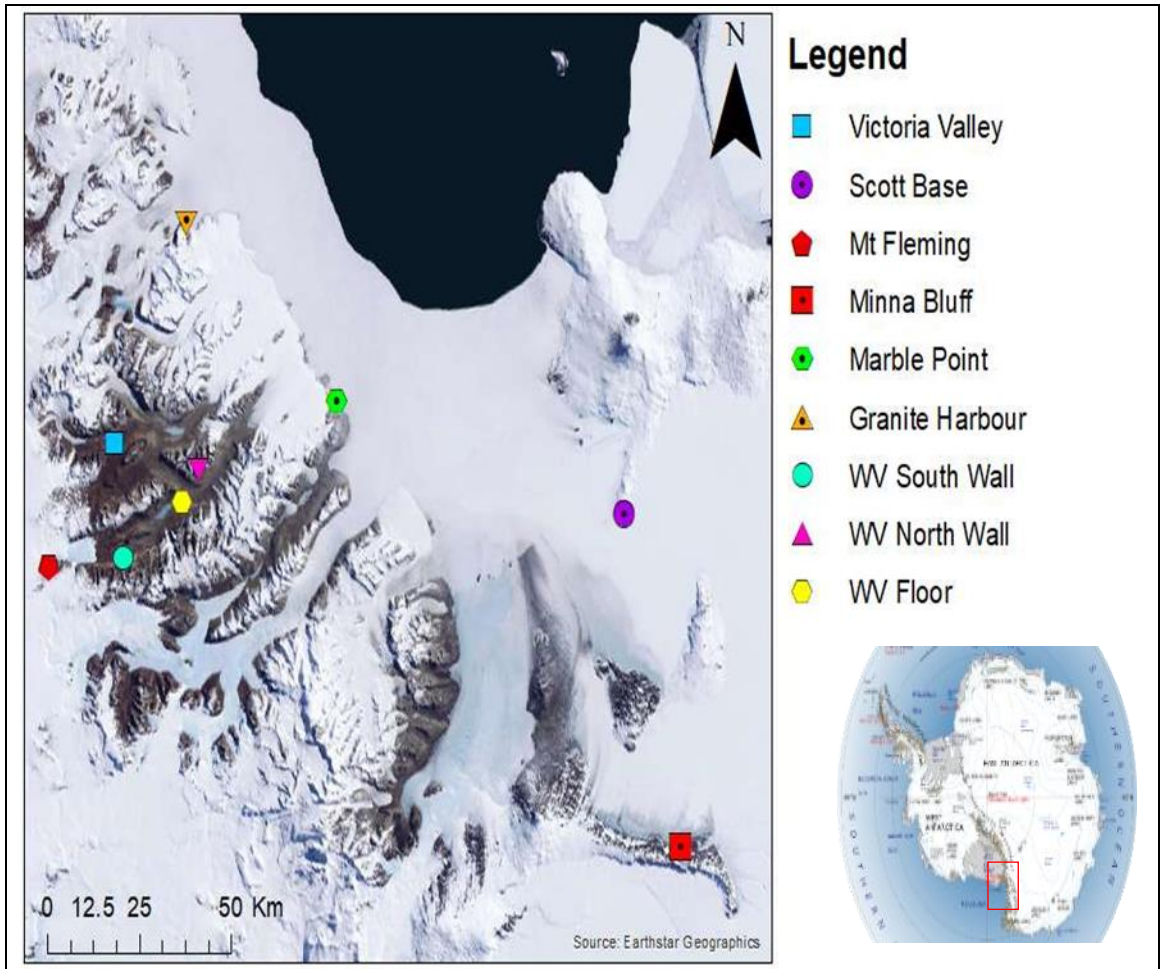


Figure 5.1: Soil climate monitoring sites location map, with the insert showing the location of the McMurdo Dry Valleys. WV = Wright Valley (Carshalton et al., 2019).

Table 5.1: Description for each site in the soil climate monitoring network, and including mean summer and winter atmospheric conditions, and mean active layer depth at each site across the stations record, from site establishment to 2018. WV = Wright Valley. Adapted from Carshalton et al. (submitted).

Site (date established)	GPS Coordinates	Site location	Site Description (elevation, aspect, slope)	Windspeed (Km/h)		Mean Air Temperature (°C)		Mean ALD (cm)
				Mean Summer	Maximum	Winte r	Summer	
Granite Harbour (2003)	77°00'23.7"S 162°31'32.4"E	On 10 m wide boulder lateral moraine ledge between coast and base of cliff	4.5 masl, North West (300°), 10°	6.24	85.70	-25.93	-1.02	90
Marble Point (1999)	77°25'10.6"S 163°40'55"E	400 m E of the Wilson-Piedmont Glacier, 620 m S of USA helicopter refuelling station	60 masl South facing (180°), 3%,	10.27	86.10	-26.59	-2.73	50
Minna Bluff (2003)	78°30'41.6"S 166°45'58"E	75 km S of Scott Base, on N side of Minna Bluff Peninsula	37 masl, North facing (360°), < 5°	20.81	160.93	-27.33	-1.70	29
Mt Fleming (2002)	77°32'42.7"S 166°17'24.6"E	Flat rocky platform on N side of Mt Fleming, near edge of Polar Plateau	1700 masl, South facing (180°), <5°	27.75	117.64	-29.96	-8.54	5
North Wall WV (2012)	77° 30' 07.9" S 162° 03' 53.1" E	On a flat gravelly terrace, overlooking the Wright Valley, east of Bull Pass	832 masl, South facing (180°), 5%	17.99	91.73	-23.27	-4.67	38
Scott Base (1999)	77°50'53.6"S 166°45'44"E	Approximately 100 m N of Scott Base on rocky mid-slope of hillside	38 masl, South East (135°), 6%	15.81	153.69	-26.97	-5.34	33
South Wall WV (2011)	77° 34' 26.0" S 161° 14' 19.6" E	On a sandy terrace 700 m above Don Juan Pond	728 masl, East facing, 5%	11.76	69.01	-23.27	-4.67	38
Victoria Valley Floor (1999)	77° 19'51.3"S 161°36'02.2"E	On the Victoria Valley floor in the centre of a patterned ground polygon. 300 m SW of Lake Victoria	410 masl, Flat	14.65	69.20	-34.77	-1.33	23
Wright Valley Floor (1999)	77°31'06.1"S 161°51'57"E	On the floor of the Wright Valley, below Bull Pass	160 masl, South facing (180°), 3%	20.98	77.25	-31.73	-1.13	49

Adlam et al. (2010) used data between 2000 and 2007 from five of the stations in the soil monitoring network, to develop an empirical model to predict ALD, the stations used were; Marble Point, Minna Bluff, Scott Base, Victoria Valley and the Wright Valley Floor. To test the Adlam et al. (2010) model, the data from the same soil climate stations were compiled from between 2000 and 2018. Data from the sites not used by Adlam et al. (2010) was included.

An effort was made to develop an improved model using Matlabs' interactive stepwise regression function "stepwise". The stepwise function allows for the manual adding and removing of variables along with the observation of changing statistical results (co-efficient value, p-value, model adjusted R^2 etc). The function also advises on the best empirical model for the supplied variables. First the same atmospheric variables used in the (Adlam (et al., 2010)) model were tested (i.e. mean summer air temperature (MSAT), mean winter air temperature (MWAT), mean summer wind speed (MSWS), mean winter wind speed (MWWS), and total summer solar radiation (TSSR)).

The addition of mean spring air temperature (MSprAT), mean summer surface temperature (MSST) (taken as the soil temperature between 0 cm and 5 cm at each site), maximum annual wind speed (MaxWS), and station altitude, metres above sea level (MASL), were also trialled. Summer variables were calculated using data from December and January, winter variables from June, July and August, and spring data from September, October and November. To calculate total summer solar radiation, the solar radiation ($W m^{-2}$) during summer months were totalled and then converted into $100kW m^{-2}$ by dividing the total by 100,000. From the 18 years of data available, 15 years of data were used (2000 – 2015) to develop the new models, and three years (2016 – 2018) were used to test the fit for each new model.

The predictions from each model were plotted, with error bars displaying the residual mean standard error (RMSE), which can also be interpreted as one standard deviation of the mean, this was selected rather than the 95% quartiles (within two standard deviations), so to be able to compare the more specific changes in each model.

The analysis was extended in Minitab using restricted maximum likelihood (REML) to reduce the level of bias due to using data from multiple sites. By using a REML method the results are safeguarded from wrong conclusions in serial correlation. Both logged and non-logged variables were explored, as well as the use of a site-specific constant, rather than one set constant for all sites as in the stepwise analysis. The measured ALD (previously reported in Carshalton et al. (submitted)/ Chapter 4) and predicted ALD from each model were compared.

5.4 Results

The model of Adlam et al. (2010) was reproduced and then tested on a further ten years of data, for the same five soil climate station sites the model was developed on, and on a further two new sites on the walls of the Wright Valley with varying results (Figure 5.2). At the Wright Valley Floor (WVF), the model provided a good fit for most years (average within ± 6.6 cm) and within one standard deviation, with a similar fit between the years the model was developed with and the years since the model was developed (Figure 5.2a). A reasonable fit was also apparent at Marble Point (Figure 5.2c) and Victoria Valley (Figure 5.2e) (± 10 cm), though there were several years where the model predicted deeper ALD's than were measured. The model performed poorly at Minna Bluff (Figure 5.2b), constantly predicting a deeper ALD than was measured ($> +25$ cm). The Adlam et al. (2010) model overestimated ALD on the WV South Wall for all years tested ($> +32$ cm), but at the WV North Wall two of the five years tested (current length of the record at the WV North Wall) were a reasonable fit ($< \pm 15$ cm) (Figure 5.2f-g).

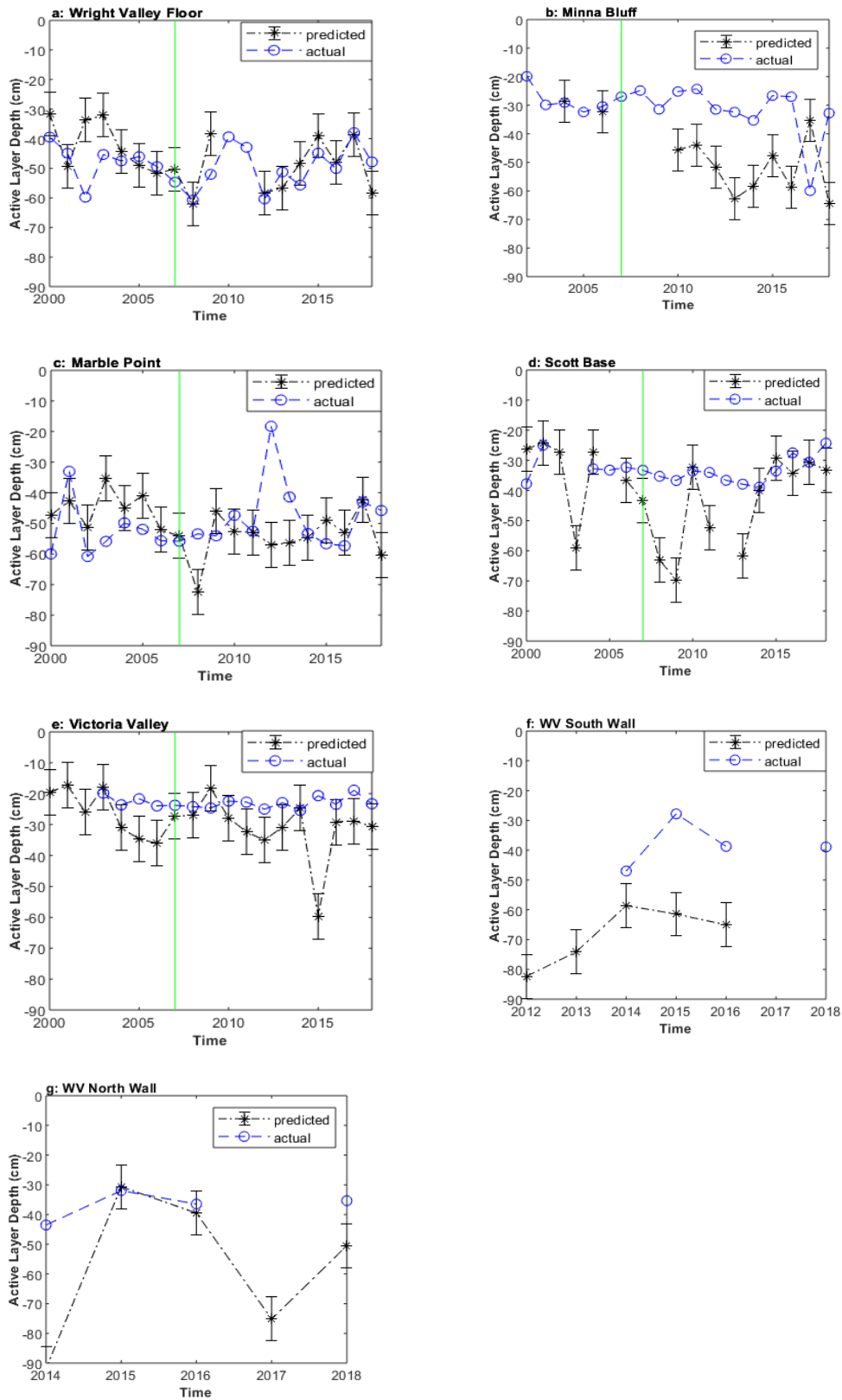


Figure 5.2: Measured ALD plotted with ALD predicted using the equation of Adlam et al. (2010), the model was developed using data from 1999 to 2007, which is plotted on the left hand side of each graph (left of green line), and on the right hand side of the line is the results since the model was developed. Graphs f and g were not used to develop the model.

A range of stepwise equations were explored using the same variables as Adlam et al. (2010), as well as altitude, spring air temperature, maximum wind speed and summer surface temperature. In total 19 equations were developed, 13 using data from the same five soil climate station sites as Adlam et al. (2010), and four using data from all sites, with varying results (Appendix 5). To assess how useful the models were the statistics of each model were analysed. The predicted ALD and actual measured ALD for each site were visually compared in the further three years of data not used to develop each model. Here the four models with the highest R^2 are discussed (Table 5.2 and Table 5.3).

Table 5.2: The four empirical model equations developed using stepwise analysis, to predict ALD* in the McMurdo Sound Region. Adlam et al. (2010) model also given.

Model	Equation
Adlam	$ALD = 222 + 5.69(MSAT) + 3.63(MWAT) - 10.6(TSSR) - 2.84(MSWS)$
8	$ALD = 71.53 - 0.07(MASL) + 3.23(MSST) + 3.596(MSAT) + 1.172(MWAT)$
12	$ADL = 191 + 3.44(MWAT) + 2.4(MSAT) + 2.84(MSST) - 13.86(TSSR)$
14	$ALD = 56.2 + 2.5(MSAT) + 0.55(MWAT) + 0.34(MSST)$
15	$ALD = 60.4 + 3.5(MSST) - 0.08(MASL) - 2.597(MWWS) + 1.115(MSprAT)$

*where ALD denotes ALD, MSAT is mean summer (DJ) air temperature, MWAT is mean winter (JJA) air temperature, MSprAT is mean spring (SON) air temperature, TSSR is total summer solar radiation (DJ), MSWS is mean summer windspeed, MASL is altitude, MSST is mean summer surface temperature, and MWWS is mean winter windspeed.

Table 5.3: Statistics of most viable stepwise multiple regression models. The number of years of data and number of sites used in development, along with the variation explained, the efficiency of the model (f-stat), where a larger number is preferred, and the residual mean standard error (RMSE). The same statistics for the model of Adlam et al. (2010) are also given from previously unpublished data (Personal communication, Littler 2019).

Model	Years	Sites	Adj R^2	f-stat	RMSE	p-value
Adlam	8	5	0.69	19.74	7.36	<0.0001
8	16	5	0.75	38.5	7.17	<0.0001
12	16	5	0.66	25.4	8.33	<0.0001
14	16	8	0.49	27	10.5	<0.0001
15	16	5	0.63	29	10.3	<0.0001

Statistically, the addition of a site-specific constant (altitude) in model 8, increased the variation explained by the model (adjusted $R^2 = 0.75$) compared to the Adlam et al. (2010) model by adjusted $R^2 = 0.69$ (Table 5.2), and was statistically the best model. Model 8 also had the highest f-statistic (38.5), and lowest residual mean standard error (RMSE) (7.2), (Table 5.2).

Model 8 was developed using 16 years of data across five soil climate station sites. When model 8 was used to predict the ALD the data showed an improved fit to Adlam et al. (2010) at all the low altitude sites (Figure 5.3), with a great fit at the WVF (Figure 5.3a) and at Victoria Valley (Figure 5.3e) (average within $< \pm 5$ cm). A good fit at Scott Base (± 10 cm) (Figure 5.3d). And a reasonable fit at Marble Point (± 15 cm) (Figure 5.3c) and at Minna Bluff (± 18 cm) for most years (Figure 5.3b). Model 8 was not able to accurately predict the ALD for the higher altitude sites at Mt Fleming (+146 cm) and on the walls of the Wright Valley ($> +40$ cm).

To see if the overall model could be improved for the higher altitude sites a model without altitude was trialled, keeping the same conditions as model 8, resulted in model 12 (Table 5.2). Without altitude included in the equation for model 12, the variation explained decreased (adjusted $R^2 = 0.65$) and the residual increased by one from 7.2 to 8.3. On the five sites it was designed on the further three years tested showed similar results to model 8 (Figure 5.4a-e). The model still did not accurately predict the ALD at the higher altitude sites, though the results were improved (Figure 5.4f-h) ($> +25$ cm).

Several models were developed using data from all eight soil climate station sites, between 1999 and 2015, with the best model being model 14 (Figure 5.5). Model 14 had a lower variance (adjusted $R^2=0.49$) than other models and a large residual mean standard error (10.5). However, the plotted results worked well at the higher altitude sites, with a good fit at; Mt Fleming (± 11 cm), the WV South Wall (± 6 cm), and the WV North Wall ($< \pm 5$ cm), (Figure 5.5f-h). The difference between the measured and predicted ALD was calculated on only 4 data points for the WV wall sites. Model 14 was not able to show the fluctuation of ALD at the five lower altitude sites both in years where the data was used to create the model (1999 – 2015) and subsequent years (2016 – 2018), as accurately as Adlam et al. (2010) or models 8, 12 and 15 discussed here ($> \pm 15$ cm) (Figure 5.5a-e).

Warmer or cooler spring temperatures were hypothesised to drive the timing of maximum depth of thaw and the potential maximum ALD each year. Cooler, less sunny, and more stormy conditions may lead to shallower ALD's later in the season. Thus, spring air temperature was trialed as a model predictor both in a model with all eight sites, which showed no significance, and across the five lower altitude sites. Model 15 (Table 5.2, Figure 5.6) was the most significant of the spring predictor models (adjusted $R^2= 0.63$), and it also included mean winter temperature (Table 5.2). Model 15 provided a good fit in the test years (2016 - 2018), particularly at Marble Point and Scott Base ($< \pm 10$ cm) (Figure 5.6c and d) and at Minna Bluff (± 11 cm) (Figure 5.6b).

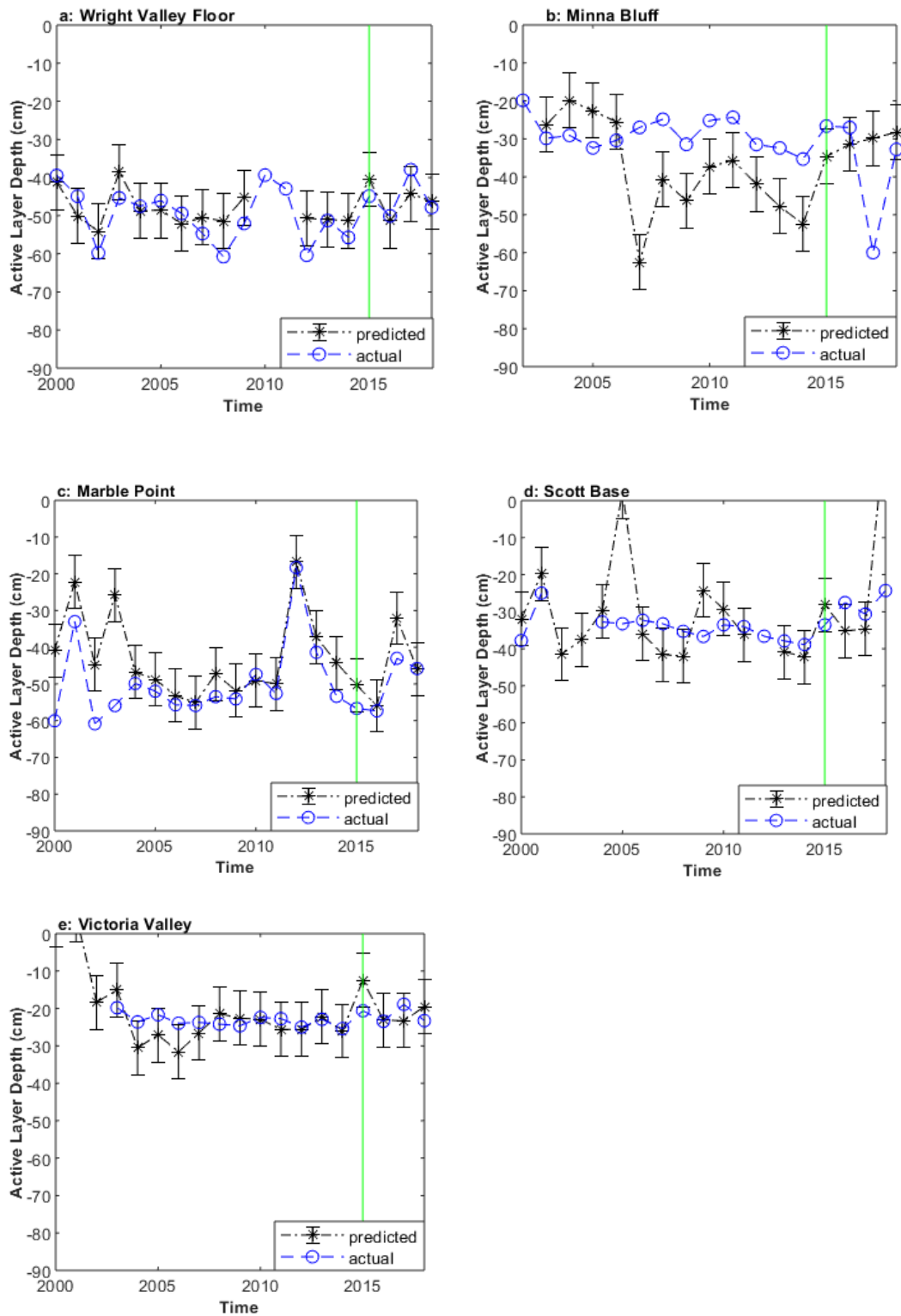


Figure 5.3: Measured ALD plotted with predicted ALD using the equation for model 8. The model was developed using data from 1999 to 2015, which is plotted on the left-hand side of each graph (left of vertical line), and on the right-hand side of the line is the results since the model was developed.

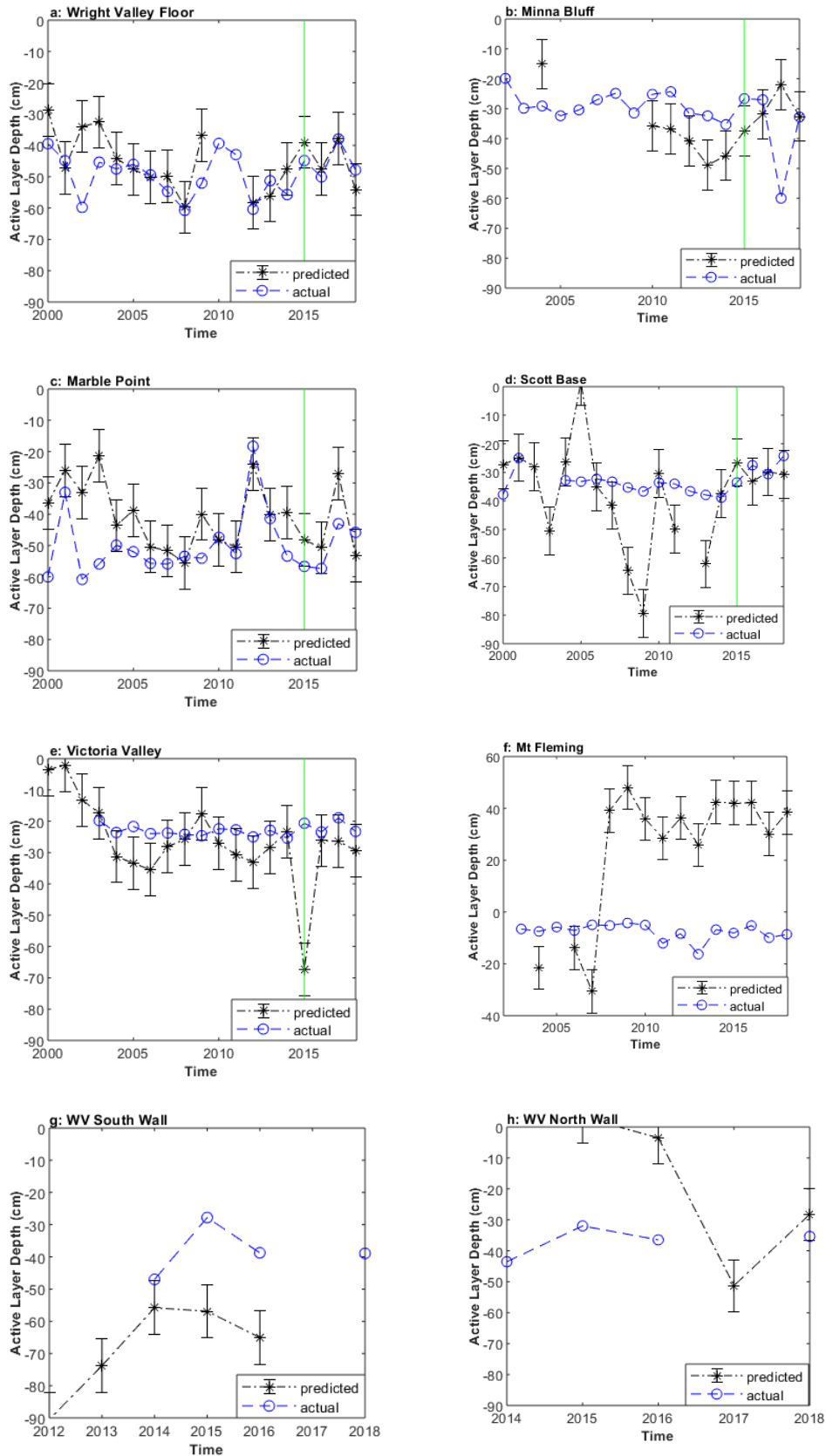


Figure 5.4: Measured ALD plotted with predicted ALD using the equation for model 12. The model was developed using data from 1999 to 2015, which is plotted on the left-hand side of each graph (left of vertical line), and on the right-hand side of the line is the results since the model was developed. Graphs f-h were not used to develop the model.

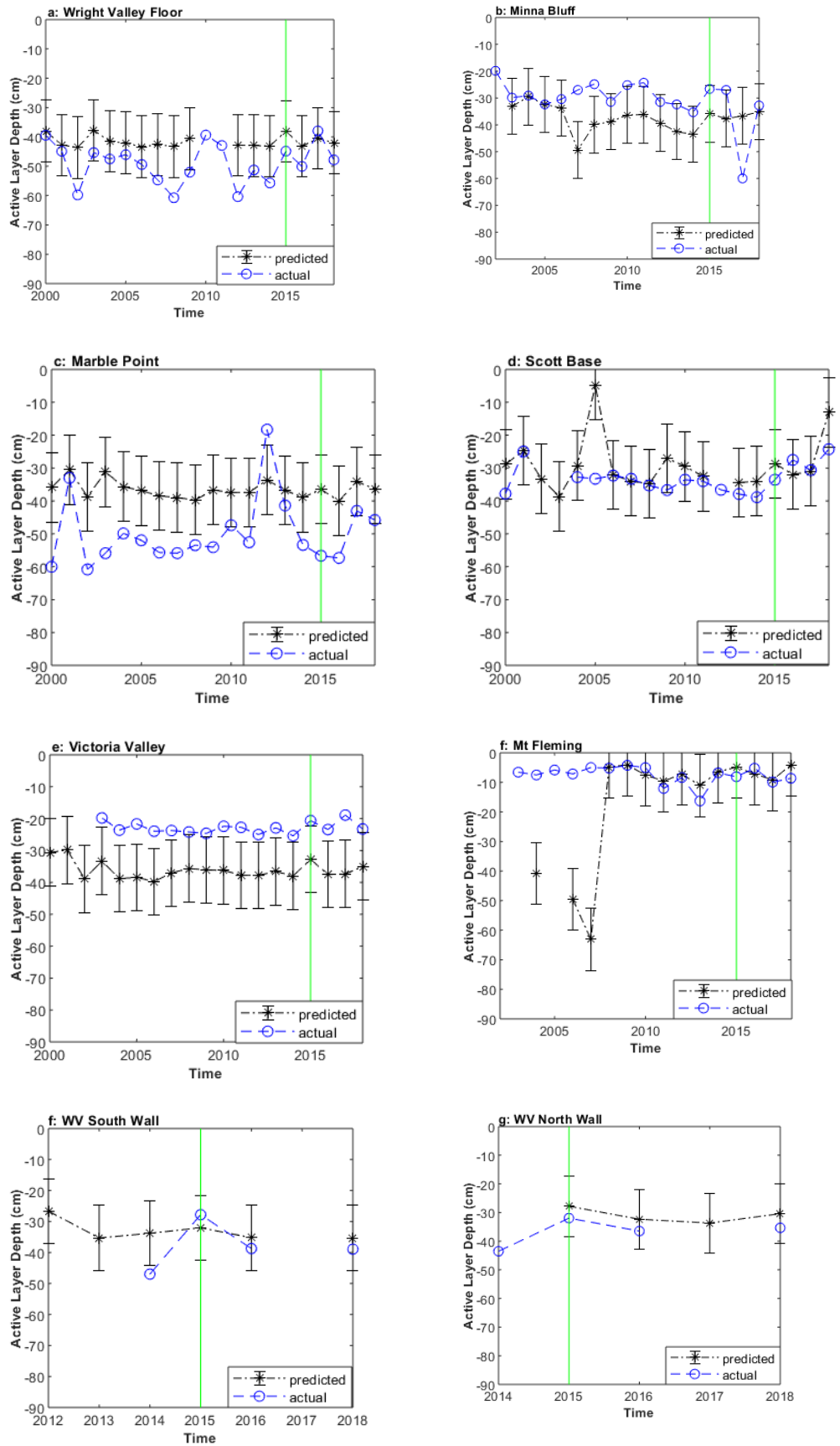


Figure 5.5: Measured ALD plotted with predicted ALD using the equation for model 14 the model was developed using data from 1999 to 2015, which is plotted on the left hand side of each graph (left of vertical line), and on the right hand side of the line is the results since the model was developed.

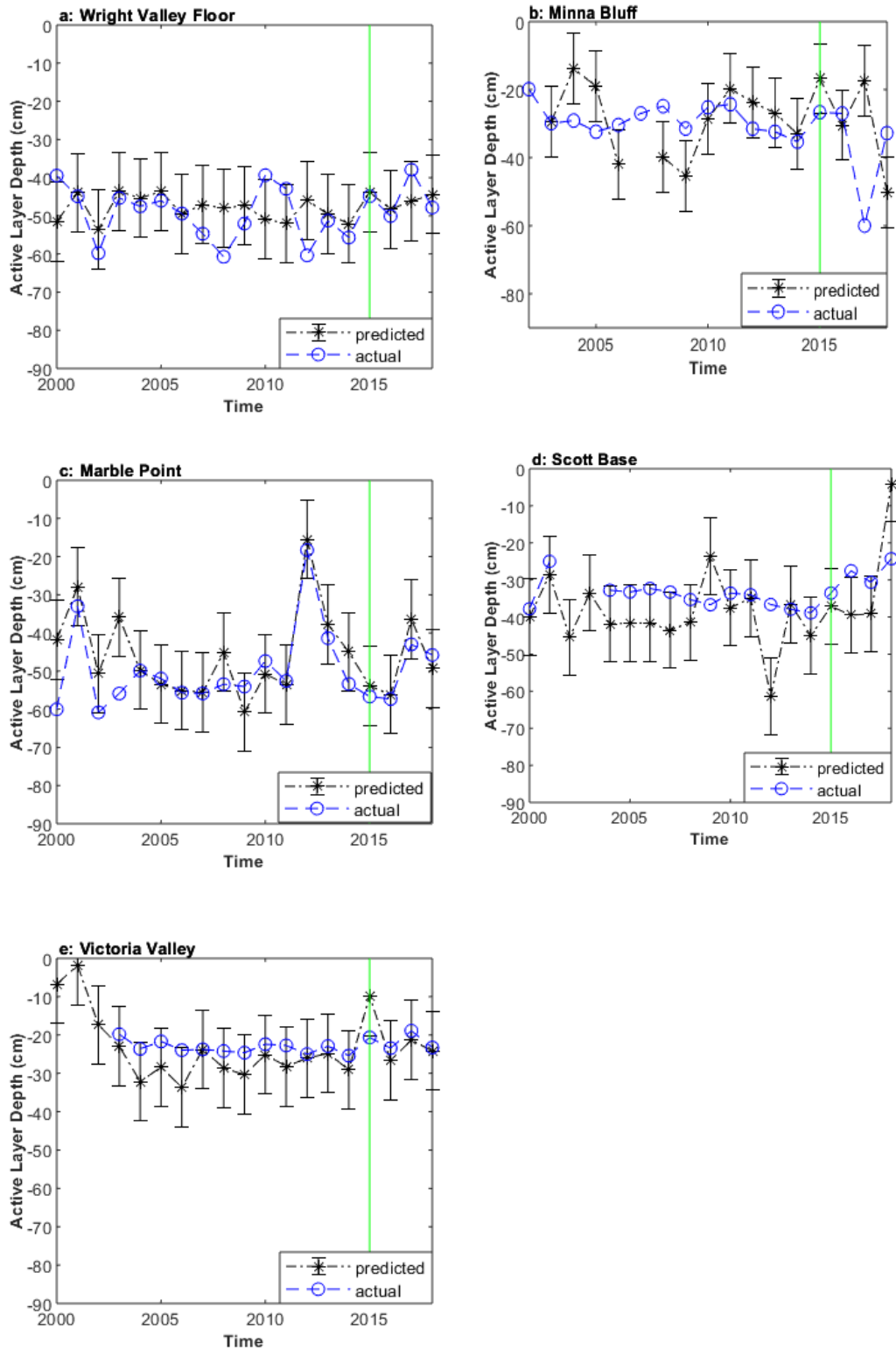


Figure 5.6: Measured ALD plotted with predicted ALD using the equation for model 15. The model was developed using data from 1999 to 2015, which is plotted on the left-hand side of each graph (left of vertical line), and on the right-hand side of the line is the results since the model was developed.

To reduce bias in the model introduced from using multiple sites, the restricted maximum likelihood (REML) method was also trailed for several models. A REML model was developed using data from the five low altitude soil climate station sites, with an undefined constant. The best model developed had an Adjusted $R^2 = 0.77$, a p-value < 0.003 and can be written as:

$$\log\text{ALD} = x + 0.028(\text{MSAT}) + 0.08(\text{TSSR})$$

Where $\log\text{ALD}$ is the ALD to the \log_{10} (cm), x is the site-specific constant, MSAT is the mean summer air temperature ($^{\circ}\text{C}$), and TSSR is the total summer solar radiation (100 kW m^2).

5.5 Discussion

5.5.1 Model options

Model 8 accounted for the most variation in ALD ($R^2 = 0.75$, $p < 0.001$), and gave the best prediction of ALD at most sites. Model 8 included altitude (MASL), mean summer air temperature (MSAT), mean winter air temperature (MWAT), and summer surface temperature (MSST). While model 8 did not work well when extrapolated to the three higher altitude sites ($> +40 \text{ cm}$), it predicted ALD on average within $\pm 10 \text{ cm}$ for most years at the five soil climate station sites it was based on. Model 8, is best applied to coastal and inland sites between sea level and 500 m, where it describes more of the variation in ALD than the model developed by Adlam et al. (2010) for the same sites (Adjusted $R^2 = 0.69$, $p < 0.001$).

The Adlam et al. (2010) model was better able to predict the ALD on the walls of the WV than Model 8 and produced reasonable results when compared to the subsequently recorded ALDs, at the five lower altitude sites it was developed from ($< \pm 15 \text{ cm}$) except Minna Bluff ($> + 25 \text{ cm}$). At Marble Point, the shallow ALD in 2011 was likely due to snow cover (Carshalton et al., submitted), which is a natural occurrence that neither the model of Adlam et al. (2010) nor models here can predict, as is not a variable monitored by the soil monitoring network. The model of Adlam et al. (2010) is more versatile and was better able to predict the ALD at the walls of the WV.

5.5.2 High altitude modelling

The aim was to produce a model that could predict across all Antarctic ice-free areas. However, due to the vastly different characteristics at Mt Fleming (on the edge of the Polar Plateau) compared to the lower altitude sites, neither model 8 or the model of Adlam et al. (2010) extrapolated well enough to predict the ALD at Mt Fleming ($> +47$ cm).

The environmental conditions at Mt Fleming include higher mean summer wind speeds, cooler mean summer and mean winter air temperatures as well as being at a much higher altitude (1700 m) (Table 5.1). Though the inclusion of wind data was trialled in model development it did not improve the predictive capacity. High-altitude data from Mt Fleming was included in the development of model 14 (Figure 5.5) to cover the full range of conditions, along with data from the WV walls. Model 14 predicted the ALD at Mt Fleming well for all but the first three years (± 5 cm) and reasonably well on the walls of the Wright Valley (± 13 cm), however model 14 was not able to replicate the small between-year changes in ALD at the lower altitude sites ($> \pm 20$ cm).

With no other soil climate stations >1000 m in altitude and the mid-altitude Wright Valley wall sites having only five years of data (with no winter data due to winter power failures) it was difficult to develop a robust model to predict the shallow measured ALDs at high altitude sites such as Mt Fleming. Therefore, more data from higher altitude sites is needed to improve the models.

5.5.3 Relative change model

A further model was developed using the REML method, which was better suited to modelling the pattern of between year variation in ALD. The model was developed with no set constant, this created a model that was not fixed to the ordinate axis but creates a predictive pattern that can be shifted up or down to meet a starting data point. The REML model is therefore, able to predict the change in ALD between years rather than the independent measured ALD. To determine the constant for a site, either a one-off measurement of the ALD, or the average ALD for the area, if known, could be used. The predicted ALD can then be plotted backwards or forwards with time. This creates a relative change model. By allowing for a site-specific constant a more accurate model was developed.

The REML modelling was an interesting experiment. However, the method needs to be worked with further to be useful for application across Antarctica. It currently could be useful interpolating between data-sets, or within data-sets with missing data.

5.5.4 Limitations

There were several limitations with the data for the model development. Most sites had some missing data due to lack of power at the end of August beginning of September in some years when batteries failed to charge, consequently, mean winter and spring temperatures could not be accurately determined for all years and sites.

The solar radiation values were uncharacteristically low at the soil climate station site on the South Wall of the WV compared to the other sites in the SCS network. This is possibly due to a calibration issue with the solar radiation sensor. However the lower measured solar radiation may also be due to natural shading in summer due to the steep walls of the valley adjacent to the site.

None of the soil climate monitoring stations had snow monitoring and snow cover is likely to have an effect on ALD ((Carshalton et al., submitted)/ Chapter 4). Snow cover has a dampening effect on soil temperatures in summer and therefore reduces ALD, through increased the albedo at the soil surface, reducing the amount of solar radiation warming the soil, and insulating the soil from changes in air temperature. The effects of snow cover on soil temperature are well known, along with a measurable difference in temperature between snow-covered soil, bare soil, and the surrounding air temperatures (Guglielmin et al., 2012; Hrbáček et al., 2016). Snow cover can also insulate and keep the soil warm in winter. Extended summer snow cover has been recorded in the soil climate station record at both Marble Point and at the South Wall of the WV in some summers, with the effect on ALD evident in 2011 at Marble Point (Carshalton et al., submitted).

5.5.5 Future work

While the four models described here have been tested on the three years of data (2016 - 2018) not used to develop them, to test the robustness of the preferred models (model 8 and model 14) would require the models be trialled at other sites

in Antarctica. The usefulness of any model is for it to be successful at predicting ALD at sites it has not been prepared with, with model 8 the opportunities to test the model are somewhat limited due to the inclusion of surface temperature which many atmospheric climate stations do not measure. An attempt to source complementary data to test the models, both from the RSR and the wider Antarctic area, was not successful in time to submit this thesis.

Through finding a correlation between mean surface temperature recorded at soil climate stations and ALD, this work could be extended by exploring whether surface temperature and timing and duration of snow cover, calculated from satellite-derived images can accurately predict ALD. If successful, and ground-truthing can be carried out, a remote sensing-based model will allow for a regional modelling of the Antarctic soil climate, which would be particularly useful in areas that are not accessible and to reduce human footprint and costs associated with soil climate station maintenance and data retrieval. Previous work has shown success in ground-truthing of surface temperature and satellite-derived surface temperatures (Brabyn et al., 2014). Further modelling work utilising the top of the permafrost model (TTOP) (Smith and Riseborough, 1996; Riseborough et al., 2008) and satellite surface data has also shown successful results (Obu et al., 2019). The mean annual temperatures at the top of the permafrost was predicted Antarctica-wide, and verified using some of the same data used in this paper to between +0.8 °C to -4.2 °C (Obu et al., 2019).

5.6 Conclusion

A soil climate monitoring network was developed in 1999 and has been continuously monitoring active layer and permafrost temperatures, and above-ground atmospheric variables, at nine sites in the Ross Sea Region. The purpose of this paper was to develop an improved empirical model for predicting ALD using atmospheric climate variables, and to test the model of Adlam et al. (2010), who previously worked with the same data set.

The model of Adlam et al. (2010) was tested by plotting the measured (actual) ALD against the ALD predicted by their equation, with reasonable results ($< \pm 20$ cm) over ten years at four of the five sites their model was developed on. When applied to the sites on the WV walls the model of Adlam et al. (2010) was able to predict the ALD (± 15 cm North Wall, $> \pm 20$ cm South Wall). Nineteen models

were developed, one with the inclusion of mean surface summer temperature and altitude, was accepted as the final improved model (Model 8) had an adjusted $R^2 = 0.75$ and a p-value < 0.0001 , and was able to predict the ALD within ± 10 cm at the five low altitude soil climate station sites.

When applied to three higher altitude sites (700 m – 1700 m), Model 8 was unable to accurately predict ALD, with predictions overestimating measured ALDs by + 32 cm to + 100 cm. This is most likely due to the extrapolation beyond the range of parameters used to develop the models across the low altitude and high-altitude sites, and lack of a long and complete data record for the higher altitude sites. The Adlam et al. (2010) model predicted mid to high altitude sites more accurately than Model 8 (± 15 cm - ± 50 cm), however, Model 8 predicted ALD more accurately at lower altitude sites (an improvement of 4-5 cm at each site). Both Model 8 and the model of Adlam et al. (2010) have their uses and while model 8 explains more of the variation in ALD at low altitude sites which make up five of the eight soil climate station sites investigated here, the model of Adlam et al. (2010) may be more versatile, as currently only a small number of the atmospheric climate monitoring sites scattered across Antarctica measure surface temperature (which is a parameter included in model 8).

An alternative model to both model 8 and Adlam et al. (2010) is model 14 ($R^2=0.49$), which used data from all sites in the network except Granite Harbour. Model 14 provided a good fit between the measured and predicted ALDs for the high-altitude sites ($< \pm 11$ cm) however at the lower altitude site it failed to show the intricate variation accurately but provided a reasonable fit ($< \pm 20$ cm). Model 14 would be the best option, of the models explored here, to produce a general large scale, low-resolution model of the ALD across Antarctica.

To determine the robustness of the improved model, it would be advantageous to test model 8 and model 14 with data from other Antarctic sites. This work helps add to the understanding of how atmospheric and soil climate variables are linked, and extends the work in characterising the soil climate, particularly in inaccessible regions. Including surface temperature in ALD prediction models will allow future investigation into the utility of remotely sensed data to predict ALD in non-monitored areas, and at a regional scale.

5.7 Acknowledgements

This research was partly funded by Landcare Research - Ross Sea Region Terrestrial Data Analysis research programme, MBI contract no. C09X1413. Logistic support was provided by Antarctica New Zealand. Thanks to John Kimble, Ron Paetzold, Don Huffman, Iain Campbell, Jackie Aislabie and Deb Harms for assisting in the initial climate station establishment. Thanks to Ray Littler for statistical assistance with the REMS modelling and Karin Brian for assisting with the coding for the stepwise analysis. Thanks to Chris Morcom, Dean Sandwell, Fraser Morgan and Aaron Wall for ongoing technical support. Funding assistance for Annette Carshalton was provided by the Broad Memorial Fund.

Chapter Six

Discussion and Conclusion

6.1 Introduction

Eighteen years of soil and atmospheric data (1999 – 2018) from nine soil climate stations (SCS) in the Ross Sea Region (RSR) of Antarctica, were analysed to investigate soil climate and change through time. The aims of this chapter are to summarise the findings of the thesis and discuss the implications of the work. A discussion of the limitations of this study and where future research should head are also included.

6.2 Summary

6.2.1 Thesis objectives

The main objective of this thesis was to analyse and report on the state of the active layer and the overall soil climate of the McMurdo Dry Valleys adjacent coastal sites. The specific goals were to:

- A. Characterise the depth of the active layer and the condition of permafrost in the RSR between 1999 and 2018;
- B. Assess the seasonal and annual temperature cycles and look for significant trends in the dataset;
- C. Assess the link between the soil climate and large scale climate systems such as the Southern Oscillation Index (SOI), the Southern Annular Mode (SAM) and the Amundsen Sea Low (ASL);
- D. Test the model developed by Adlam *et al.* (2010), who worked with data from 2000 – 2008 from the same soil climate network, using a further 10 years of data (2009 – 2018); and
- E. Attempt to develop an improved model from atmospheric climate variables and soil surface temperature.

A: Active layer and permafrost characteristics of the SCS network

Between 1999 and 2003 seven SCS were set up, followed by two further stations in 2011 and 2012. Soil moisture and temperature to a depth of between 90 cm and

1.2 m (which in the RSR is within the permafrost) are continuously monitored. Each SCS also measures atmospheric variables including solar radiation, air temperature, and relative humidity and windspeed and direction. Hourly measurements from each sensor are recorded to dataloggers, with the data downloaded annually in summer. The SCS are spread across the RSR, with six stations creating an altitudinal transect from Mt Fleming on the edge of the Polar Plateau (1700 m), through two sites on the walls of the Wright Valley (832 m and 728 m), and two sites on the valley floors at Victoria Valley (410 m) and Wright Valley (160 m), concluding at a coastal site at Marble Point (60 m). Four sites create a coastal latitudinal transect from Minna Bluff in the south ($78^{\circ}30'41.6''\text{S}$) through stations at Scott Base and Marble Point concluding with a station at Granite Harbour ($77^{\circ}00'23.7''\text{S}$).

Assessment of soil data reliability was carried out at each SCS by comparing the temperature data at about 45 cm, from the year after the SCS was initiated and 2018 (Chapter 3) The data from the MRC and Campbell probes were highly correlated ($R^2 > 0.9$). Mean annual soil temperature at 15 cm depth ranged across the SCS between -23.3°C (Mt Fleming) and -14.5°C (Granite Harbour), while mean summer temperature (December – January) at 15 cm depth across the SCS ranged between -9°C (Mt Fleming) and $+4.5^{\circ}\text{C}$ (Granite Harbour). The mean annual air temperature is similar to that of shallow soil (15 cm) with temperature ranging between -24°C (Mt Fleming) to -16°C (Granite Harbour). The mean winter air temperatures ranged between -34.8°C (Victoria Valley) and -23°C (WV North Wall) and the mean summer air temperatures ranged between -1°C (Granite Harbour) and -8.5°C (Mt Fleming). The maximum wind speed recorded was at Minna Bluff (161 km h^{-1}) which is the maximum recording the sensor on the site can take, the sensor has previously been blown away. The mean summer wind speed ranged between 12 km h^{-1} (WV South Wall) and 28 km h^{-1} (Mt Fleming).

The soils at each site have been previously described with most of the soil classified as Typic Haplorthels (Table 3.1). All sites other than the SCS on the WVF and the WV North Wall have ice-cemented permafrost.

Active layer depth

Up to 12 sensors at different depths ranging from the surface to a depth of 1.2 m were used to calculate the active layer depth (ALD). With the maximum summer

temperature for each sensor found and plotted against its depth. The point where the plotted line between the measured points crossed the 0°C isotherm was taken as the ALD for each site and each summer.

The shallowest ALD were at Mt Fleming with a mean of 8 cm \pm 12 cm over 16 years and the deepest at Granite Harbour where the ALD is $>$ 90 cm over 15 years. On the walls of the Wright Valley the ALD ranged between 27 cm and 47 cm across five years, with the South wall having slightly shallower depths most year, possibly due to lower incoming solar radiation. At Victoria Valley SCS, the mean ALD depth was 25 cm \pm 6.5 over 16 years. The Wright Valley Floor (49 \pm 23 cm) and Marble Point (50 cm \pm 42.5 cm) have similar ALD's and the longest continuous record with 18 years of data. Marble Point has a larger range in ALD due to an unusually shallow ALD in 2011. Which is likely to be because of extensive snow cover observed at the station that year. At Minna Bluff the mean ALD was 29 cm \pm 11 cm, with nine years of data. The ALD at Scott Base was similar to Minna Bluff (33 cm \pm 14 cm) over 17 years, there are some gaps in the record in the early 2000's. The mean ALD decreased with increasing altitude ($R^2=0.71$) and increased with increasing latitude ($R^2=0.66$).

B: Permafrost temperature and active layer depth trends with time

Trend assessments were done for ALD and the mean annual temperature at the top of the permafrost at each site for the length of the record at the site, using the Mann-Kendall test. The null hypothesis was that there would be significant ($p < 0.05$) warming or cooling trends in the ALD or in the mean annual permafrost temperature.

The null hypothesis was rejected at all sites, meaning that there were no significant patterns of warming or cooling in either ALD or permafrost temperature at any of the SCS between 2000 and 2018. However, all sites showed marked between season and interannual variation.

C: Relationship to large scale climate systems

Wavelet analysis was undertaken using de-seasonalised temperature data from the top of the permafrost for four stations (Mt Fleming, Wright Valley Floor, Marble Point, and Victoria Valley) and the data from the regional (Amundsen Sea Low (ASL)) and continental climate systems (Southern Annular Mode (SAM) and the

Southern Oscillation Index (SOI)) all of which potentially drive variation in permafrost temperature.

Cross wavelet analysis showed high energy relationships ($p < 0.05$) between de-seasonalised top of the permafrost temperature and the Amundsen Sea Low (ASL) at a yearly period, the Southern Annular Mode (SAM) at a 1-2 year period, and the Southern Oscillation Index (SOI) at 1 and 3 year periods, for all four sites studied. Cohen *et al.* (2013) reported that the ALD has a correlation with the SAM and SOI. While Clem and Fogt (2013), Schlosser *et al.* (2018), and Stuecker *et al.* (2017) all reported a link between local warming events and the SAM, SOI and ASL.

D & E: Active layer depth modelling

Adlam *et al.* (2010) developed a model to predict ALD that utilised air temperature, solar radiation and wind speed, using data from five sites between 1999 and 2007. The Adlam *et al.* (2010) model was tested with a further ten years of data (1999 – 2018) from the same five sites, and was also tested on an additional three mid to high altitude sites. The Adlam *et al.* (2010) model provided a reasonable fit for most sites, predicting the ALD on average across all years within ± 12 cm of the measured values, but did not work well at Minna Bluff (-27 cm) the WV South Wall (± 32 cm) or at Mt Fleming (+47 cm).

A further 19 models were trialled to improve on the model of Adlam *et al.* (2010), with four potential improvements developed. Model 8 was statistically the best model (Adjusted $R^2=0.75$, p value < 0.001), compared to the Adlam *et al.* (2010) model (Adjusted $R^2=0.69$, p value < 0.001). Model 8 used altitude, mean summer surface temperature, mean summer air temperature and mean winter air temperature, with data taken from five sites, to predict ALD within on average ± 8.5 cm of the measured ALD across the record at most sites. Model 8 did not accurately predict ALD at higher altitude sites ($> +36$ cm - +146 cm).

An alternative model (Model 14) that used data from all sites except Granite Harbour (Adjusted $R^2=0.49$, p value < 0.001) was developed which used mean summer air temperature, mean winter air temperature and mean summer surface temperature, and produced a good fit at high altitude sites (± 11 cm at Mt Fleming, ± 6 cm at WV South Wall, ± 4.5 cm at VW North Wall). However, model 14 did

not accurately predict with detail the smaller scale between year variation typically seen at the lower altitude sites (on average $< \pm 20$ cm). Model 14 could be used to produce a general large scale, low resolution model of the ALD across Antarctica.

Data from Granite Harbour was not used for modelling, as the site has an unusual micro topography and sub-surface water flow causes a deeper ALD than the typical wider area. The soil climate station was installed at Granite Harbour to capture the environmental characteristics and soil climate of a biologically important “site of special scientific interest” (Botany Bay) which is an exceptional microclimate atypical of the wider area.

6.3 Discussion

6.3.1 Implications of research

Global warming is a topical issue as the International Panel for Climate Change (IPCC) predicts that global mean surface air temperatures will be 1°C higher between 2016 and 2035 compared to the mean between 1850 and 1900; and that the mean global long term temperatures in 2100 will be 1.5°C to 4°C greater than mean temperatures between 1850 and 1900 (IPCC, 2014), with the effects warming theorised to be amplified at the poles. Several studies have reported that warming trends are detectable in the Antarctic, both in terrestrial environments (Guglielmin & Cannone, 2012; Goddard, 2013; Ramos *et al.*, 2017), the atmospheric climate (Vaughan *et al.*, 2001; Steig *et al.*, 2009; Schneider *et al.*, 2012; Bromwich *et al.*, 2013; Oliva *et al.*, 2017). However cooling has also been reported in the atmospheric climate record (Turner *et al.*, 2016) and in the soil climate (Doran *et al.*, 2002) along with a shallowing of ALD (Goyanes *et al.*, 2014; Hrbacek *et al.*, 2016; Ramos *et al.*, 2017; Oliva *et al.*, 2017).

The findings in my work do not support the idea that warming is currently occurring in the RSR; in accordance with the findings of Adlam (2009). As well as supporting findings from the Antarctic Peninsula that show ALD is only experiencing between-year variation (Almeida *et al.*, 2017; Hrbáček *et al.*, 2017; de Pablo *et al.*, 2018).

Research findings of Goddard (2013) detected a weak warming trend in air and soil temperature at Marble Point and Granite Harbour, however my results show

neither of these trends have continued. If the predicted global warming was to affect the environment in the RSR, an increase in air temperature would have clear ramifications on the soil environment, with warmer soil temperatures and an associated deepening of the ALD. Wavelet analysis has shown that there is a relationship between ALD the climatic systems such as SAM, SOI and ASL, on differing time scales, and these findings are similar to findings by other researchers linking climatic systems and sea ice (Schlosser *et al.*, 2018).

It is important to highlight the uniqueness of the SCS network, as it is one of the largest and longest-running above and below-ground soil climate networks in Antarctica. The SCS network offers the opportunity to create a strong baseline understanding of the soil climate in the RSR and monitor the effects a changing climate may have on the active layer and permafrost.

While the four models discussed and the Adlam et al (2010) model all have their merits, no one model can be considered the best. The Adlam et al (2010) model is useful as it utilises commonly monitored atmospheric variables, and does not use surface temperature data, which only a small number of Antarctic climate stations monitor. Model 8 is the most statistically robust, and offers the most explanation, while model 14 greater captures the variation across all altitudes, but at a lower resolution.

6.3.2 Limitations of this research

The RSR soil climate monitoring network while one of the longest continuous soil climate monitoring networks and has several limitations. Firstly, most stations, bar the WVF and Victoria Valley stations, have days to weeks of data missing in late winter and early spring in some years, due to the batteries running out. There are also other times of the year where some stations have stopped recording data though the reason is not always known. Thus, it is not possible to calculate annual or seasonal results at all sites. While there appears to be no calibration or drift issues with soil temperature (Chapter 3), there may be an issue in the solar radiation data at the WV South Wall, as the total summer values here are up to 300,000 W m² lower than other sites in the network. However, this may be due to natural shading from the adjacent valley wall.

When assessing both the RSR soil climate dataset, and other climate monitoring datasets for long term trends, and potentially predicting if warming or cooling will occur, it is important to reiterate that climate should be discussed over the average of 30 years or more (WMO-No.100, 2018). The dataset used in this study does not currently have enough data to significantly add to the discussion on climate change, although it is still providing critical information to understanding the wider soil climate in the RSR. The dataset over the last 18 years has created a baseline against which future change can be detected and the SCS sites cover a range of environments with potentially have different terrestrial ecosystems. Therefore, the RSR SCS network continues to increase in scientific value as its duration continues and as the dataset grows.

6.3.3 Future research

This thesis is the third MSc thesis to work on the data from the soil climate monitoring network, the first worked on data up to 2007 (Adlam, 2009) and the second with data up to 2012 (Goddard, 2013) across seven sites. Thus here I investigate a further six years of data which includes data from two new sites on the walls of the Wright Valley. While all three MSc theses have covered a range of the available data, there are still data that have not previously analysed and there is still a large amount of further research that can be undertaken, both using the RSR soil climate network data as well as data from other complementary datasets. These include:

- Further modelling to test back in time with the use of longer atmospheric datasets such as the meteorological data from Scott Base (1953 – present).
- It would be beneficial to test the improved model on further datasets that the model was not developed on. While this was attempted, data from other researchers in other regions of Antarctica was not able to be obtained in time to be included in this study.

The mean summer surface temperature is a good predictor for ALD, so satellite data could be explored in the future as both the MODIS and Landsat satellites groups collect imagery in the infrared scale and could be used to calculate surface temperature and air temperature. Along with this, the advancement in satellite data resolution, and the increased frequency of image and data collection, satellite data could help with the assessment of snow cover, which current monitoring stations

cannot do. Thus, explaining more variation in ALD and improving modelling efforts.

Previous work in the Miers Valley, RSR shows that the Landsat 7 thermal band data correlates strongly with surface temperature (Brabyn *et al.*, 2014). Obu and others (2019) showed MODIS satellite data modelled temperature at the top of the permafrost compared well to measured mean annual permafrost temperatures within the Ross Sea region (+0.8 °C to -4.2 °C) and similarly around the rest of Antarctica (Obu *et al.*, 2019). These studies show that remote sensing data is a viable option to follow.

The use of satellite data allows for the remote monitoring of areas that are inaccessible either due to cost, remoteness or special protection placed on areas due to their outstanding environmental, scientific, historic, aesthetic or wilderness values (e.g. Antarctic Specially Protected Areas, ASPA). It also allows for modelled maps of larger areas such as full valleys, regions or possibly all ice-free land on the Antarctic continent.

6.4 Conclusion

The soil climate monitoring network is one of the longest continuous running soil climate monitoring programs in Antarctica (1999 – 2019) and has created a valuable baseline for understanding the RSR soil climate. This thesis has ten main findings:

- The active layer depth (ALD) showed strong between year variation and ranged between an average of 8 cm at Mt Fleming and > 90 cm at Granite Harbour.
- ALD decreased with increasing altitude ($R^2= 0.71$) and increased with increasing latitude ($R^2= 0.66$).
- Trend analysis was undertaken using a non- parametric trend test. No long term trends of warming or cooling were found in ALD or in permafrost temperature at any of the nine SCS.
- All sites experienced strong between season and inter-annual variation in soil and air temperatures.
- A significant ($p < 0.05$) relationship between de-seasonalised permafrost temperature and three large scale climatic systems (the Amundsen Sea Low,

Southern Annular Mode, and the Southern Oscillation Index) on multi-year time scales.

- The Adlam et al. (2010) model (Adj $R^2= 0.69$) was tested on additional years of data and was reasonably robust predicting the ALD across the five lower altitude sites (Minna Bluff, Wright Valley Floor, Scott Base, Marble Point, and Victoria Valley) on average within ± 12 cm. The Adlam et al. (2010) model would be useful in predicting the ALD at sites that only collect atmospheric climate data.
- Model 8 was the most statistically significant model (Adj $R^2= 0.75$) developed and used surface temperature, air temperature and altitude. This model predicted the ALD across the low altitude sites on average within ± 8.5 cm of the measured ALD.
- Model 8 offers the opportunity for future work using satellite imagery, which has been shown to have been successfully used in modeling surface temperature (Brabyn *et al.*, 2014) and permafrost temperature (Obu *et al.*, 2019).
- Model 14 provides an alternative model, which while statistically weaker (Adj $R^2= 0.49$) used data from eight sites and predicted the mid to high altitude sites well (± 11 cm) and the low altitude site reasonably (on average ± 15 cm). Model 14 could be used as a low resolution/ large scale model that can be used at a range of altitudes.

It is important to highlight the uniqueness of the SCS network, as it is one of the largest and longest-running above and below-ground soil climate networks in Antarctica. The SCS network offers the opportunity to create a strong baseline understanding of the soil climate in the RSR and monitor the effects a changing climate may have on the active layer and permafrost. While no trends of warming or cooling were found in permafrost temperature or ALD the inter-annual variability indicates the need for a longer record to fully comprehend the potential patterns at each site.

The dataset does have a few limitations. Many of the sites have a gap in data collection, particularly at the end of winter where the batteries run out. There does not appear to be any calibration issue with the soil temperature data, as all sensors fit a similar pattern. There is possibly a calibration issue with the solar radiation sensor at the WV South Wall, as the total summer values are up to $300,000 \text{ W m}^2$

lower each year than other sites in the network. However, this may be due to natural shading from the adjacent valley wall.

The soil climate station network dataset still has not been fully studied, with more data added annually as the project continues to run. There is still a number of sensors (e.g. relative humidity and net radiation) with data that has not been analysed and future study is recommended. There is also the opportunity for further modelling work with the two models (model 8 and model 14) requiring further development and testing with data not used to develop them, along with the opportunity to work with satellite data to develop a regional understanding of the state of the active layer, particularly in inaccessible areas.

References

- Adlam, L. S. (2009). *Soil climate and permafrost temperature monitoring in the McMurdo Sound region, Antarctica*. Masters thesis, University of Waikato, Hamilton, New Zealand.
- Adlam, L. S., Balks, M. R., Guglielmin, M., Baio, F., & Campbell, D. I. (2009). *Borehole establishment for ice-cemented core sampling and permafrost temperature monitoring at Marble Point and Wright Valley, Antarctica*. University of Waikato. Antarctic Research, Unit Special Report No. 2. Hamilton, N.Z.: Hamilton, N.Z. : Antarctic Research Unit, University of Waikato.
- Adlam, L. S., Balks, M. R., Seybold, C. A., & Campbell, D. I. (2010). Temporal and spatial variation in active layer depth in the McMurdo Sound Region, Antarctica. *Antarctic Science*, 22(1), 45-52.
- Agresti, A. (2010). *Analysis of Ordinal Categorical Data*. New York: John Wiley & Sons.
- Almeida, I. C. C., Schaefer, C. E. G. R., Michel, R. F. M., Fernandes, R. B. A., Pereira, T. T. C., de Andrade, A. M., Francelino, M. R., Fernandes Filho, E. I., & Bockheim, J. G. (2017). Long term active layer monitoring at a warm-based glacier front from maritime Antarctica. *Catena*, 149, 572-581.
- Anisimov, O. A., Shiklomanov, N. I., & Nelson, F. E. (1997). Global warming and active-layer thickness: results from transient general circulation models. *Global and Planetary Change*, 15(3), 61-77.
- Balks, M. R., Campbell, D. I., Campbell, I. B., & Claridge, G. G. C. (1995). *Interim results of 1993/94 soil climate, active layer and permafrost investigations at Scott Base, Vanda and Beacon Heights, Antarctica*. Hamilton, N.Z.: Hamilton, N.Z. : Antarctic Research Unit, University of Waikato.
- Balks, M. R., & O'Neill, T. A. (2016). Soil and permafrost in the Ross Sea Region of Antarctica: Stable or dynamic? *Cuadernos de Investigacion Geografica*, 42(2), 415-434.
- Bertler, N. A. N., Barrett, P. J., Mayewski, P. A., Fogt, R. L., Kreutz, K. J., & Shulmeister, J. (2004). El Niño suppresses Antarctic warming. *31*(15).
- Bockheim, J., Campbell, I. B., & Claridge, G. G. C. (2015). *The soils of Antarctica*. Cham, Switzerland: Springer.
- Bockheim, J., & McLeod, M. J. G. (2006). Soil formation in Wright Valley, Antarctica since the late Neogene. *137*(1-2), 109-116.
- Bockheim, J. G. (2015). *Cryopedology*. Springer.

- Bockheim, J. G., Campbell, I. B., & McLeod, M. (2007). Permafrost distribution and active-layer depths in the McMurdo Dry Valleys, Antarctica. *18*(3), 217-227.
- Bockheim, J. G., & Hinkel, K. M. (2005). Characteristics and Significance of the Transition Zone in Drained Thaw-Lake Basins of the Arctic Coastal Plain, Alaska. *Arctic*, *58*(4), 406-417.
- Brabyn, L., Zawar-Reza, P., Stichbury, G., Cary, C., Storey, B., Laughlin, D. C., Katurji, M. J. E. M., & Assessment. (2014). Accuracy assessment of land surface temperature retrievals from Landsat 7 ETM + in the Dry Valleys of Antarctica using iButton temperature loggers and weather station data. *186*(4), 2619-2628.
- Campbell, I. B., & Claridge, G. G. C. (1987). *Antarctica: Soils, weathering processes and environment*. Elsevier Science Pub. Co. Inc., New York, NY; None.
- Carshalton, A. G., Balks, M., O'Neill, T. A., Bryan, K. R., & Seybold, C. A. (submitted). Climatic influences on Active Layer Depth between 2000 and 2018 in the McMurdo Dry Valleys, Ross Sea Region, Antarctica. Hamilton, New Zealand.
- Clem, K. R., & Fogt, R. L. (2013). Varying roles of ENSO and SAM on the Antarctic Peninsula climate in austral spring. *118*(20), 11,481-11,492.
- Cohen, L., Dean, S., & Renwick, J. (2013). Synoptic Weather Types for the Ross Sea Region, Antarctica. *Journal of Climate*, *26*(2), 636-649.
- Conovitz, P. A., MacDonald, L. H., & McKnight, D. M. (2006). Spatial and Temporal Active Layer Dynamics along Three Glacial Meltwater Streams in the McMurdo Dry Valleys, Antarctica. *Arctic, Antarctic, and Alpine Research*, *38*(1), 42-53.
- Correia, A., Vieira, G., & Ramos, M. (2012). Thermal conductivity and thermal diffusivity of cores from a 26 meter deep borehole drilled in Livingston Island, Maritime Antarctic. *Geomorphology*, *155*, 7-11.
- de Pablo, M. A., Ramos, M., Molina, A., & Prieto, M. (2018). Thaw depth spatial and temporal variability at the Limnopolar Lake CALM-S site, Byers Peninsula, Livingston Island, Antarctica. *Science of The Total Environment*, *615*, 814-827.
- Doran, P. T., McKay, C. P., Clow, G. D., Dana, G. L., Fountain, A. G., Nylen, T., & Lyons, W. B. (2002a). Valley floor climate observations from the McMurdo dry valleys, Antarctica, 1986–2000. *107*(D24), ACL 13-1-ACL 13-12.
- Doran, P. T., Priscu, J. C., Lyons, W. B., Walsh, J. E., Fountain, A. G., McKnight, D. M., Moorhead, D. L., Virginia, R. A., Wall, D. H., Clow, G. D., Fritsen, C. H., McKay, C. P., & Parsons, A. N. (2002b). Antarctic climate cooling and terrestrial ecosystem response. *Nature*, *415*(6871), 517-520.

- Fisher, D. A., Lacelle, D., Pollard, W., Davila, A., & McKay, C. P. (2016). Ground surface temperature and humidity, ground temperature cycles and the ice table depths in University Valley, McMurdo Dry Valleys of Antarctica. *121*(11), 2069-2084.
- Florides, G., & Kalogirou, S. (2019). *Annual ground temperature measurements at various depths*.
- Food and Agriculture Organization of the United Nations. (2015). *World Reference Base for Soil Resources 2014: International Soil Classification System for Naming Soils and Creating Legends for Soil Maps*. World Soil Resources Reports 106. Rome, Italy. 192p.
- Garratt, J. R. (1994). Review: the atmospheric boundary layer. *Earth-Science Reviews*, *37*, 89-134.
- Goddard, H. E. (2013). *Investigation of air and soil climate across the latitudinal and altitudinal gradient of the Ross Sea region of Antarctica*. Masters thesis, University of Waikato, Hamilton, New Zealand.
- Grinsted, A., Moore, J. C., & Jevrejeva, S. (2004). Application of the cross wavelet transform and wavelet coherence to geophysical time series. *Nonlin. Processes Geophys.*, *11*(5/6), 561-566.
- Guglielmin, M. (2006). Ground surface temperature (GST), active layer and permafrost monitoring in continental Antarctica. *17*(2), 133-143.
- Guglielmin, M. (2012). Advances in permafrost and periglacial research in Antarctica: A review. *Geomorphology*, *155*, 1-6.
- Guglielmin, M., Balks, M. R., Adlam, L. S., & Baio, F. (2011). Permafrost thermal regime from two 30-m deep boreholes in southern Victoria Land, Antarctica. *Permafrost and Periglacial Processes*, *22*(2), 129-139.
- Guglielmin, M., & Cannone, N. J. C. C. (2012). A permafrost warming in a cooling Antarctica? , *111*(2), 177-195.
- Guglielmin, M., Worland, M. R., & Cannone, N. (2012). Spatial and temporal variability of ground surface temperature and active layer thickness at the margin of maritime Antarctica, Signy Island. *Geomorphology*, *155*, 20-33.
- Hartge, K. H. (2016). *Essential soil physics : an introduction to soil processes, functions, structure and mechanics*. (1st English language edition.. ed.). COLLINGWOOD: COLLINGWOOD CSIRO PUBLISHING.
- Hillel, D. (2003). *Introduction to Environmental Soil Physics*. Burlington, UNITED STATES: Elsevier Science & Technology.
- Hosking, J. S., Orr, A., Bracegirdle, T. J., & Turner, J. (2016). Future circulation changes off West Antarctica: Sensitivity of the Amundsen Sea Low to projected anthropogenic forcing. *43*(1), 367-376.

- Hosking, J. S., Orr, A., Marshall, G. J., Turner, J., & Phillips, T. (2013). The Influence of the Amundsen–Bellingshausen Seas Low on the Climate of West Antarctica and Its Representation in Coupled Climate Model Simulations. *26*(17), 6633-6648.
- Hrbáček, F., Kňázková, M., Nývlt, D., Láska, K., Mueller, C. W., & Ondruch, J. (2017). Active layer monitoring at CALM-S site near J.G.Mendel Station, James Ross Island, eastern Antarctic Peninsula. *Science of The Total Environment*, 601-602, 987-997.
- Hrbáček, F., Láska, K., & Engel, Z. (2016). Effect of Snow Cover on the Active-Layer Thermal Regime – A Case Study from James Ross Island, Antarctic Peninsula. *27*(3), 307-315.
- Ikard, S. J., Gooseff, M. N., Barrett, J. E. and Takacs-Vesbach, C. (2009). Thermal characterisation of active layer across a soil moisture gradient in the McMurdo Dry Valleys, Antarctica. *Permafrost and Periglacial Process*.(20), 27-39.
- IPCC. (2014). How will permafrost, the active layer and water availability in Antarctic soils and marine sediments change in a warming climate, and what are the effects on ecosystems and biogeochemical cycles?
- Jenny, H. (1941). *Factors of soil formation; a sytem of quantitative pedology*.
- Kaimal, J. C., & Finnigan, J. J. (1994). *Atmospheric boundary layer flows their structure and measurement*. New York: New York : Oxford University Press.
- Kane, D. L., Hinkel, K. M., Goering, D. J., Hinzman, L. D., & Outcalt, S. I. (2001). Non-conductive heat transfer associated with frozen soils. *Global and Planetary Change*, 29(3), 275-292.
- Kennicutt, M. C., Chown, S. L., Cassano, J. J., Liggett, D., Peck, L. S., Massom, R., Rintoul, S. R., Storey, J., Vaughan, D. G., Wilson, T. J., Allison, I., Ayton, J., Badhe, R., Baeseman, J., Barrett, P. J., Bell, R. E., Bertler, N., Bo, S., Brandt, A., Bromwich, D., Cary, S. C., Clark, M. S., Convey, P., Costa, E. S., Cowan, D., Deconto, R., Dunbar, R., Elfring, C., Escutia, C., Francis, J., Fricker, H. A., Fukuchi, M., Gilbert, N., Gutt, J., Havermans, C., Hik, D., Hosie, G., Jones, C., Kim, Y. D., Le Maho, Y., Lee, S. H., Leppe, M., Leitchenkov, G., Li, X., Lipenkov, V., Lochte, K., López-Martínez, J., Lüdecke, C., Lyons, W., Marensi, S., Miller, H., Morozova, P., Naish, T., Nayak, S., Ravindra, R., Retamales, J., Ricci, C. A., Rogan-Finnemore, M., Ropert-Coudert, Y., Samah, A. A., Sanson, L., Scambos, T., Schloss, I. R., Shiraishi, K., Siegert, M. J., Simões, J. C., Storey, B., Sparrow, M. D., Wall, D. H., Walsh, J. C., Wilson, G., Winther, J. G., Xavier, J. C., Yang, H., & Sutherland, W. J. (2014). A roadmap for Antarctic and Southern Ocean science for the next two decades and beyond. *Antarctic Science*, 27(1), 3-18.
- King, J. C. (1997). *Antarctic meteorology and climatology / J.C. King and J. Turner*. Cambridge atmospheric and space science series. Cambridge, England: Cambridge University Press.

- Lacelle, D., Lapalme, C., Davila, A. F., Pollard, W., Marinova, M., Heldmann, J., & McKay, C. P. (2016). Solar Radiation and Air and Ground Temperature Relations in the Cold and Hyper-Arid Quartermain Mountains, McMurdo Dry Valleys of Antarctica. *27*(2), 163-176.
- Lau, K.-M., & Weng, H. (1995). Climate Signal Detection Using Wavelet Transform: How to Make a Time Series Sing. *76*(12), 2391-2402.
- Lee, J. R., Raymond, B., Bracegirdle, T. J., Chadès, I., Fuller, R. A., Shaw, J. D., & Terauds, A. (2017). Climate change drives expansion of Antarctic ice-free habitat. *Nature*, *547*, 49.
- Linell, K. A., & Tedrow, J. C. F. (1981). *Soil and permafrost surveys in the arctic*. Oxford: Oxford University Press.
- Marshall, G. J. (2003). Trends in the Southern Annular Mode from Observations and Reanalyses. *16*(24), 4134-4143.
- Martin, M. A. R., J. (2016). *A Brief History of the Research Stations and Refuges of the British Antarctic Survey and its Predecessors*. Natural Environment Research Council - British Antarctic Survey 2016. <https://www.bas.ac.uk/wp-content/uploads/2015/03/British-Antarctic-Stations-Refuges-v6.2-2016.pdf>.
- Mauro, G., Michele Dalle, F., & Nicoletta, C. (2014). Permafrost warming and vegetation changes in continental Antarctica. *Environmental Research Letters*, *9*(4), 045001.
- Michel, R. F. M., Schaefer, C. E. G. R., Poelking, E. L., Simas, F. N. B., Fernandes Filho, E. I., & Bockheim, J. G. (2012). Active layer temperature in two Cryosols from King George Island, Maritime Antarctica. *Geomorphology*, *155–156*, 12-19.
- Obu, J., Westermann, S., Vieira, G., Abramov, A., Balks, M., Bartsch, A., Hrbáček, F., Kääb, A., & Ramos, M. (2019). Pan-Antarctic map of near-surface permafrost temperatures at 1 km² scale. *The Cryosphere Discuss.*, *2019*, 1-38.
- Oliva, M., Hrbacek, F., Ruiz-Fernández, J., de Pablo, M. Á., Vieira, G., Ramos, M., & Antoniades, D. (2017a). Active layer dynamics in three topographically distinct lake catchments in Byers Peninsula (Livingston Island, Antarctica). *CATENA*, *149*, 548-559.
- Oliva, M., Navarro, F., Hrbacek, F., Hernandez, A., Nyvlt, D., Pereira, P., Ruiz-Fernandez, J., & Trigo, R. (2017b). Recent regional climate cooling on the Antarctic Peninsula and associated impacts on the cryosphere. *Sci Total Environ*, *580*, 210-223.
- Péwé, T. L. (1999). *Permafrost*. Retrieved July 16, 2019, from <https://www.britannica.com/science/permafrost/Ice-content>.

- Ramos, M., Vieira, G., de Pablo, M. A., Molina, A., Abramov, A., & Goyanes, G. (2017). Recent shallowing of the thaw depth at Crater Lake, Deception Island, Antarctica (2006–2014). *CATENA*, *149*, 519-528.
- Riseborough, D., Shiklomanov, N., Eitzelmüller, B., Gruber, S., & Marchenko, S. (2008). Recent advances in permafrost modelling. *Permafrost and Periglacial Processes*, *19*(2), 137-156.
- Ropelewski, C. F., & Jones, P. D. (1987). An extension of the Tahiti-Darwin Southern Oscillation Index. *Monthly Weather Review*, *115*, 2161-2165.
- Sauer, T., & Horton, R. (2005). *Soil Heat Flux*.
- Schaefer, C., Michel, R., Delpupo, C., O. Senra, E., Bremer, U., & Bockheim, J. (2016). *Active layer thermal monitoring of a Dry Valley of the Ellsworth Mountains, Continental Antarctica*. (Vol. 149).
- Schlosser, E., Haumann, F. A., & Raphael, M. N. (2018). Atmospheric influences on the anomalous 2016 Antarctic sea ice decay. *The Cryosphere*, *12*(3), 1103-1119.
- Seybold, C. A., Balks, M. R., & Harms, D. S. (2010). Characterization of active layer water contents in the McMurdo Sound region, Antarctica. *Antarctic Science*, *22*(6), 633-645.
- Seybold, C. A., Harms, D. S., Balks, M., Aislabie, J., Paetzold, R. F., Kimble, J., & Sletten, R. (2009). Soil Climate Monitoring Project in the Ross Island Region of Antarctica. *Soil Horizons*, *50*(2).
- Shukla, M. (2014). *Soil physics : an introduction*. Boca Raton : CRC Press.
- Smerdon, J. E., Pollack, H. N., Cermak, V., Enz, J. W., Kresl, M., Safanda, J., & Wehmler, J. F. (2006). Daily, seasonal, and annual relationships between air and subsurface temperatures. *Journal of Geophysical Research: Atmospheres*, *111*(D7).
- Soil Survey Staff, S. (1999). *Soil taxonomy: A basic system of soil classification for making and interpreting soil surveys. 2nd edition*. Natural Resources Conservation Service. U.S. Department of Agriculture Handbook 436.
- Speirs, J. C., McGowan, H. A., Steinhoff, D. F., & Bromwich, D. H. (2013). Regional climate variability driven by foehn winds in the McMurdo Dry Valleys, Antarctica. *33*(4), 945-958.
- Stuecker, M. F., Bitz, C. M., & Armour, K. C. (2017). Conditions leading to the unprecedented low Antarctic sea ice extent during the 2016 austral spring season. *44*(17), 9008-9019.
- Torrence, C., & Compo, G. P. (1998). A Practical Guide to Wavelet Analysis. *79*(1), 61-78.
- Turner, J., Lu, H., White, I., King, J. C., Phillips, T., Hosking, J. S., Bracegirdle, T. J., Marshall, G. J., Mulvaney, R., & Deb, P. (2016). Absence of 21st

century warming on Antarctic Peninsula consistent with natural variability. *Nature*, 535, 411.

Ugolini, F., & Bockheim, J. (2008). Antarctic soils and soil formation in a changing environment: A review. *Geoderma*, 144, 1-8.

Uxa, T. (2017). Discussion on 'Active Layer Thickness Prediction on the Western Antarctic Peninsula' by Wilhelm et al. (). *Permafrost and Periglacial Processes*, 28(2), 493-498.

Waelbroeck, C. (1993). Climate-soil processes in the presence of permafrost: a systems modelling approach. *Ecological Modelling*, 69(3), 185-225.

Wilhelm, K., & Bockheim, J. (2016). Influence of soil properties on active layer thermal propagation along the western Antarctic Peninsula. *Earth Surface Processes and Landforms*, 41(11), 1550-1563.

Wilhelm, K., Bockheim, J., & Kung, S. (2015). *Active Layer Thickness Prediction on the Western Antarctic Peninsula*. (Vol. 26).

WMO-No.100. (2018). *Guide to Climatological Practices*.

Zawar-Reza, P., & Katurji, M. (2014). Antarctic Climate and Soils. In D. A. Cowan (Ed.), *Antarctic Terrestrial Microbiology: Physical and Biological Properties of Antarctic Soils* (pp. 279-292). Berlin, Heidelberg: Springer Berlin Heidelberg. https://doi.org/10.1007/978-3-642-45213-0_15.

Appendices

Appendix I

Soil Profile Descriptions

Introduction

The soil profile was described, using the USDA taxonomic standards, at each site by the team who initiated each soil climate station. The soil probes were installed in the same hole and the surface was restored to its original condition. Soil samples were taken for further analysis and those results are available at:

https://www.nrcs.usda.gov/wps/portal/nrcs/detail/soils/survey/climate/?cid=nrcs142p2_053772

Below are the direct copies of the soil profile descriptions for each site, with the author accredited. These descriptions are available in their original form at the same site given above. Chapter three gives an overview of each site and soil profile figures.

Granite Harbour

Described by Megan Balks

Date January 2003

Profile description

Depth

0 – 2 cm

Description

Desert pavement comprises about 50% granite boulders greater than 80 cm in diameter, some up to 5 m in diameter, 30% granite boulders and stones of less than 80 cm diameter, 10% sand and 10 % granite gravel. Boulders are rounded and weathering by grains falling off. A small amount of iron oxidation is visible on some boulders. The matrix is gravelly coarse sand which comprises angular mineral grains from the granite, colours are those of individual minerals, minimal chem. weathering, dry, loose, distinct smooth boundary.

2 – 10 cm

Dull yellowish brown (10YR5/4 dry, 10YR 4/4 moist) gravelly coarse sand which comprises rounded mineral grains from granite, moderately weathered with a trace (<1%) of silt and clay and some iron oxides, dry, loose, no salts seen, diffuse smooth boundary.

10 – 30 cm

Gravelly coarse angular sand, minimal chemical weathering, colours are those of granite minerals (pink, white, grey, black), loose, dry, no salts seen, distinct wavy (+/- 10 cm) boundary.

30 – 70 cm

Dull yellowish brown (10YR4/3) loamy fine sand, sand is very uniform and well sorted, and does not have the individual granite minerals obvious (maybe a beach deposit?) moist, firm in-situ (holds vertical walls in pit), few angular stones (about 10 %), few granite gravels (about 5%), occasional lenses of coarse granite sand (ghosts of boulders), irregular distinct boundary.

70 – 80 cm

Gravelly coarse sand, 70% strongly interlocking stones and boulders, sand is unweathered granite mineral grains in granite mineral colours, this horizon is interpreted as a buried former desert pavement, indistinct irregular boundary.

80 – 90+ cm

Ice cemented sands with many rocks.

Minna Bluff

Described by Megan Balks

Date 11th January 2003

Profile description

Depth	Description
0 – 4 cm	Desert pavement. Gravelly coarse sand, colours are those of individual mineral grains, dry, salt accumulation beneath some rocks (1 sample). The desert pavement comprised dominantly basalts and dolerites, including scoreacious and porphoritic basalts. Granites (pink, red, grey and white dominated) were common with a range of other rock types seen occasionally including Beacon sandstone, weathered marble, angular conglomerates and shale. The pavement materials were generally moderately rounded and smoothed, a few with desert varnishing. (Generally more weathered than Marble Point). The pavement comprised about 5% large boulders (>30 cm diameter), 10% medium boulders (20-30 cm diameter), 20 % stones (5-20 cm diameter) and remainder gravel and coarse sand. Distinct, smooth boundary.
4 – 10 cm	Brown (10YR4/4) gravelly loamy sand (estimate 2% silt and clay in <2mm fraction), moisture content of < 2 mm fraction was 15 %, loose, gravel content variable - ranging from about 30 to 70 %, no salts seen, diffuse boundary.
10 – 30 cm	Dark brown (10YR3/3) gravelly loamy sand (estimate 2% silt and clay in <2mm fraction), slightly moist (< 2mm fraction was 10 %), very loose, gravel content variable - ranging from about 30 to 70 %, measured as 64% by weight > 5.6 mm, 17% by weight 5.6 – 2 mm and 19% < 2mm, no salts seen, sharp smooth boundary.
30 – 60 cm	Dull yellowish brown (10YR4/3) gravelly icy sandy silt loam (estimate 60% silt and 10% clay in <2mm fraction), ice saturated (>50% ice), ice-cemented, very sticky when melted, gravel content about 30 %, boulders about 1%, no salts seen, diffuse smooth boundary.
60 – 80+ cm	Grayish yellow brown (10YR4/2) gravelly icy sandy silt loam (estimate 60% silt and 10% clay in <2mm fraction), ice saturated (>50% ice), ice-cemented, very sticky when melted, gravel content about 10 %, boulders about 1%, no salts seen.

Marble Point

Described by John M Kimble, Iain Campbell, Megan Balks, Ron Paetzold

Date: 15th January 1999

Profile description

Depth

0 – 3 cm A

Description

Very dark greyish brown (10YR 3/2) very gravelly sand, dark greyish brown (10YR 4/2), dry; single grain; loose, loose, non-cemented, non-sticky, non-plastic; non-smeary; low toughness; 1 percent 75- to 250-millimeter marble fragments and 1 percent 75- to 250-millimeter gneiss fragments and 1 percent 75- to 250-millimeter granite fragments; strong effervescence, by HCl, 1 normal; clear smooth boundary. Lab sample # 99P01648.

3 – 15 cm C1

Dark brown (10YR 3/3) very gravelly sand, brown (10YR 4/3), dry; strong single grain; loose, loose, non-cemented, non-sticky, non-plastic; non-smeary; low toughness; 1 percent 75- to 250-millimeter marble fragments and 1 percent 75- to 250-millimeter gneiss fragments; very slight effervescence, by HCl, 1 normal; clear smooth boundary. Lab sample # 99P01649.

15 – 32 cm C2

Dark brown (10YR 3/3) very gravelly sand, brown (10YR 5/3), dry; strong single grain; loose, loose, non-cemented, non-sticky, non-plastic; non-smeary; low toughness; 1 percent 75- to 250-millimeter marble fragments and 1 percent 75- to 250-millimeter gneiss fragments and 1 percent 75- to 250-millimeter granite fragments; slight effervescence, by HCl, 1 normal; clear smooth boundary. Lab sample # 99P01650.

32 – 45 cm C3

Dark brown (10YR 3/3) very gravelly sand, greyish brown (10YR 5/2), dry; strong single grain; loose, loose, non-cemented, non-sticky, non-plastic; non-smeary; low toughness; 1 percent 75- to 250-millimeter marble fragments and 1 percent 75- to 250-millimeter gneiss fragments and 1 percent 75- to 250-millimeter granite fragments; strong effervescence, by HCl, 1 normal; clear smooth boundary. Lab sample # 99P01651.

45 – 69 cm C4

Brown (10YR 4/3) very gravelly sand, pale brown (10YR 6/3), dry; strong single grain; loose, loose, non-cemented, non-sticky, non-plastic; non-smeary; low toughness; 1 percent 75- to 250-millimeter marble fragments and 1 percent 75- to 250-millimeter gneiss fragments and 1 percent 75- to 250-millimeter granite fragments; violent effervescence, by HCl, 1 normal; clear smooth boundary. Lab sample # 99P01652.

69 – 100 cm C5

1 percent 75- to 250-millimeter marble fragments. Lab sample # 99P01653.

Scott Base

Described by John M Kimble

Date 15th January 1999

Profile description

Depth	Description
0 – 1 cm C1	Very dark greyish brown (10YR 3/2) gravelly sandy loam, greyish brown (10YR 5/2), dry; moderate fine and medium lenticular platy, and single grain; very friable, soft, non-sticky, non-plastic; 30 percent angular 2- to 75-millimeter basaltic-ash; non-effervescent, by HCl, 1 normal; abrupt smooth boundary. Lab sample # 99P01667.
1 – 7 cm C2	Very dark greyish brown (10YR 3/2) gravelly sandy loam, pale brown (10YR 6/3), dry; moderate very fine and fine single grain; loose, loose, non-sticky, non-plastic; 30 percent angular 2- to 75-millimeter basaltic-ash; non-effervescent, by HCl, 1 normal; clear smooth boundary. Lab sample # 99P01668.
7 – 15 cm C3	Dark greyish brown (10YR 4/2) gravelly sandy loam, brown (10YR 5/3), dry; moderate very fine and fine single grain; loose, loose, non-sticky, non-plastic; 35 percent angular 2- to 75-millimeter basaltic-ash; non-effervescent, by HCl, 1 normal; clear smooth boundary. Lab sample # 99P01669.
15 – 30 cm C4	Brown (10YR 4/3) gravelly sandy loam, brown (10YR 5/3), dry; moderate very fine and fine single grain; loose, loose, non-sticky, non-plastic; 35% angular 2- to 75- millimetre basaltic-ash; non-effervescent, by HCl, 1 normal; abrupt smooth boundary. Lab sample # 99P01670.
30 – 45 cm C5	Lab sample # 99P01671.

Victoria Valley

Described by Megan Balks and Ron Sletten

Date 10th January 2002

Profile description

Depth	Description
0-2 cm	Desert pavement, weakly weathered (10YR7/2 dry, 10YR5/2 wet), gravelly sand, (estimate 70% gravel, 30% sand), colors of individual sand grains are evident, occasional thin (<0.5mm) intermittent salt accumulations on base of stones, <1% moisture, distinct smooth boundary;
2-8 cm	Weakly cemented (10YR7/2 dry, 10YR5/2 wet) gravelly sand (estimate 20% gravel, 77% sand, 3% silt), gravels are predominantly 10-50 mm in diameter, weakly weathered, sub-angular, cementation is sufficient to hold an overhang of up to 20 cm, 2% moisture, distinct smooth boundary;
8-40 cm	Unweathered, stratified gravelly sand (estimate 20% gravel, 77% sand, 3% silt), gravels are predominantly 10-50 mm in diameter, weakly weathered, sub-angular. Colours are those of individual sand grains and range from dark grey to white, occasional pebble layer is evidence of former surface horizon, 2% moisture, sharp smooth boundary;
40-120+ cm	Ice cemented material essentially similar to the horizon above as evidenced by drill hole to install MRC probe.

Wright Valley North Wall

Described by Cathy Seybold and Holly Goddard

Date 17th January 2012

Profile description

Depth		Description
0 – 1 cm	C1	Desert pavement, weathered, polished and some pitted stones and gravels with 50% grey (10YR 6/1 dry) and 50% black (10YR 2/1 dry) coarse sand (5% of surface); single grain; loose, non-cemented, non-sticky and non-plastic; non-effervescent (1N-HCl); surface stones (65 mm to 2 m) cover about 5% of surface, cobbles cover about 5% of surface, and gravels cover about 85% of surface; fragment kinds are 85% granite, 10% dolerite; abrupt smooth boundary.
1 – 23 cm	C2	Light olive brown (2.5Y 5/4 dry) gravelly coarse sand; single grain; loose, non-cemented, non-sticky, and non-plastic; non-effervescent (1N-HCl); 5% stones and 20% gravel; non-oxidized; finely stratified throughout; 0.7% by wt. water content; clear smooth boundary.
23 – 79 cm	2Ck	Light olive brown (10YR 5/3 moist) very gravelly fine sand; massive; very friable, non-sticky and non-plastic; slightly effervescent (1N-HCl); 15% stones, 15% cobbles and 20% gravel; non-oxidized; 4.0% by wt. water content; gradual wavy boundary.
79 – 120 cm	2C	Greyish brown (10YR 5/2 moist) very gravelly sand; non-oxidized, massive; very friable, non-sticky and non-plastic; non-effervescent (1N-HCl); 15% stones, 10% cobbles and 25% gravel, non-oxidized; 5.8% by wt. water content.

Wright Valley South Wall

Described by Malcolm McLeod and Cathy Seybold

Date 11th January 2011

Profile description

Depth	Description
0 – 1 cm Cn1	Desert pavement, weathered, polished and some pitted boulders and gravels with yellowish brown (10YR 5/4 moist) coarse sand (5% of surface); single grain; loose, non-cemented, non-sticky and non-plastic; non-effervescent (1N-HCl); very few salt/carbonate accumulations under stones; surface boulders (65 mm to 2 m) cover about 15% of surface, cobbles cover about 25% of surface, and gravels cover about 55% of surface; fragment kinds are 85% granite, 10% dolerite; surface is flattened; abrupt smooth boundary.
1 – 24 cm Cn2	Light yellowish brown (2.5Y 6/3 moist) stony sand; single grain; loose, non-cemented, non-sticky, and non-plastic; non-effervescent (1N-HCl); 15% stones and 5% cobbles; clear wavy boundary.
24 – 70 cm 2Cfm1	30% Yellowish brown (10YR 5/5 moist) and 70% strong brown (7.5YR 4/6 moist) very gravelly sand; single grain; loose, frozen, non-sticky and non-plastic; non-effervescent (1N-HCl); 5% stones, 10% cobbles and 40% gravel; oxidized surfaces; gradual wavy boundary.
70 – 120 cm 2Cfm2	Yellowish brown (10YR 5/5 dry) very gravelly sand; single grain; loose, frozen, non-sticky and non-plastic; non-effervescent (1N-HCl); 5% stones, 15% cobbles and 35% gravel; oxidized surfaces.

Wright Valley Floor

Described by John M Kimble

Date 1st December 1999

Profile description

Depth		Description
0 – 3 cm	C1	Very dark greyish brown (10YR 3/2) very gravelly sand, light brownish grey (10YR 6/2), dry; single grain; loose, loose, non-cemented, non-sticky, non-plastic; slight effervescence, by HCl, 1 normal; abrupt smooth boundary. Lab sample # 99P01658.
3 – 12 cm	C2	Brown (10YR 4/3) silt loam, brown (10YR 5/3), dry; very friable, slightly hard, non-cemented, non-sticky, non-plastic; brittle; slight effervescence, by HCl, 1 normal; abrupt irregular boundary. Lab sample # 99P01659.
12 – 18 cm	C3	Brown (10YR 5/3) silt loam, light grey (10YR 7/2), dry; massive, and single grain; loose, slightly hard, non-cemented, non-sticky, non-plastic; brittle; slight effervescence, by HCl, 1 normal; clear smooth boundary. Lab sample # 99P01660.
18 – 28 cm	C4	Dark greyish brown (10YR 4/2) silt loam, light grey (10YR 7/2), dry; massive, and single grain; loose, slightly hard, non-cemented, non-sticky, non-plastic; brittle; slight effervescence, by HCl, 1 normal; clear smooth boundary. Lab sample # 99P01661.
28 – 38 cm	C5	Brown (10YR 4/3) silt loam, very pale brown (10YR 7/3), dry; massive, and single grain; loose, slightly hard, non-cemented, non-sticky, non-plastic; brittle; slight effervescence, by HCl, 1 normal; clear smooth boundary. Lab sample # 99P01662.
38 – 51 cm	C6	Brown (10YR 5/3) silt loam, light brownish grey (10YR 6/2), dry; massive, and single grain; loose, slightly hard, non-cemented, non-sticky, non-plastic; brittle; slight effervescence, by HCl, 1 normal; clear smooth boundary. Lab sample # 99P01663.
51 – 78 cm	C7	Brown (10YR 5/3) silt loam, light brownish grey (10YR 6/2), dry; massive, and single grain; loose, slightly hard, non-cemented, non-sticky, non-plastic; brittle; slight effervescence, by HCl, 1 normal; clear smooth boundary. Lab sample # 99P01664.
78 – 109 cm	C8	Brown (10YR 4/3) gravelly silt loam, very pale brown (10YR 7/3), dry; massive; loose, slightly hard, non-

cemented, non-sticky, non-plastic; brittle; slight effervescence, by HCl, 1 normal; clear smooth boundary. Lab sample # 99P01665.

109 – 130 cm C9 Greyish brown (10YR 5/2) gravelly silt loam, light grey (10YR 7/2), dry; massive, and single grain; loose, slightly hard, non-cemented, non-sticky, non-plastic; brittle; strong effervescence, by HCl, 1 normal.

Mt Fleming

Described by Megan Balks

Date 5th January 2002

Profile description

Depth

0-2 cm

Description

Desert pavement, very strongly weathered, polished and pitted boulders and gravels with (10YR6/3 dry, 10YR5/4 moist) coarse sand, surface boulders cover about 60% of surface, are up to 1 m in diameter, and have strong desert varnish and ventifaction. Dolerite is dominant with sandstone and granite also present; gravels are subangular, desert varnished, many ventifacted, dolerite and quartz dominate, sands are coarse, loose and weathered to FeO colours, about 2% moisture, distinct irregular boundary.

2-8 cm

Strongly weathered bouldery gravelly, (10YR6/6 dry, 10YR5/4 moist) coarse sand (estimate 98% sand, 2% silt), common 0.5-0.8 cm thick, white, salt crusts under larger stones. About 20% 10-40 cm diameter boulders, angular, some strongly weathered (so fall apart when disturbed), dolerite dominant, but granite and sandstone also present. About 30% gravels, angular (rocks split to gravel size), weakly to strongly weathered, dolerite dominant with granite, sandstone and some rounded quartz pebbles, about 7% moisture (following recent snow), distinct, irregular boundary.

-8-20 cm

Weakly weathered gravelly (2.5Y7/2 dry, 2.5Y5/2 moist) silty sand (estimate 70% fine sand, 30% silt), no salts visible, about 10% unweathered angular gravel, with an occasional (10%) up to 20 cm diameter, non to weakly weathered, angular boulder, about 5% moisture, diffuse, smooth boundary.

20-45 cm

Relatively unweathered gravelly (2.5Y6/2 dry, 2.5Y4/2 moist) silty sand. About 10% unweathered, angular gravel and rocks, about 2% moisture, sharp distinct boundary.

45-70+ cm

Ice cemented ground, similar material to the horizon above but with sufficient water to cement (16% moisture, sample appeared to be saturated when thawed). (2.5Y5/1 wet).

Appendix II

Soil Climate Station Instrumentation

Introduction

Six main variables are measured across the soil climate station (SCS) network. The instruments used are generally similar, with the main difference being when an upgraded version of an instrument becomes available it is used. More detailed list of each SCS instrumentation can be found at:

https://www.nrcs.usda.gov/wps/portal/nrcs/detail/soils/survey/climate/?cid=nrcs142p2_053772

Instrumentation tables

Table II.1: All SCS measure soil moisture using the same probe type (that has been renamed as the Hydra-Probe, from the before Vitel M/T probe), here the depth range that soil moisture is measured, installation date and the specifications of the probes are presented.

SCS	Probe Type	Soil Moisture		Measurement Range	Tolerance
		Depth Range	Date Installed		
WV North Wall	Hydra-Probe	2 - 50 cm	2012	0 - 100%	± 0.01wfv
South Wall	Hydra-Probe	3 - 25 cm	2011	0 - 100%	± 0.01wfv
Granite Harbour	Vitel Soil M/T	2.5 - 75 cm	2003	0 - 100%	± 0.01wfv
Marble Point	Vitel Soil M/T	2.5 - 80 cm	1999	0 - 100%	± 0.01wfv
Minna Bluff	Vitel Soil M/T	25 - 94 cm	2003	0 - 100%	± 0.01wfv
Mt Fleming	Vitel Soil M/T	7.5 - 30 cm	2002	0 - 100%	± 0.01wfv
Scott Base	Vitel Soil M/T	2-40 cm	1999	0 - 100%	± 0.01wfv
Victoria Valley	Vitel Soil M/T	3-33 cm	1999	0 - 100%	± 0.01wfv
WV Floor	Vitel Soil M/T	2-120 cm	1999	0 - 100%	± 0.01wfv

Table II.2: Three types of soil temperature probes are present at each soil climate station (SCS), here the probe type, the depth range of the sensors, installation date and the specifications of each probe are presented. WV = Wright Valley

Soil Temperature					
SCS	Probe Type	Depth Range	Date Installed	Measurement Range	Tolerance
WV North Wall	Campbell 107	1 - 75 cm	2012	-35°C - +50°C	± 0.2°C
	Hydra-Probe	2 - 25 cm		-10°C - +60°C	± 0.3°C
	MRC	0 - 120 cm		-30 - +75°C	± 0.01°C
WV South Wall	Campbell 107	1 - 75 cm	2011	-35°C - +50°C	± 0.2°C
	Hydra-Probe	2 -25 cm		-10°C - +60°C	± 0.3°C
	MRC	0 - 120 cm		-30 - +75°C	± 0.01°C
	Vitel Soil				
Granite Harbour	M/T	2.5 - 75 cm	2003	-30°C - +36°C	± 0.3°C
	Campbell 107	2 - 90 cm		-35°C - +50°C	± 0.2°C
	MRC	0 - 90 cm		-30 - +75°C	± 0.01°C
	Vitel Soil				
Marble Point	M/T	2 - 80 cm	1999	-10°C - +60°C	± 0.3°C
	Campbell 107	surface		-35°C - +50°C	± 0.2°C
	MRC	0 - 120 cm		-30 - +75°C	± 0.01°C
	Vitel Soil				
Minna Bluff	M/T	10 - 38 cm	2003	-10°C - +60°C	± 0.3°C
	Campbell 107	5 - 85 cm		-35°C - +50°C	± 0.2°C
	MRC	0 - 105 cm		-30 - +75°C	± 0.01°C
	Vitel Soil				
Mt Fleming	M/T	7.5-30 cm	2002	-10°C - +60°C	± 0.3°C
	Campbell 107	2-75 cm		-35°C - +50°C	± 0.2°C
	Vitel Soil				
Scott Base	M/T	2-40 cm	1999	-10°C - +60°C	± 0.3°C
	Campbell 107	2-25 cm		-35°C - +50°C	± 0.2°C
	MRC	0-120 cm		-30 - +75°C	± 0.01°C
	Vitel Soil				
Victoria Valley	M/T	3-33 cm	1999	-10°C - +60°C	± 0.3°C
	Campbell 107	3-33 cm		-30°C - +36°C	± 0.2°C
	MRC	0-120 cm		-30 - +75°C	± 0.01°C
	Vitel Soil				
WV Floor	M/T	2-120 cm	1999	-10°C - +60°C	± 0.3°C
	Campbell 107	Surface-42 cm		-35°C - +50°C	± 0.2°C
	MRC	0-120 cm		-30 - +75°C	± 0.01°C

Table II.3: At most sites the air temperature is monitored with two probes, the Campbell 107 and 109 measure only air temperature, while the Campbell HMP 35C and HMP 45C monitor both air temperature and relative humidity (Table II.4). Here the probe type, the height of the sensors, installation date and the specifications of each probe are presented. WV = Wright Valley

SCS	Probe type	Air Temperature			
		Height Installed	Date installed	Measurement Range	Tolerance
WV North Wall	Campbell 109	1.6 m	2012	-50°C - +70°C	± 0.2°C
	HMP 45C	2 m		-40°C - +60°C	± 0.4°C
WV South Wall	Campbell 109	1.6 m	2011	-50°C - +70°C	± 0.2°C
	HMP 45C	2 m		-40°C - +60°C	± 0.4°C
Granite Harbour	Campbell 107	2 m	2003	-35°C - +50°C	± 0.2°C
	HMP45C	1.6 m		-40°C - +60°C	± 0.4°C
Marble Point	Campbell 107	3 m	1999	-35°C - +50°C	± 0.2°C
	HMP 45C	1.6 m		-40°C - +60°C	± 0.4°C
Minna Bluff	Campbell 107	2 m	2006	-35°C - +50°C	± 0.2°C
	HMP 35C	2 m	2003	-35°C - +50°C	± 0.4°C
Mt Fleming	HMP45C	1.6 m	2002	-40°C - +60°C	± 0.4°C
	HMP35C	1.2 m	2000 - 2004	-35°C - +50°C	± 0.2°C
Scott Base	HMP45C	1.6 m	2005 - 2009	-40°C - +60°C	± 0.4°C
	Campbell 109	1.6 m	2010	-50°C - +70°C	± 0.2°C
Victoria Valley	HMP45C	2 m	1999	-35°C - +50°C	± 0.4°C
	Campbell 109	2 m	2010	-40°C - +60°C	± 0.2°C
WV Floor	RM Young RTD	2 m	1999	-50°C - +50°C	± 0.3°C
	HMP45C	2 m	2008	-40°C - +60°C	± 0.4°C

Table II.4: Relative above ground humidity is measured at the SCS using either the Campbell HMP 45C or Campbell HMP 35C sensor. The relative above ground humidity sensors were installed during set up at all SCS other than at the WV Floor. Here the probe type, the installation height, installation date, and the specifications of each probe are presented. WV= Wright Valley

SCS	Probe	Relative Air humidity Probe			
		Height Installed	Date installed	Measurement range	Tolerance
WV North Wall	HMP 45C	2 m	2012	0 - 100%	± 2%
WV South Wall	HMP 45C	1.6 m	2011	0 - 100%	± 2%
Granite Harbour	HMP 45C	1.6 m	2003	0 - 100%	± 2%
Marble Point	HMP 45C	1.6 m	1999	0 - 100%	± 2%
Minna Bluff	HMP 35C	2 m	2003	0 - 100%	± 2%
Mt Fleming	HMP45C	1.6 m	2002	0 - 100%	± 2%
Scott Base	HMP45C	2 m	1999	0 - 100%	± 2%
Victoria Valley	HMP45C	2 m	1999	0 - 100%	± 2%
WV Floor	HMP45C	2 m	2008	0 - 100%	± 2%

Table II.5: Incoming solar radiation is monitored at all sites with the same instrument manufactured by LiCor. Here the probe type, the installation height and date and the specifications of the probe are presented. WV= Wright Valley

SCS	Probe type	Incoming Solar Radiation pyranometer			
		Height Installed	Date installed	Spectrum Waveband	Tolerance
WV North Wall	LiCor LI200X	2.2 m	2012	400 - 1100nm	± 3%
WV South Wall	LiCor LI200X	2.2 m	2011	400 - 1100nm	± 3%
Granite Harbour	LiCor LI200X	3 m	2003	400 - 1100nm	± 3%
Marble Point	LiCor LI200X	3 m	1999	400 - 1100nm	± 3%
Minna Bluff	LiCor LI200X	3 m	2003	400 - 1100nm	± 3%
Mt Fleming	LiCor LI200X	3 m	2002	400 - 1100nm	± 3%
Scott Base	LiCor LI200X	3 m	1999	400 - 1100nm	± 3%
Victoria Valley	LiCor LI200X	2 m	1999	400 - 1100nm	± 3%
WV Floor	LiCor LI200X	3 m	1999	400 - 1100nm	± 3%

Table II.6: Wind Speed was monitored originally with a Met One sensor, replacements after 2005 and at the newer sites the RM Young sensor has been installed, it can monitor faster speeds. Here the probe type, the height installed, the sensor specifications and year installed to year replaced are presented. WV= Wright Valley.

SCS	Probe type	Wind Speed & Direction			
		Height Installed	Date installed	Measurement range (ms ⁻¹)	Tolerance (ms ⁻¹)
WV North Wall	RM Young Sensor	2.2 m	2012	0 - 100	± 0.3
WV South Wall	RM Young Sensor	2.2 m	2011	0 - 100	± 0.3
Granite Harbour	Met One		2003 - 2012	0 - 45	± 0.11
	RM Young Sensor	3 m	2012	0 - 100	± 0.3
Marble Point*	Met One	3 m	1999 - 2009	0-45	± 0.11
	RM Young		2009	0 -100	± 0.3
Minna Bluff*+	Met One	3 m	2003- 2007	0 - 45	± 0.11
	RM Young		2007	0 -100	± 0.3
Mt Fleming	Met One	3 m	2002 - 2008	0 -45	± 0.11
	RM Young		2008	0 - 100	± 0.3
Scott Base*	Met One	3 m	1999- 2009	0 - 45	± 0.11
	RM Young		2009	0 - 100	± 0.3
Victoria Valley*	Met One	3 m	1999	0 - 45	± 0.11
WV Floor*	Met One	3 m	1999-2006	0-45	± 0.11
	RM Young		2007	0 - 100	± 0.3

* Denotes that the original Met One sensor damaged (blown away) and replaced with a second Met One sensor.

+ Denotes that the RM Young sensor was damaged after original installation and replaced with a second RM Young sensor.

Appendix III

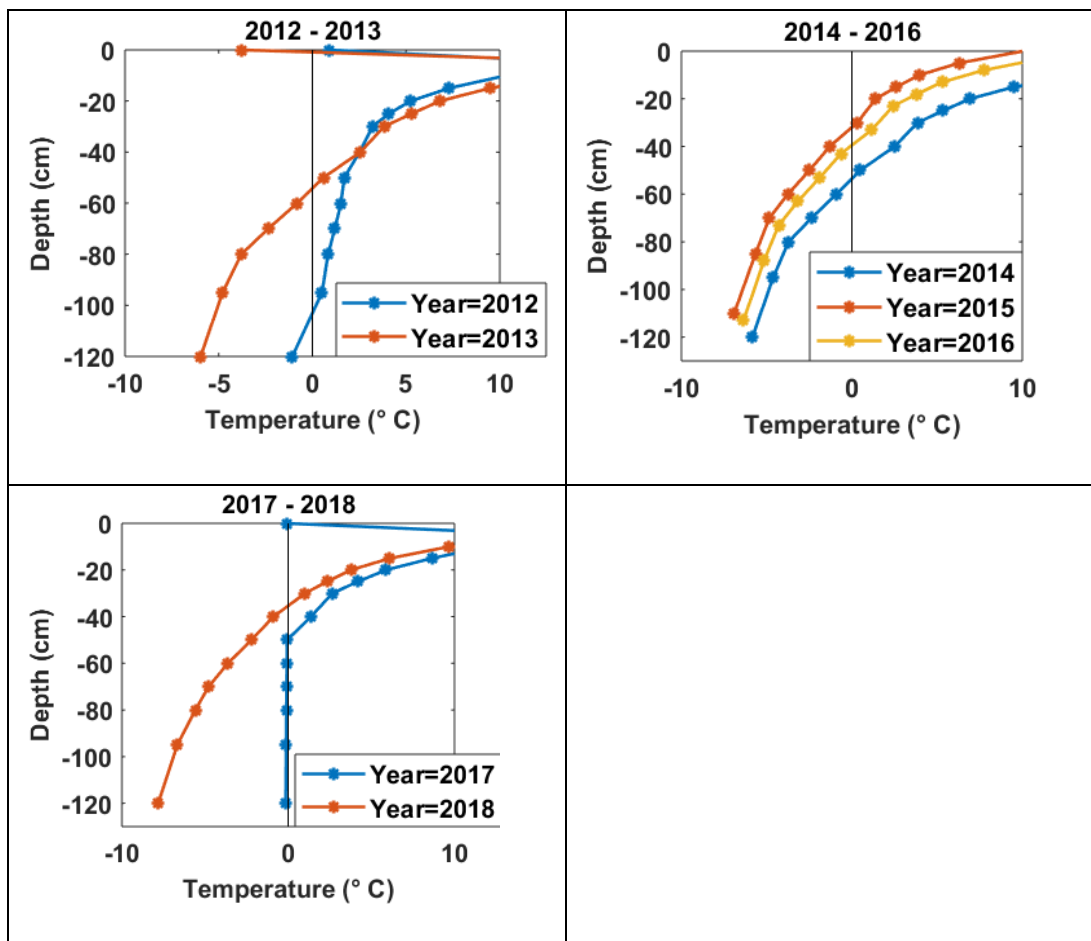
Active Layer Depth Determination

Introduction

Here presented are the figures developed in Matlab to determine the maximum active layer depths (ALD) at each soil climate station, presented in chapter 4. The ALD was determined by plotting the maximum summer (December and January) temperature for each sensor down the soil profile, and then using the “ginput” function to determine where the temperature profile crossed the 0°C isotherm. Where the profile crossed the isotherm more than once, the shallower depth (i.e. closest to the ground surface) was taken. Years where the multiple sensors reported the same temperature along the profile were discarded.

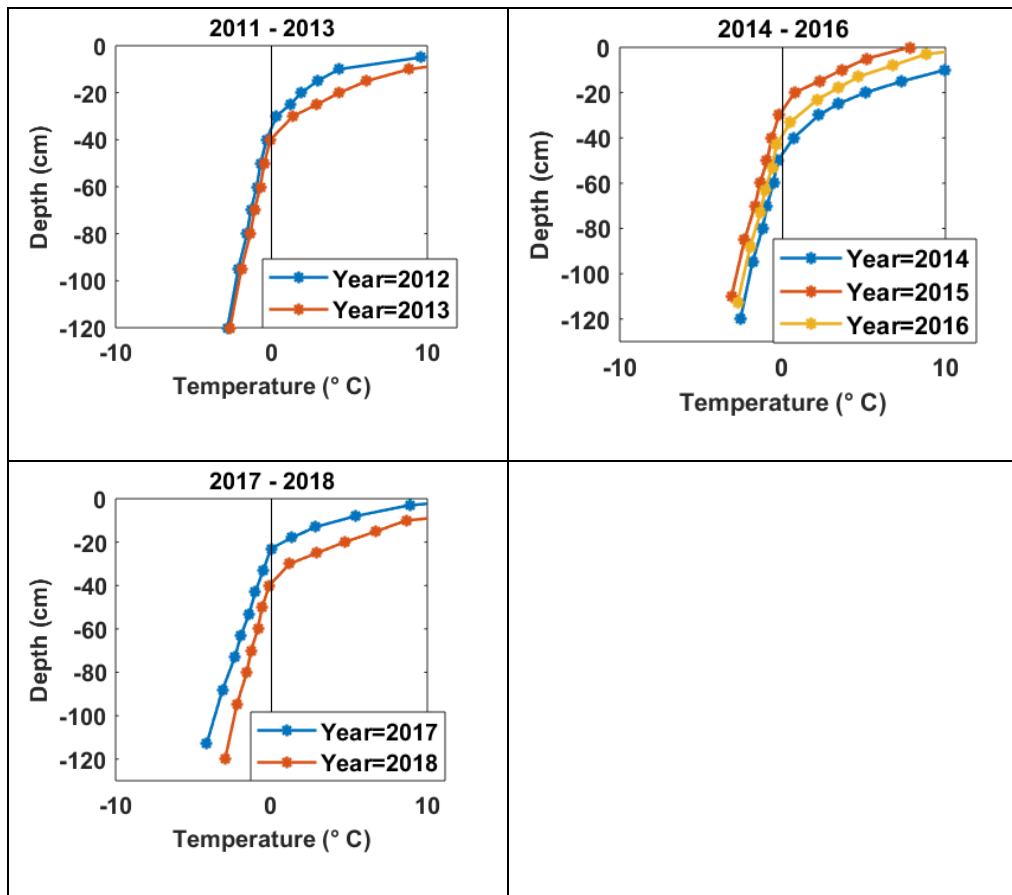
Wright Valley North Wall

Table III.1: Maximum soil temperature for each summer at the Wright Valley North Wall, the legend denotes the year at the end of each summer.



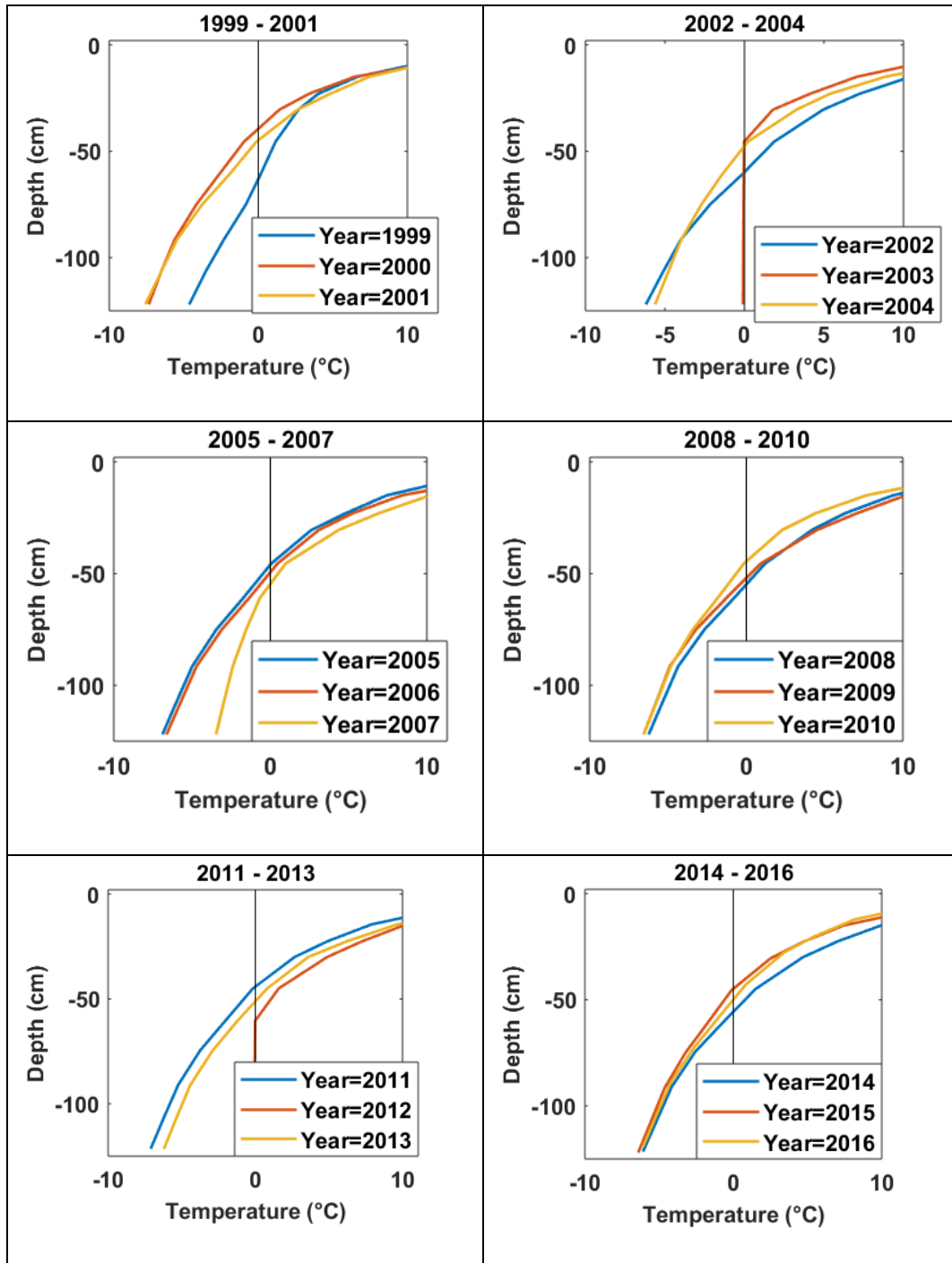
Wright Valley South Wall

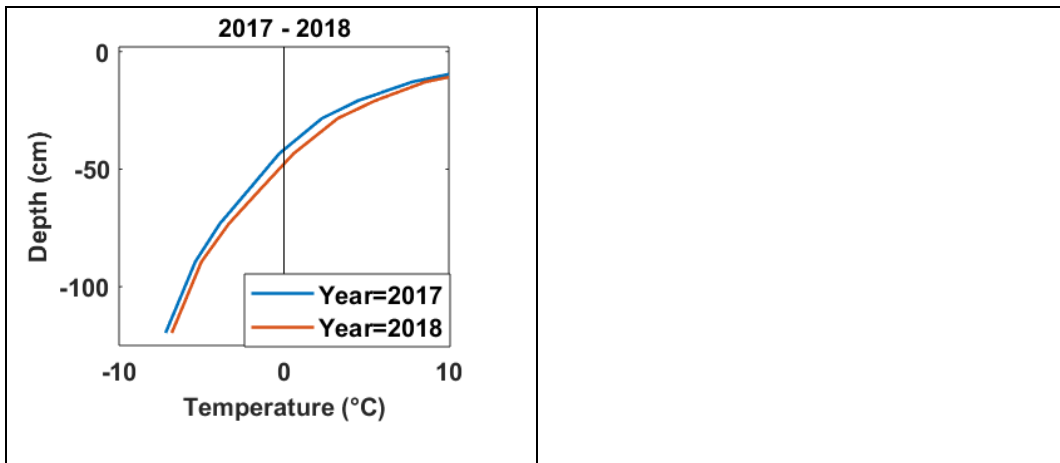
Table III.2: Maximum soil temperature for each summer Wright Valley South Wall, the legend denotes the year at the end of each summer.



Wright Valley Floor

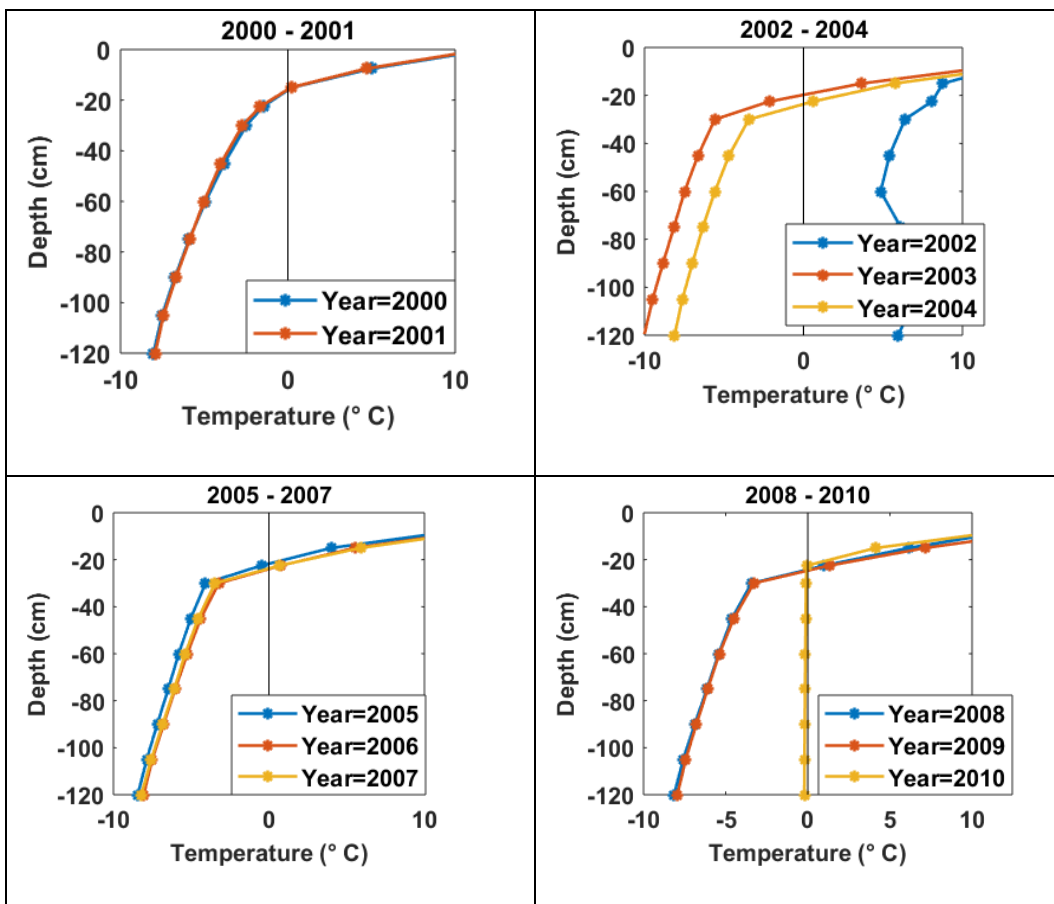
Table III.3: Maximum soil temperature for each summer at the Wright Valley Floor, the legend denotes the year at the end of each summer.

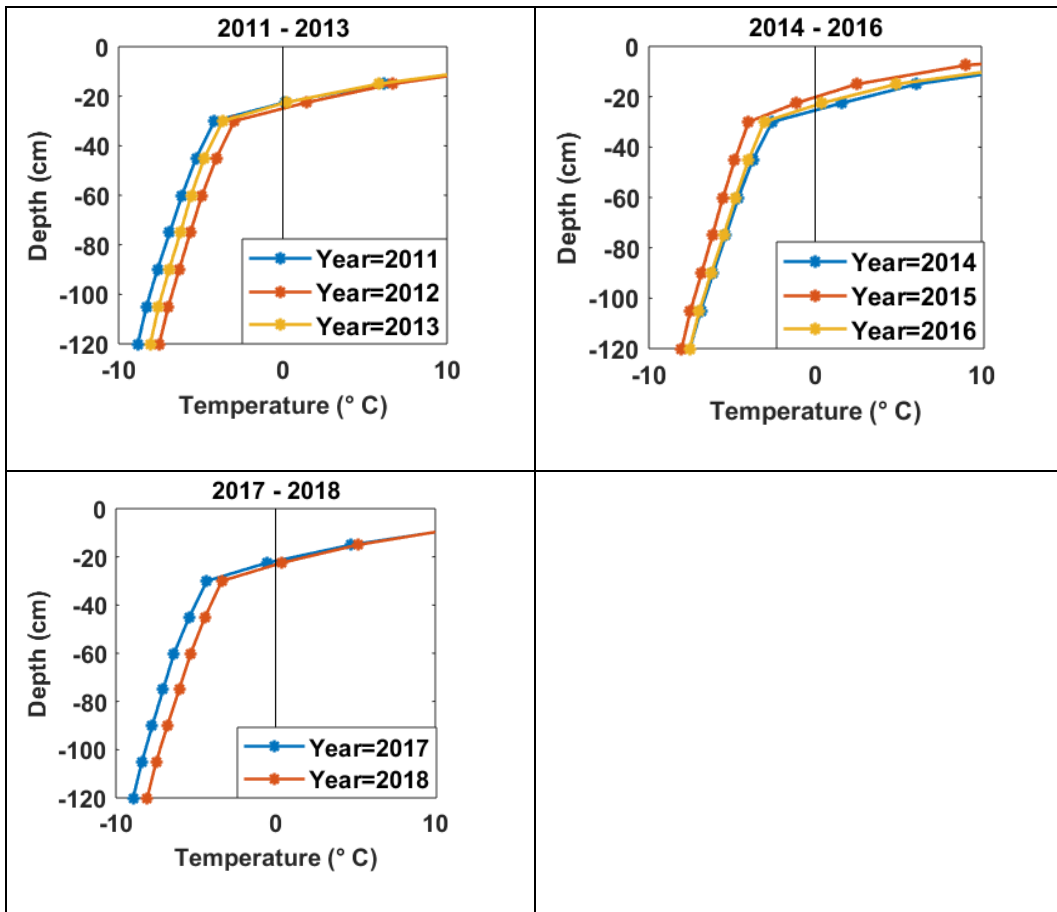




Victoria Valley

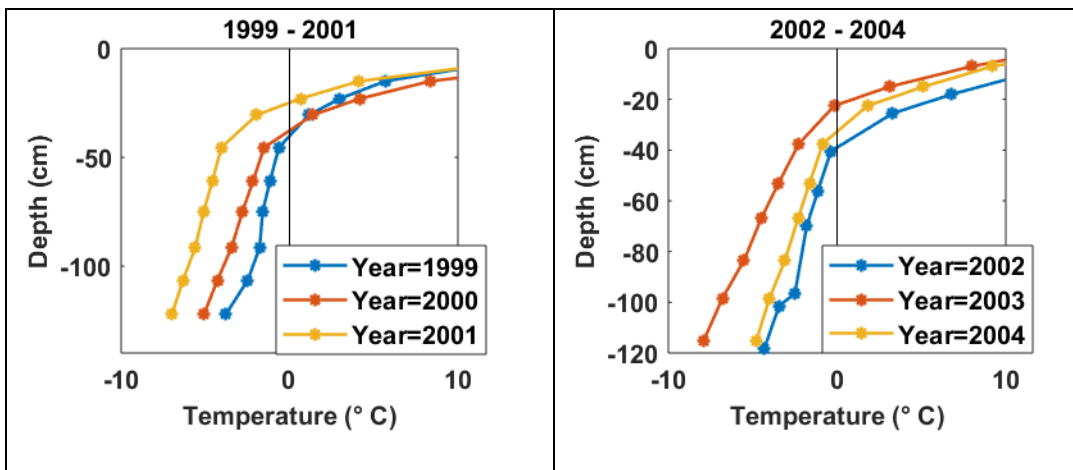
Table III.4: Maximum soil temperature for each summer at Vitoria Valley. The legend denotes the year at the end of each summer. Note that in the 2001/2002 summer the soil probe was excavated and moved from the edge of a shrink swell crack to the centre of a polygon in patterned ground.

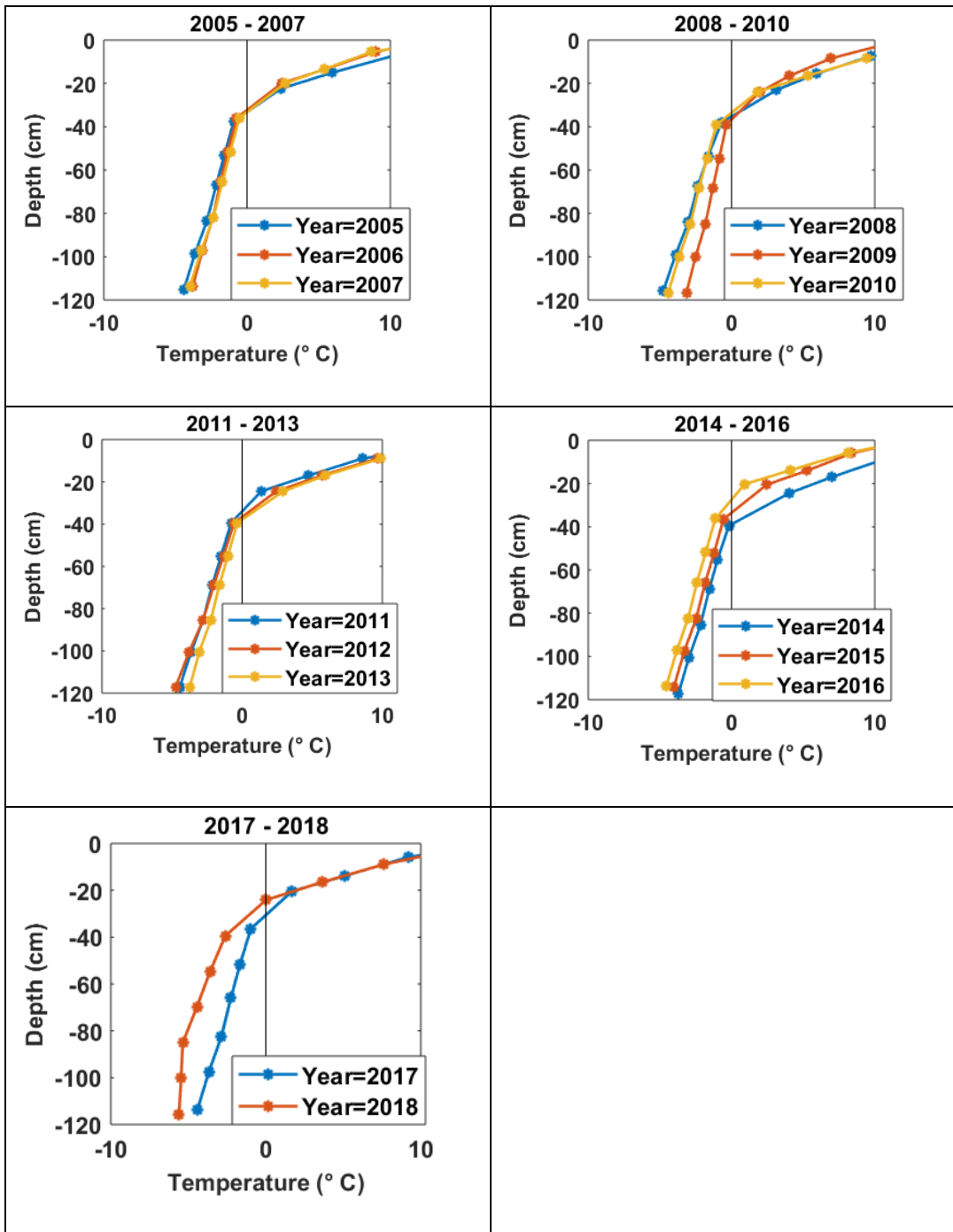




Scott Base

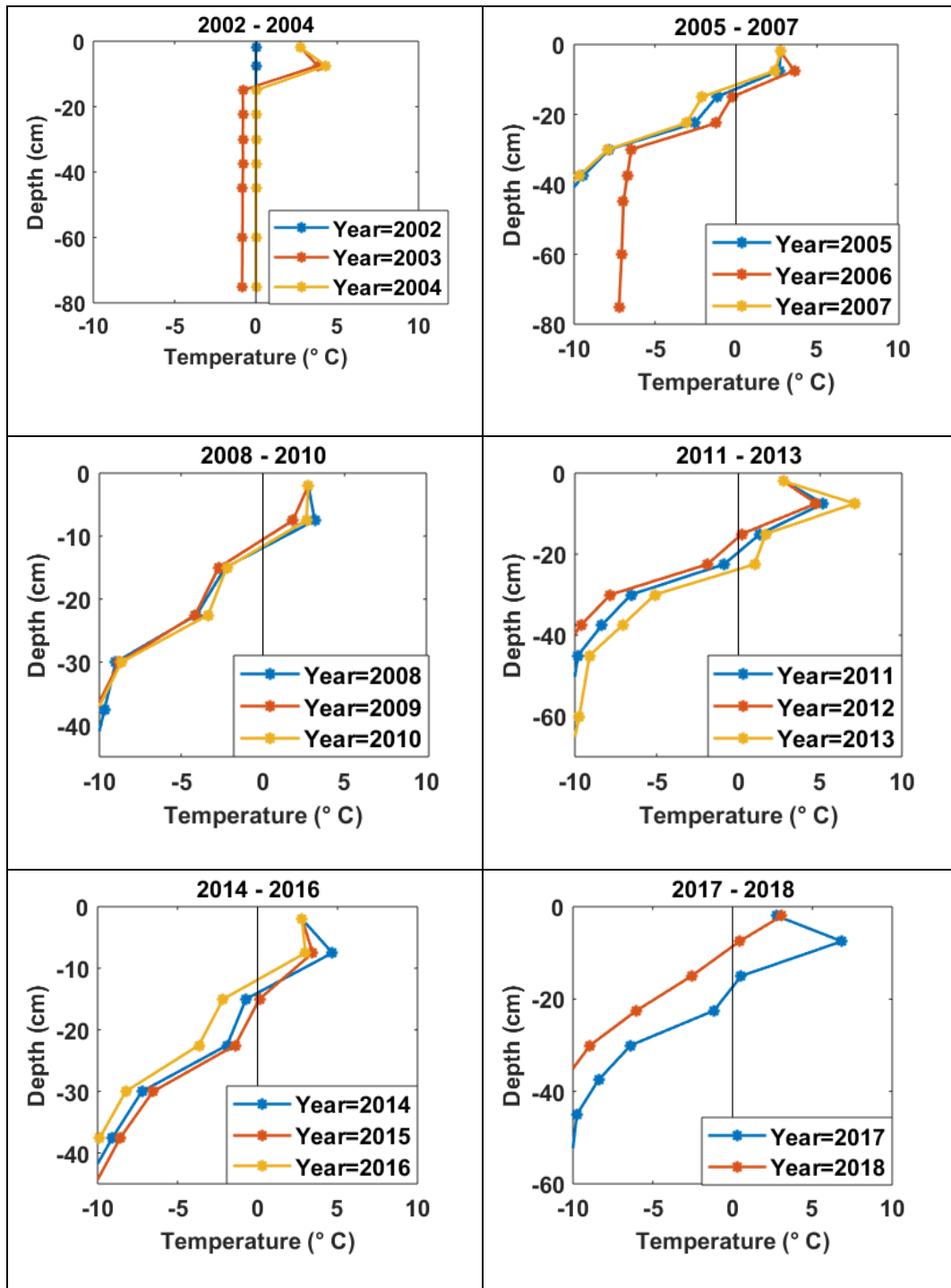
Table III.5: Maximum soil temperature for each summer at Scott Base, the legend denotes the year at the end of each summer.





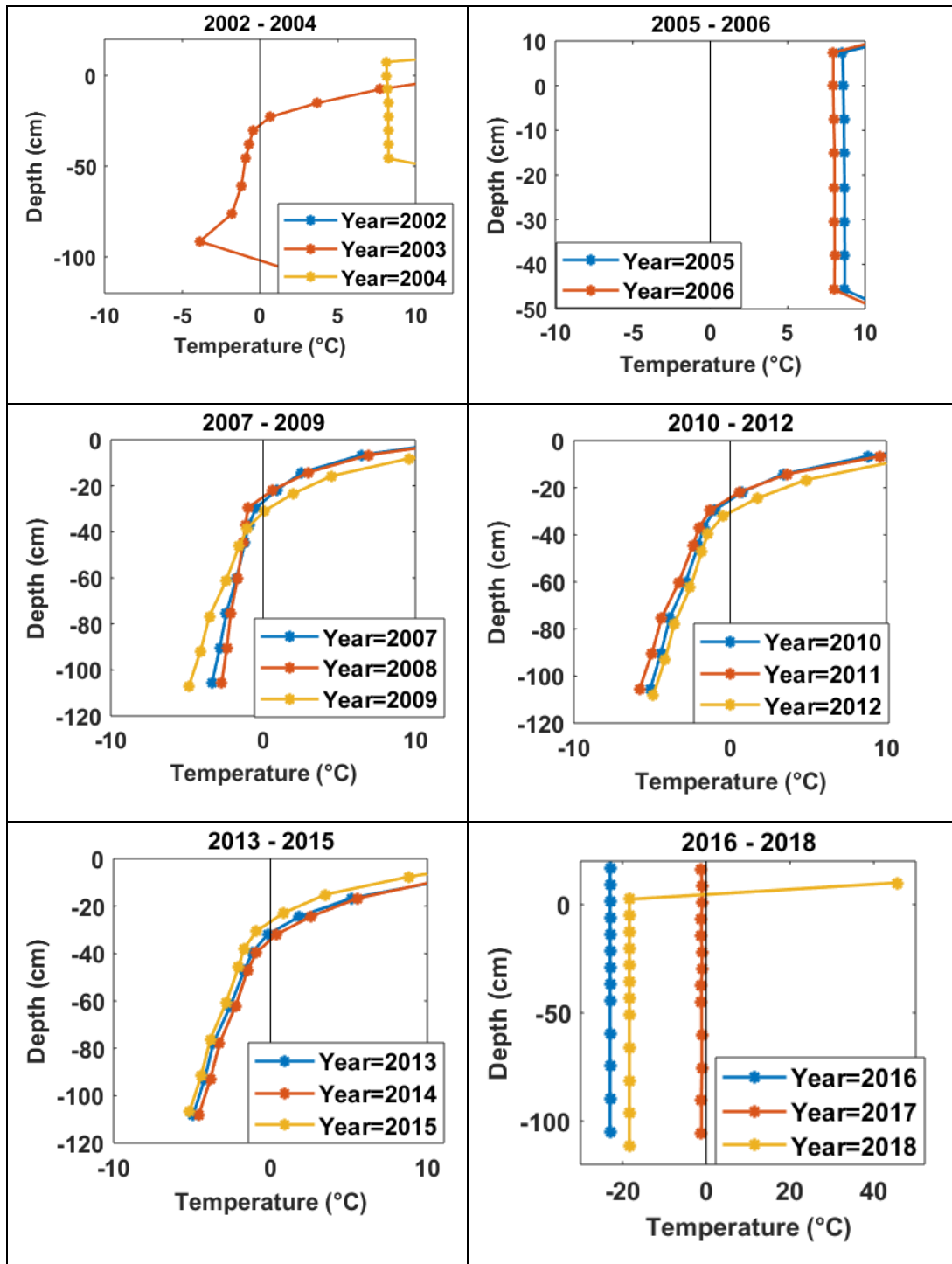
Mt Fleming

Table 6.6: Maximum soil temperature for each summer at Mt Fleming, the legend denotes the year at the end of each summer.



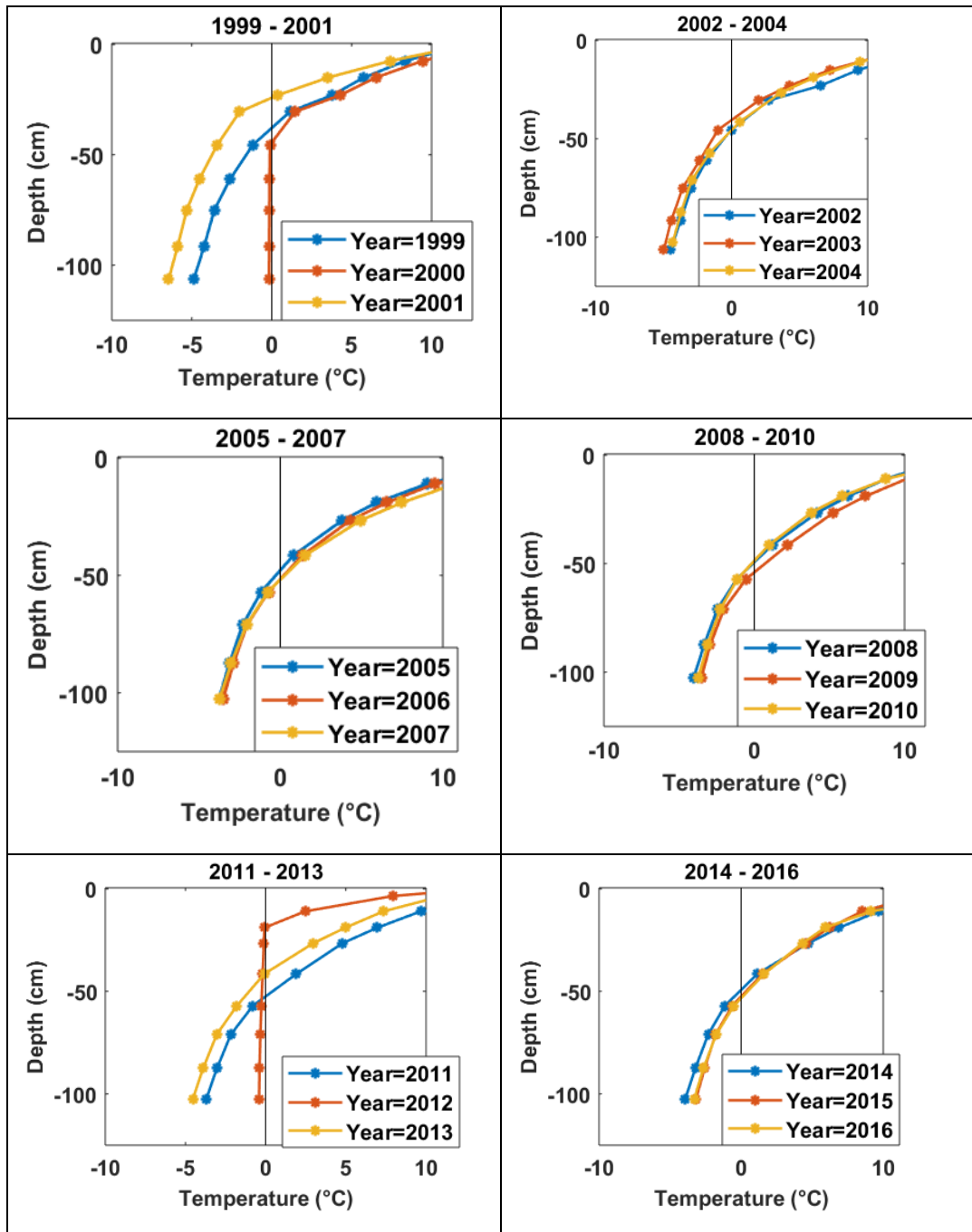
Minna Bluff

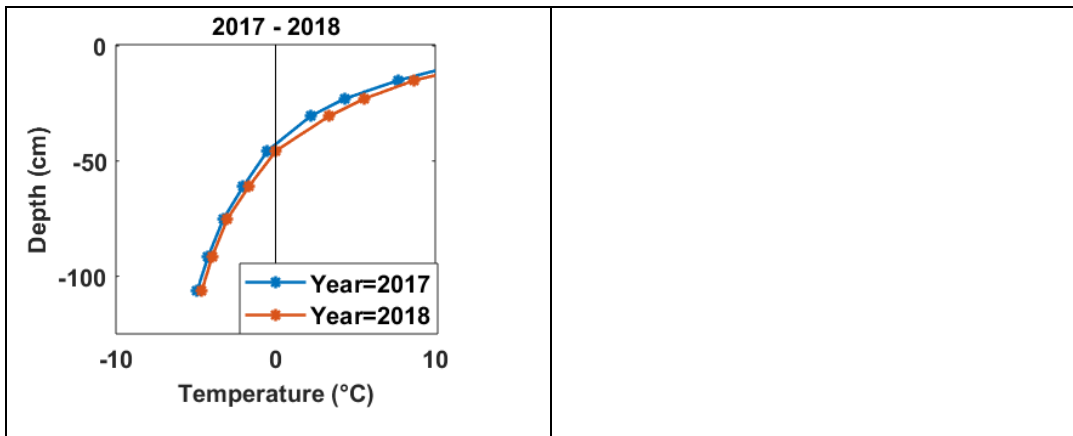
Table 6.7: Maximum soil temperature for each summer at Minna Bluff, the legend denotes the year at the end of each summer. Note ALD's from the 2003/ 2004 – 2005/ 2006 and the 2015/2016 -2016/2017 summers were discarded



Marble Point

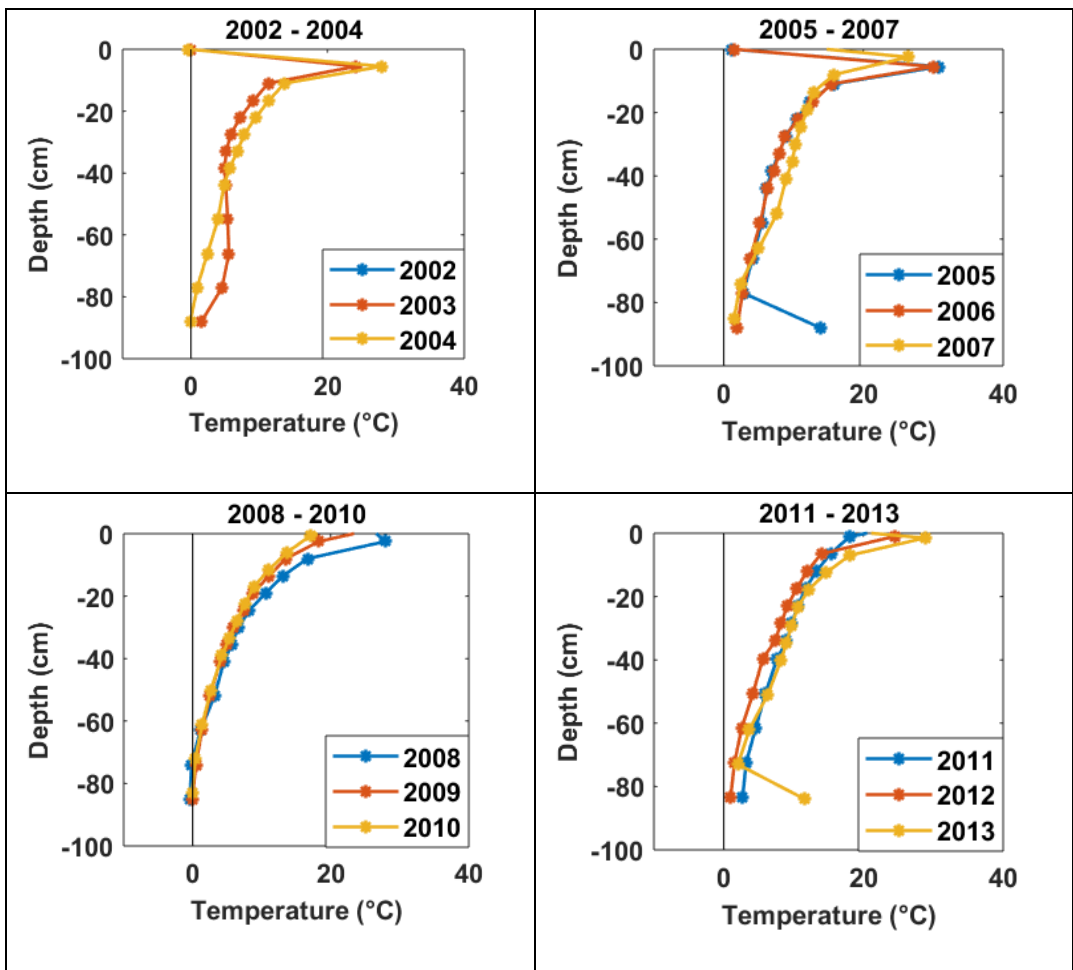
Table III.8: Maximum soil temperature for each summer at Marble Point. The legend denotes the year at the end of each summer.

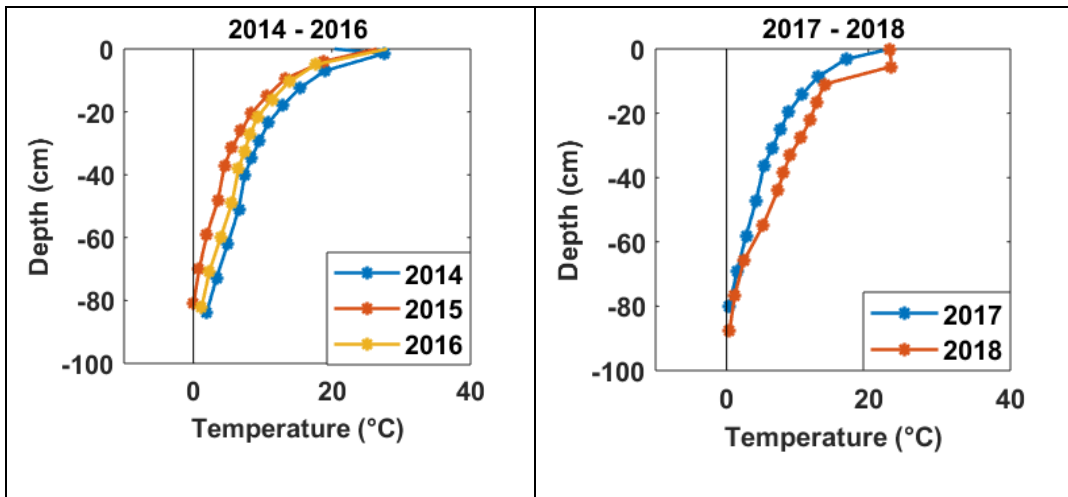




Granite Harbour

Table III.9: Maximum soil temperature for each summer at Granite harbour. The legend denotes the year at the end of each summer.





Appendix IV

Cross wavelet Analysis Graphs

Introduction

This appendix presents both the high and low amplitude cross-wavelet graphs between the climate drivers; the Southern Annular Mode (SAM), the Southern Oscillation Index (SOI) and the Amundsen Sea Low (ASL), and the soil climate stations. The results were summarised in Chapter four (Table 4.3 and Table 4.4).

High amplitude cross wavelet results

Marble Point

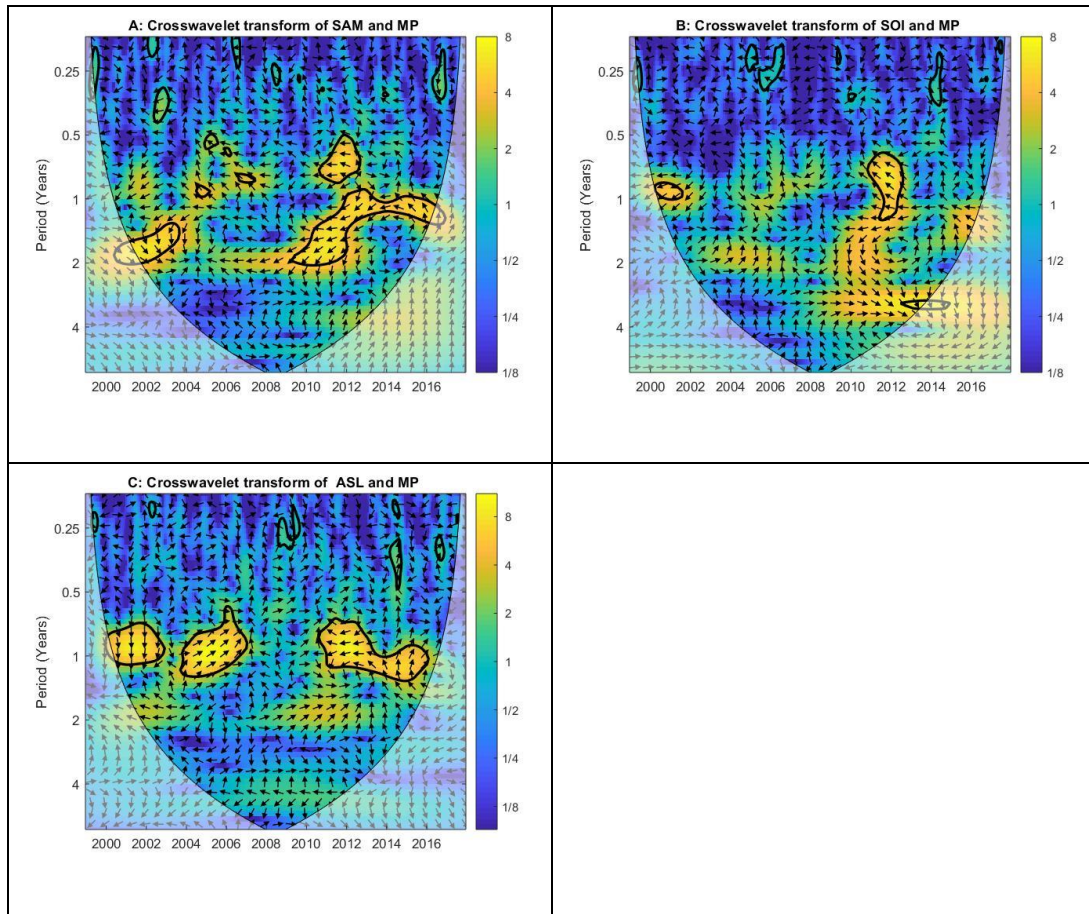


Figure IV.1: Cross wavelet transform between de-seasonalised permafrost temperature data at Marble Point (MP) and climate drivers. a: Southern Annular Mode (SAM); b: Southern Oscillation Index (SOI); c: Amundsen Sea Low pressure (ASL). The amplitude is displayed by the colour bar. Yellow corresponds to strong signal (amplitude) and areas within the black contours are significant ($p < 0.05$). Data in the paler shaded areas are influenced by the ‘edge effect’ and so are less reliable. Arrows correspond to phase relationships, where pointing right is in phase, points left is out of phase, and pointing downward means the climate driver leads the soil temperature by a quarter cycle.

Victoria Valley

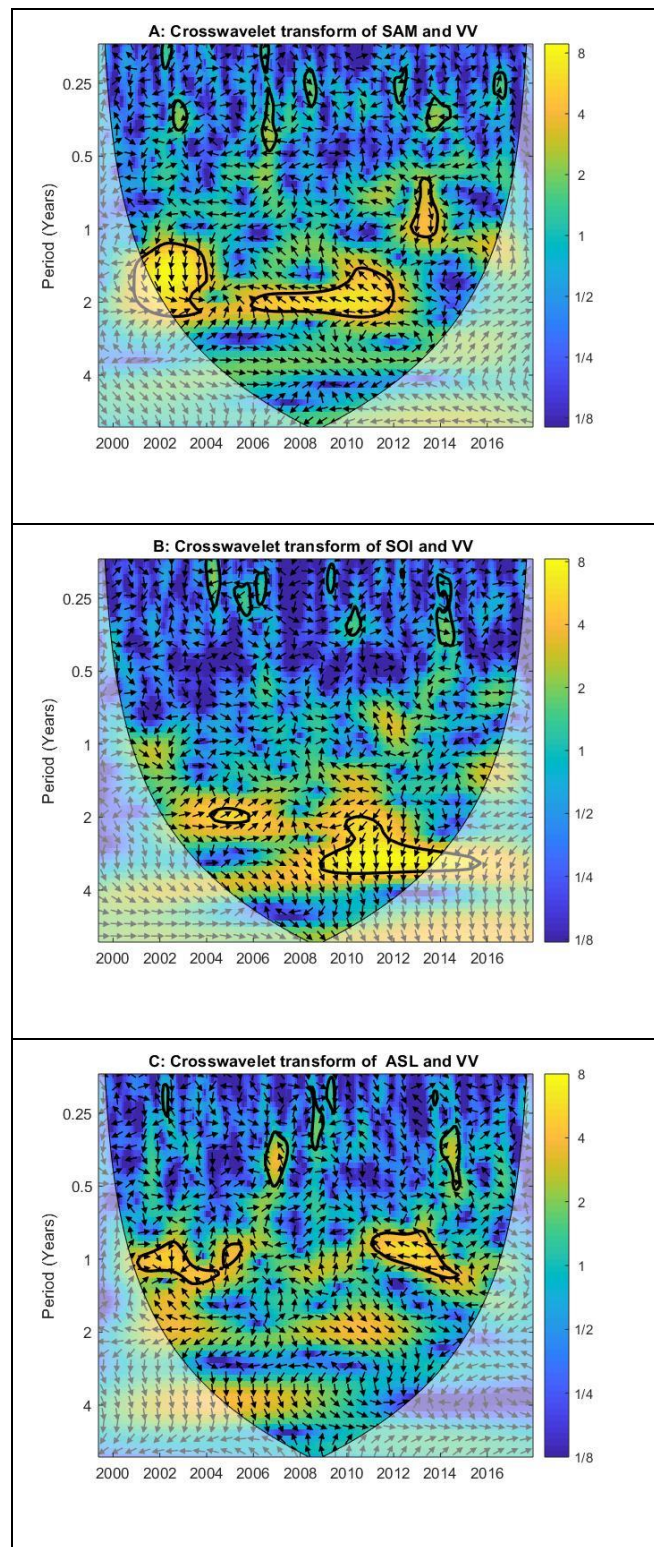


Figure IV.2: Cross wavelet transform between de-seasonalised permafrost temperature data at Victoria Valley (VV) and climate drivers. a: Southern Annular Mode (SAM); b: Southern Oscillation Index (SOI); c: Amundsen Sea Low pressure (ASL). The amplitude is displayed by the colour bar. Yellow corresponds to strong signal (amplitude) and areas within the black contours are significant ($p < 0.05$). Data in the paler shaded areas are influenced by the ‘edge effect’ and so are less reliable. Arrows correspond to phase relationships, where pointing right is in phase, points left is out of phase, and pointing downward means the climate driver leads the soil temperature by a quarter cycle.

Mt Fleming

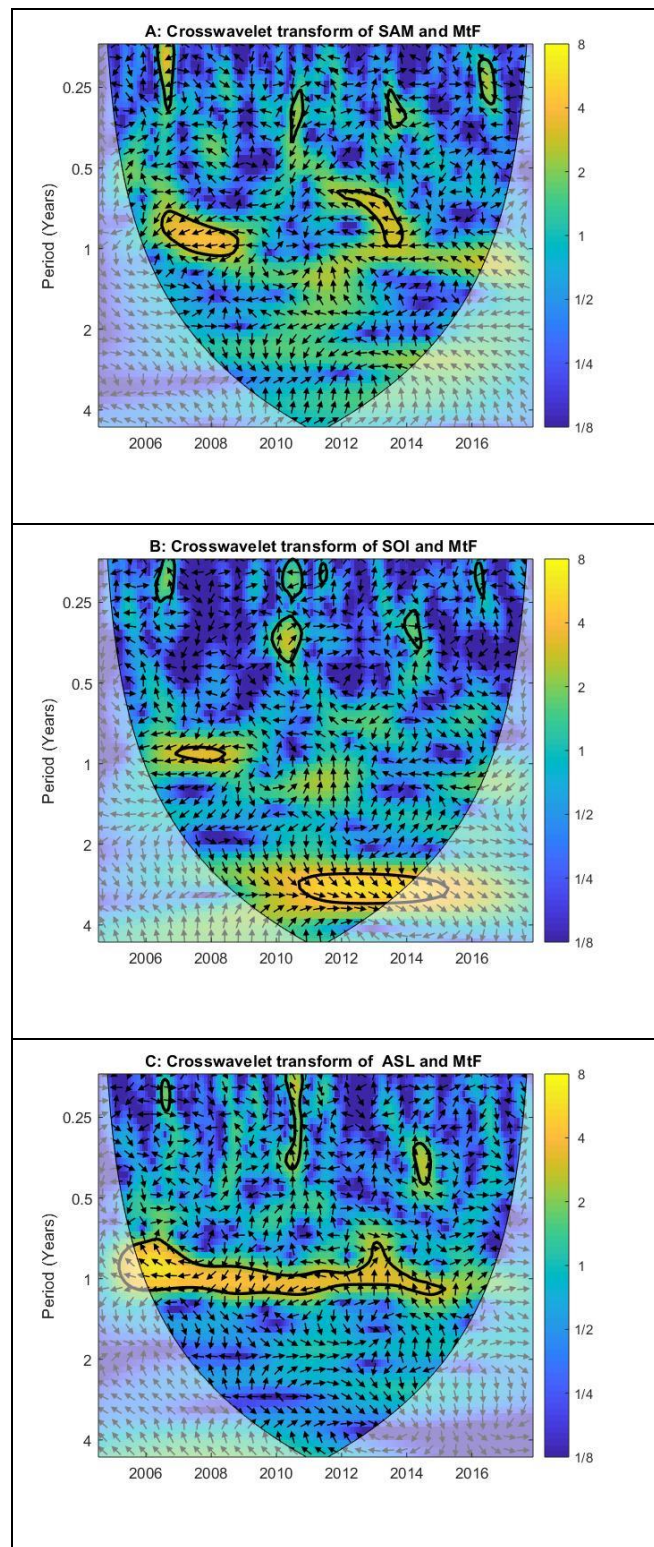


Figure IV.3: Cross wavelet transform between de-seasonalised permafrost temperature data at Mt Fleming (MtF) and climate drivers. a: Southern Annular Mode (SAM); b: Southern Oscillation Index (SOI); c: Amundsen Sea Low pressure (ASL). The amplitude is displayed by the colour bar. Yellow corresponds to strong signal (amplitude) and areas within the black contours are significant ($p < 0.05$). Data in the paler shaded areas are influenced by the ‘edge effect’ and so are less reliable. Arrows correspond to phase relationships, where pointing right is in phase, points left is out of phase, and pointing downward means the climate driver leads the soil temperature by a quarter cycle.

Low amplitude cross wavelet results

Marble Point

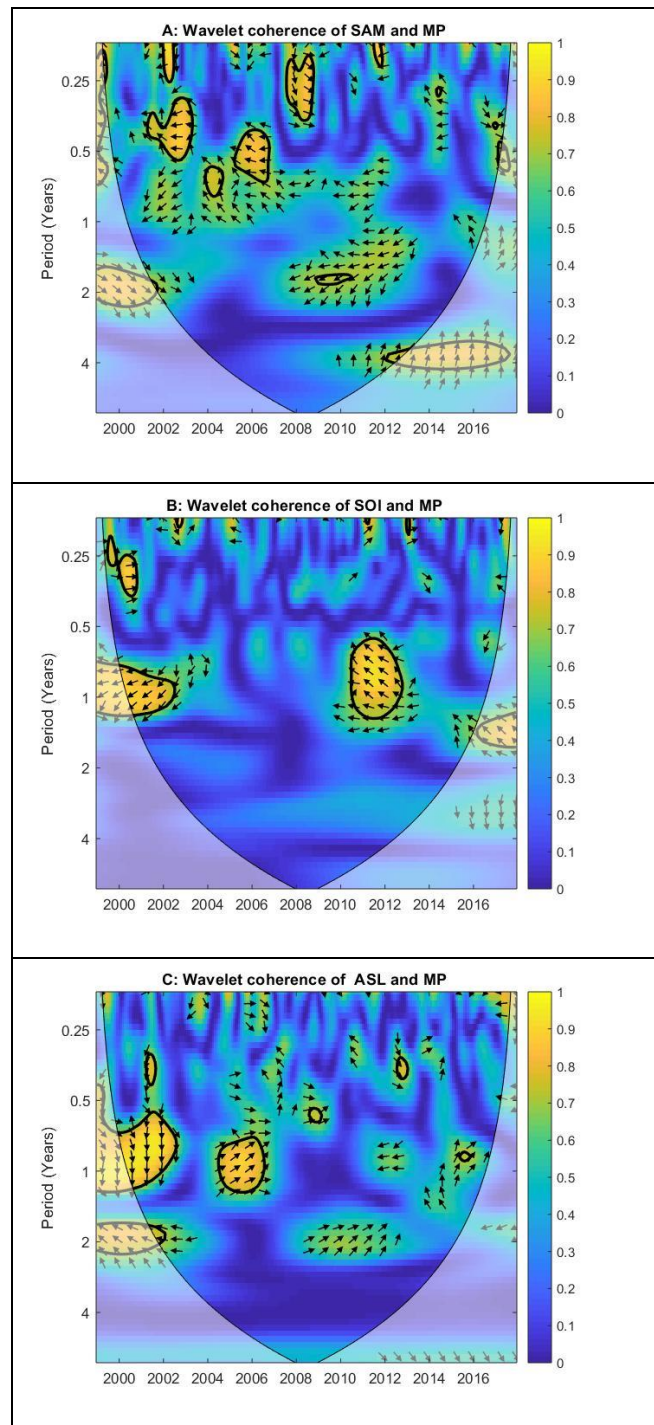


Figure IV.4: Cross wavelet transform with high amplitude periods removed, to identify significant periods with a low energy, between transform between de-seasonalised permafrost temperature data at Marble Point and climate drivers. a: (SAM); b: (SOI); c: (ASL). The amplitude is displayed by the colour bar (note change in scale to figures 1-3). Areas within the black contours are significant ($p < 0.05$). Data in the paler shaded areas are influenced by the 'edge effect' and so are less reliable. Arrows correspond to phase relationships, where pointing right is in phase, points left is out of phase, and pointing downward means the climate driver leads the soil temperature by a quarter cycle.

Wright Valley Floor

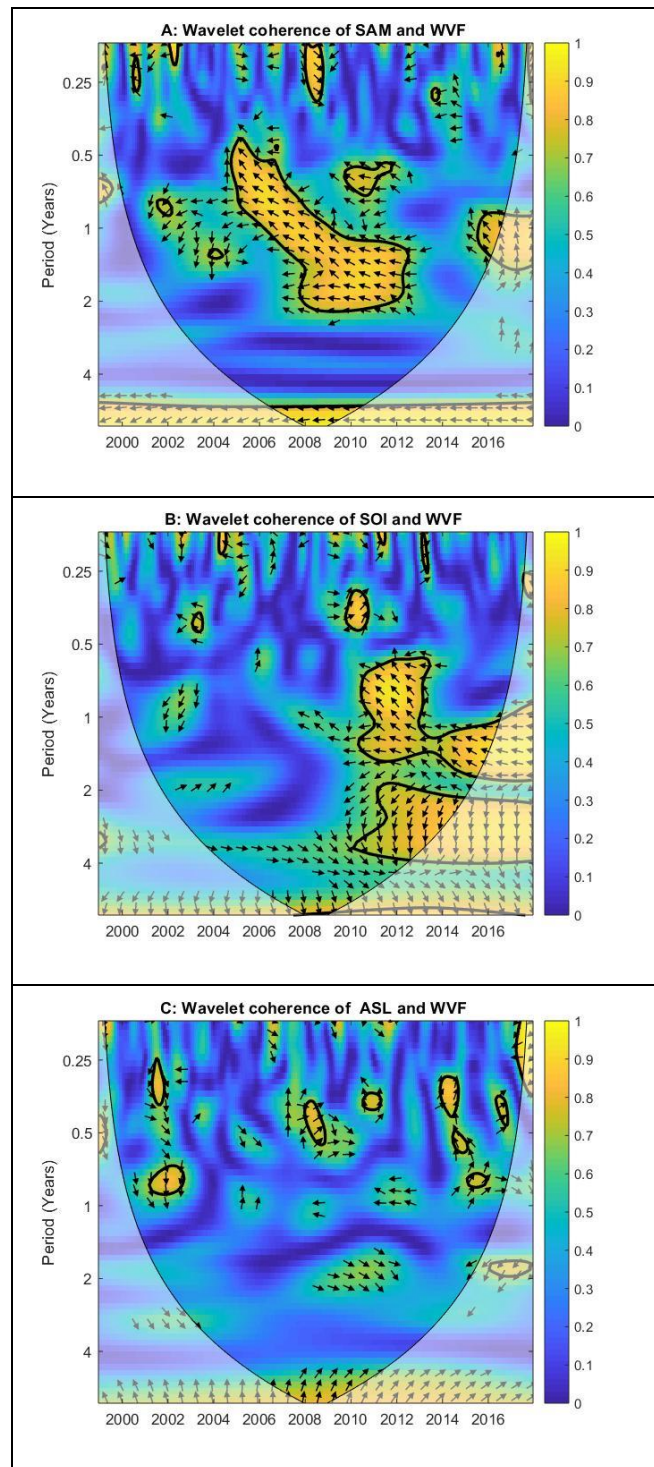


Figure IV.5: Cross wavelet transform with high amplitude periods removed, to identify significant periods with a low energy, between transform between de-seasonalised permafrost temperature data at the Wright Valley Floor and climate drivers. a: (SAM); b: (SOI); c: (ASL). The amplitude is displayed by the colour bar (note change in scale to figures 1-3). Areas within the black contours are significant ($p < 0.05$). Data in the paler shaded areas are influenced by the ‘edge effect’ and so are less reliable. Arrows correspond to phase relationships, where pointing right is in phase, points left is out of phase, and pointing downward means the climate driver leads the soil temperature by a quarter cycle.

Victoria Valley

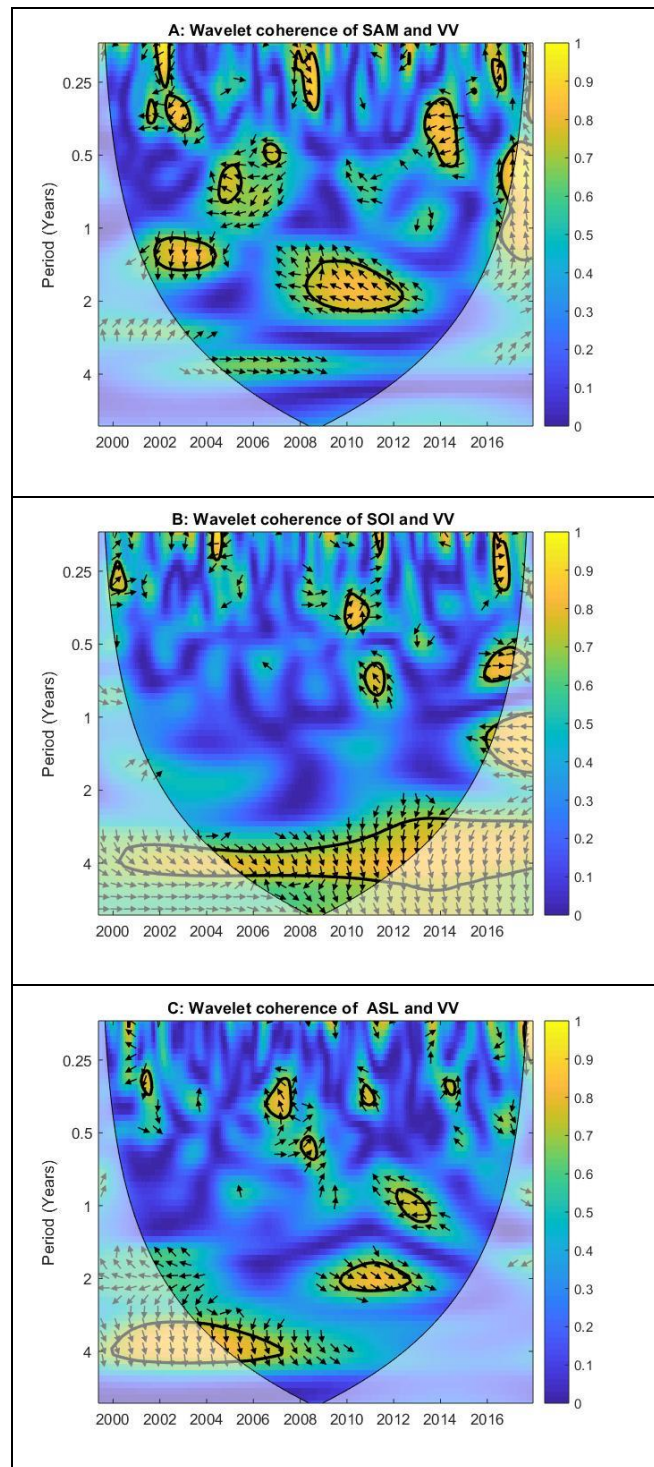


Figure IV.6: Cross wavelet transform with high amplitude periods removed, to identify significant periods with a low energy, between transform between de-seasonalised permafrost temperature data at Victoria Valley and climate drivers. a: (SAM); b: (SOI); c: (ASL). The amplitude is displayed by the colour bar (note change in scale to figures 1-3). Areas within the black contours are significant ($p < 0.05$). Data in the paler shaded areas are influenced by the ‘edge effect’ and so are less reliable. Arrows correspond to phase relationships, where pointing right is in phase, points left is out of phase, and pointing downward means the climate driver leads the soil temperature by a quarter cycle.

Mt Fleming

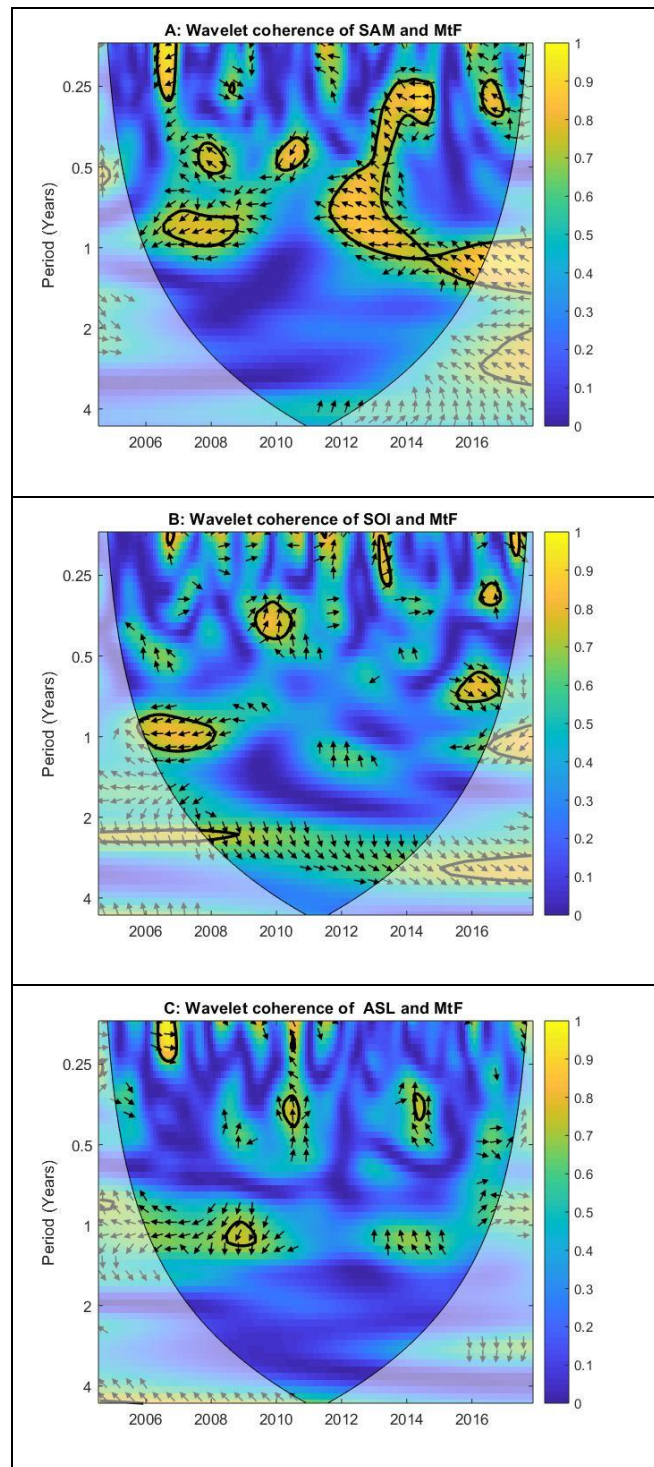


Figure IV.7: Cross wavelet transform with high amplitude periods removed, to identify significant periods with a low energy, between transform between de-seasonalised permafrost temperature data at Mt Fleming and climate drivers. a: (SAM); b: (SOI); c: (ASL). The amplitude is displayed by the colour bar (note change in scale to figures 1-3). Areas within the black contours are significant ($p < 0.05$). Data in the paler shaded areas are influenced by the ‘edge effect’ and so are less reliable. Arrows correspond to phase relationships, where pointing right is in phase, points left is out of phase, and pointing downward means the climate driver leads the soil temperature by a quarter cycle.

Appendix V

Predictive Model Options

Introduction

Appendix five presents all 19 equations developed using step wise analysis, with the best four models discussed in chapter 5. Variables used to develop the models are presented (Table V.1), along with each model equation (Table V.2) and the statistical analysis of each model (Table V.3). Summer variables were determined from December and January data, winter variables from June, July and August data and spring variables from September, October and November data.

Table V.1: The acronyms for each variable used in the modelling efforts along with their respective units.

Variable	Meaning	Units
ALD	Active layer depth	cm
MASL	Altitude	m
MSAT	Mean summer air temperature	°C
MWAT	Mean winter air temperature	°C
MSprAT	Mean spring air temperature	°C
MSST	Mean summer surface temperature	°C
TSSR	Total summer solar radiation	100 kW m ⁻²
MSWS	Mean summer wind speed	km hr ⁻¹
MWWS	Mean winter wind speed	km hr ⁻¹

Table V.2: List of models, with their equations developed using the Step wise analysis method.

Model	Equation
1	ALD= 59.14 + 5.02(MSAT) -0.075(MASL)
2	ALD= 58.85 + 5.95(MSAT)-0.07(MASL)-1.140(MSWS)+ 3.925(TSSR) +0.374(MWAT)
3	ALD= 71.67 + 5.30(MSAT)-0.07(MASL) +0.43(MWAT)
4	ALD= 42 + 5.36(MSAT)-0.08(MASL) +3.88(TSSR)
5	ALD= 83.32 -0.08(MASL) + 6.43(MSAT) -3.97(MSWS)
6	ALD= 79.97 -0.08(MASL) + 6.01(MSAT) -3.71(MSWS)
7	ALD= 58.85 + 5.95(MSAT)-0.07(MASL)-1.140(MSWS)+ 3.925(TSSR) +0.374(MWAT)
8	ALD= 71.53 -0.07(MASL)+ 3.23(MSST)+ 3.596(MSAT) +1.172(MWAT)
9	ALD= 110.47 -0.06(MASL)+ 3.37(MSST)+ 2.72(MSAT)+ 1.436(MWAT)- 7.67(TSSR)
10	ALD= 43.75 -4.02(TSSR)+1.27(MSAT)
12	ALD=191+3.44(MWAT)+2.4(MSAT)+2.84(MSST)-13.86(TSSR)
13	ALD=56.5+2.6(MSAT)+0.5(MWAT)
14	ALD=56.2=2.5(MSAT)+0.55(MWAT)+0.34(SSST)
15	ALD=60.4+3.5(MSST)-0.08(MASL)- 2.597(MWWS)+1.115(MSprAT)
16	ALD=74.14 +2.258(MSST)+1.71(MWAT)
17	ALD=47.5665 +3.878(MSST)-0.09(MASL)- 3.435(MSWS)+1.954(MSSAT)
18	ALD=61.4+3.84(MSST)-0.08(MASL)- 3.699(MSWS)+1.61(MSAT)+0.807(MSprAT)
19	ALD=110.6 +4.22(MSST)+2.243(MWAT)+1.69(MSprAT)

Table V.3: Statistics of all stepwise multiple regression models. The number of years of data used, and number of sites is given along with variation explained (Adjusted R²) the efficiency of the model (f-stat), where a larger number is preferred, and the residual mean standard error (RMSE).

Model	Years	Sites	Adj R²	f-stat	RMSE	p-Val
1	8	5	0.72	33.70	6.54	<0.001
2	8	5	0.72	14.10	6.53	<0.001
3	8	5	0.71	22.00	6.62	<0.001
4	8	5	0.74	26.99	6.35	<0.001
5	16	5	0.71	40.30	6.73	<0.001
6	16	5	0.67	37.69	6.79	<0.001
7	16	5	0.67	22.70	6.82	<0.001
8	16	5	0.75	38.50	7.17	<0.001
9	16	5	0.76	33.50	6.95	<0.001
10	16	4	0.89	94.27	3.60	<0.001
12	5	16	0.66	25.40	8.33	<0.001
13	8	16	0.48	39.00	10.66	<0.001
14	8	16	0.49	27.00	10.50	<0.001
15	5	16	0.63	29.00	10.30	<0.001
16	8	16	0.46	34.30	13.70	<0.001
17	5	16	0.61	27.70	10.49	<0.001
18	5	16	0.62	22.60	10.50	<0.001
19	5	16	0.52	11.60	25.60	<0.001